PROPERTIES OF CONCRETE WITH TIRE DERIVED AGGREGATE AND CRUMB RUBBER AS A LIGTHWEIGHT SUBSTITUTE FOR MINERAL AGGREGATES IN THE CONCRETE MIX

by

GIDEON MOMANYI SIRINGI

Presented to the Faculty of the Graduate School of
The University of Texas at Arlington in Partial Fulfillment
of the Requirements
for the Degree of

DOCTOR OF PHILOSOPHY

THE UNIVERSITY OF TEXAS AT ARLINGTON
May 2012

DEDICATION

To my dear mum, Bathseba Motugutwa for her unwavering belief in education for all her children

ACKNOWLEDGEMENTS

I would like to thank first my advisers for this project, Dr. Pranesh Aswath and Dr. Ali Abolmaali for their immense advice and guidance throughout the time of the experiments and writing of this dissertation and more so their flexibility with their schedules to accommodate my work schedule. My second thanks go to members of my dissertation committee, Dr. Jin, Dr. Hao, Dr. Lawrence and Dr. Matthys for their advice which led to further improvement of this document. I would also like to thank the Civil Engineering Technical Lab Assistants, Oleh, Paul and Jorge for their immense help around the Civil Engineering Lab Building (CELB). My thanks go also to all my fellow students whom we interacted and shared knowledge, equipment and resources at CELB.

My sincere thanks also go to Hanson Pipe and Cast in Grand Prairie, Texas, for providing most of the materials for the experiments. At Hanson, I would like to acknowledge the help provided by Vartan, Joe and Brian. I am also grateful to TXI for their understanding and allowing me to have a flexible work schedule which enabled me to attend classes at UTA and also have time for experiments.

Many thanks also go to my parents, brothers and sisters for their constant prayers. Last but not least, I would like to thank my wife for her love and understanding of my absence most of the evening and weekends which were spent in the lab and encouragement whenever things seemed difficult. Finally, thanks and praises to God for the good health and wisdom which has seen me through my study at UTA and indeed all my life.

March 23, 2012

ABSTRACT

PROPERTIES OF CONCRETE WITH TIRE DERIVED AGGREGATE AND
CRUMB RUBBER AS A LIGHTWEIGHT SUBSTITUTE
FOR MINERAL AGGREGATES IN
THE CONCRETE MIX

Gideon Momanyi Siringi, PhD

The University of Texas at Arlington, 2012

Supervising Professor: Pranesh B Aswath

Scrap tires continue to be a nuisance to the environment and this research proposes one way of recycling them as a lightweight aggregate which can substitute for mineral aggregates in concrete. Aggregates derived from scrap tires are often referred to as Tire Derived Aggregate (TDA). First, the focus is how much mineral aggregate can be replaced by these waste tires and how the properties of concrete are affected with the introduction of rubber. This is being mindful of the fact that for a new material to be acceptable as an engineering material, its properties and behavior has to be well understood, the materials must perform properly and be acceptable to the regulating agencies.

The role played by the quantity of TDA and Crumb Rubber replacing coarse aggregate and fine aggregate respectively as well as different treatment and additives in concrete on its properties are examined. Conventional concrete (without TDA) and concrete containing TDA are compared by examining their compressive strength based on ASTM C39, workability based on

ASTM C143, Splitting Tensile Strength based on ASTM C496, Modulus of Rupture (flexural strength) based on ASTM C78 and Bond strength of concrete developed with reinforcing steel based on ASTM C234.Through stress-strain plots, the rubberized concrete is compared in terms of change in ductility, toughness and Elastic Modulus.

Results indicate that while replacement of mineral aggregates with TDA results in reduction in compressive strength, this may be mitigated by addition of silica fume or using a smaller size of TDA to obtain the desired strength. The greatest benefit of using TDA is in the development of a higher ductile product with lower density while utilizing recycled TDA. From the results, it is observed that 7-10% of weight of mineral aggregates can be replaced by an equal volume of TDA to produce concrete with compressive strength of up to 4000 psi (27.5 MPa). Rubberized concrete would have higher ductility and toughness with better damage tolerance but the Elastic Modulus would be reduced.

After evaluation of rubberized concrete at elevated temperatures, it has been found that very high temperature would have adverse effects to the concrete like excessive spalling, pop-outs and cracking on the surface and therefore it is proposed to use this kind of concrete where temperature would not exceed 100°C (212°F) for extended periods.

Observation of concrete at microscopic level showed that it consists of three phases; interfacial transition zone (ITZ), bulk hydrated cement paste and aggregate. The ITZ was seen to contain micro pores and microcracks and was considered the weakest phase in concrete therefore exercises a far greater influence on the mechanical behavior of concrete than is reflected by its size. Existence of the ITZ explains why concrete strength is lower and behaves inelastically while the aggregate and cement paste if tested separately behave elastically and have higher strength than concrete.

A 3-Dimensional nonlinear Finite Element Model (FEM) for a concrete beam is proposed and developed using ABAQUS. Smeared crack model in ABAQUS is used to define material properties. The developed FEM is capable of predicting the ultimate load, deflections, Stress-

deflection/strain curves and crack initiation which are all verified against the experimental tests. ABAQUS was found to be a useful tool for modeling of concrete.

In conclusion, this research provides a clear understanding on the effects of using scrap tires as an aggregate in concrete. The pros and cons of TDA are explored, ways of overcoming the shortcomings suggested and a way of predicting concrete properties when using TDA provided.

TABLE OF CONTENTS

LIST OF ILLUSTRATIONS

Figure Page

LIST OF TABLES

CHAPTER 1

PROJECT INTRODUCTION

1.1 Motivations

Concrete is a predominant material used in construction and it competes directly with all other major construction materials like timber, steel, asphalt, and stone, because of its versatility in applications [1]. However concrete is a composite material and its properties can vary significantly depending on the choice of materials and proportions for a particular application.

The ability of concrete to be cast into any desired shape and configuration is an important characteristic that usually offsets other shortcomings. Concrete can be cast into soaring curves and columns, complex hyperbolic shells, or into massive sections used in dams, piers, and abutments. On-site construction means that local materials can be used to a large extent, thereby keeping costs down. Furthermore, by fabricating concrete on site, its properties may be tailored for the specific application.

Good-quality concrete is a very durable material and should remain maintenance free for many years when it has been properly designed for the service conditions and properly placed. Through choice of aggregates or control of paste chemistry and microstructure, concrete can be made inherently resistant to physical attack, such as from cycles of freezing and thawing or from abrasion, and from chemical attack, such as from dissolved sulfates or acids attacking the paste matrix or from highly alkaline pore solutions attacking certain aggregates.

Judicious use of mineral admixtures greatly enhances the durability of concrete. Unlike structural steel, it does not require protective coatings except in very corrosive environments. It is also an excellent material for fire resistance. Although it can be severely damaged by exposure to high temperatures, it can maintain its structural integrity for a considerable period—long after steel

buildings would have suffered irreparable damage.

However, concrete does have weaknesses that limit its use in certain applications. Concrete is a brittle material with very low tensile strength. Thus, concrete is generally not loaded in tension and reinforcing steel must be used to carry tensile loads: inadvertent tensile loading causes cracking. The low ductility of concrete also means that concrete lacks impact strength and toughness compared to metals.

Awareness of concrete weakness enables us to compensate for them, by using suitable designs and by controlling them, in part through a suitable choice of materials and construction practices [1]. New types of concrete have been developed over the years, such as fiber-reinforced concrete, shrinkage-compensated concrete, and latex-modified concrete. Concerns for harmonious co-existence between the built and the natural environment have been on the rise. There has long been a desire to create highly damage tolerant yet economic structures that require minimum maintenance and with minimum environmental impacts.

For years, material researchers have attempted to make concrete ductile. Successes have been achieved, involving fiber reinforcement in almost all cases. However, these early attempts have the limitations that either the amount of fiber required is excessive or the fibers must be continuous and aligned. These requirements lead to composites that are expensive and impossible to produce by conventional construction equipment, thus limiting the feasibility of early versions of high performance fiber reinforced concrete materials in full-scale structures.

It appears, however, that given the brittle nature of concrete, the most direct and effective approach to creating damage tolerant structures would be to embed intrinsic tensile ductility into concrete. If concrete behaves like steel in tension (highly ductile), while retaining all other advantages (e.g. extreme compressive strength), concrete structures with enhanced serviceability and safety can be readily realized.

This research will focus on looking for a solution for this worst limitation of concrete, i.e.

brittleness and very low tensile strength. Making concrete ductile would also improve impact strength and toughness of the concrete. Another issue would be to seek ways of making the concrete “green” or environmentally friendly through the choice of materials while retaining the core advantages of concrete.

Ductility is a desirable structural property because it allows stress redistribution and provides warning of impending failure. The ductile behavior will enable the concrete material to have the capacity to deform and support flexural and tensile loads, even after initial cracking.

One of the material that has been suggested as a possible replacement of mineral aggregates is rubber from used car tires. This research would focus on the use of tire chips as a Tire Derived Aggregate (TDA). TDA can be considered similar to coarse aggregate (e.g., coarse sand, gravel to crushed rock). A significant difference between mineral aggregates and TDA is that individual particles of TDA are much more deformable than those of sand, gravel, or rock. Another significant difference is that the unit weight of TDA is much lower than that of sand, gravel, or rock; therefore, TDA can be considered a lightweight aggregate. The research would also look at the effect of replacing fine aggregates (sand) with Crumb Rubber.

A lot of research continues to be done on the use of TDA. One application, referred to as rubber modified asphalt concrete (RUMAC), involves replacing some of the aggregate in the asphalt mixture with ground tires. The second, called asphalt-rubber blends/reactivates a certain percentage of the asphalt cement with ground rubber. Recycling rubber from tires for use in asphalt pavements is a promising technology. Asphalt pavements incorporating tire rubber are claimed to have twice the lifetime of ordinary asphalt, but they can cost twice as much [2]. The cost of ground (crumb) rubber probably contributes to most of this increased cost due to its high cost as shown in Table 1.1.

Scrap tires can be granulated to produce Crumb Rubber, which has a granular texture and ranges in size from very fine powder to coarse sand-sized particles. Due to its low specific gravity, Crumb Rubber can be considered a lightweight aggregate. This Crumb Rubber can then

replace sand in flowable fill to produce a lightweight material. “Experimental results indicate that Crumb Rubber can successfully be used to produce a lightweight flowable fill (1.2 to1.6 g/cm^3 [73 to 98 pcf) with excavatable 28-day compressive strengths ranging from 269 to 1194 kPa (39 to 173 psi) [3].” However as noted in Table 1.1 the cost of Crumb Rubber is high and this application may not be cost effective.

Table 1.1: Crumb Rubber and their approximate cost Range [4]

Product	Size	Applications	Approx. Cost Range
Particles	3/8–1/4"	Mulch, playground	$180–$300/ton
Coarse	1/5–1/10"	Sports Surfaces	$220–$360/ton
Medium	1/10–1/30"	Rubber Modified Asphalt, Molding	$220–$400/ton
Fine	1/40"	Rubber Modified Asphalt, Molding	$300–$1200/ton

In another experiment [5], mortar specimens were prepared using slag-modified Portland cement and 10% (by weight of mortar) of NaOH-treated rubber particles smaller than 300μm (0.012 in), from truck tires (mainly SBR rubber). Water sorption by capillarity and by immersion, resistance to acid attack, surface of fracture analysis by scanning electron microscopy and flexural strength experiments were performed. Flexural strength was reduced with the addition of the rubber (3.6 ± 0.5 MPa for the specimens with rubber, 6.5 ± 0.8 MPa for the control). On the other hand, advantageous effects of the addition of the rubber were observed on the transport properties of mortar. Sorptivity coefficient was reduced from 0.29 (control) to 0.06 mm/min$^{1/2}$. By immersion, the amount of water absorbed by the specimens with rubber was reduced by 16 %. A significant decrease in the rate of weight loss by acid attack was observed for specimens with rubber. SEM micrographs showed the presence of micro cracks in the specimens and closed pores in the specimens with rubber. These results showed that small rubber particles can improve some mortar properties even when used in a high proportion.

In the above experiment, the size of rubber used (300μm) fall under the Crumb Rubber classification and therefore the cost would be prohibitive due to the high cost of crumb rubber.

In another study [6], concrete specimens containing shredded waste tire chips were evaluated using laboratory and field tests. A total of 24 cylindrical specimens, 15 cm × 30 cm in size, were tested to determine the compressive strength of concrete at 7 and 28 days. For the dynamic tests, on the other hand, 6 New Jersey shaped concrete barriers were constructed using the identical mix designs used in the static tests. Results of the study showed that tire addition reduced the compression strength and modulus of elasticity of specimens.

Therefore the question still remains on how to economically utilize the good properties of TDA without loss of compressive strength.

Petr et al [7] in US Patent Number “US 2005/0096412 Al” claim an invention that provides a concrete composition that utilizes rubber aggregate with a distinct geometric shape. The invention prefers the source of the rubber constituting the aggregate to be used as rubber tires cut by special saws or high pressure water jets to provide a smooth finished edge. Other additional materials such as superplasticizers, fly ash, carbon fiber, fiberglass, and steel may also be mixed with the concrete compositions to vary the finish product's material properties.

The key words to be noted in this invention are “rubber aggregate with distinct geometric shape” and “cut by special saws or high pressure water jets to provide a smooth finished edge”. The shape of a cross section of individual particles of the rubber aggregate is supposed to be generally at least one of a square, a triangle, a rectangle, an octagon, a cross, and a zigzag. The rubber aggregate is generated from rubber tires that are cut such that the resulting edges are generally smooth.

By definition, TDA as an engineered product is made by cutting scrap tires into small pieces using specialized equipment, which includes shredders and shearing equipment. The final product from this kind of equipment would not have any distinct geometric shapes otherwise it would be very expensive and labor intensive to cut tires into distinct geometric shapes.

Therefore, the question still remains on how to utilize TDA in its available market form in an economically viable way to provide an engineering benefit. As seen from Table 1.2, the trend for using scrap tires in civil engineering in down wards. Some of the reasons for this trend have been high cost, environmental concerns like leaching of trace metals to the underground water system and lack of long time behavior of this material due to data not being available or not compiled into one database. Another reason is lack of consistency of TDA products.

According to the United States Environmental Protection Agency (USEPA), each year, over 270 million automobile and truck tires are removed from service and scrapped in the United States. Therefore, the need to manage scrap tires has become a necessity in most states. Examples of beneficial reuses of scrap tires in practice today include: alternative fuel source for electric generation and fuel source for cement kiln operations [8]; raw material for the production of industrial and consumer goods; and raw material for civil engineering construction [9]. The remainder of scrap tires is often disposed in various legal or illegal manners (disposal of tires in an unpermitted area).

“TDA is an engineered product made by cutting scrap tires into small pieces using specialized equipment, which includes shredders and shearing equipment. TDA is a more suitable material for reuse as aggregate when it is produced by a shearing process, in which cleanly-cut edges of the tire particles are obtained. Typically, shredders with sharp knives are used to obtain cleanly-cut edges. Screening is sometimes necessary to remove excess dirt and undesired small rubber particles [11].”

In Texas, the Department of Transportation has compiled the various applications of scrap tires as shown in Table 1.2. As can be seen, the quantity being land filled increased by 30% from 2004 to 2005, while other useful applications like in civil engineering decreased by 68% during the same period. The trend for civil engineering applications is down wards since 2001.

These numbers have not changed much as seen in Table 1.3 below as compiled by Texas Commission on Environmental Quality (TCEQ) based on 2007 data. According to the

TECQ data, amount being used in civil engineering is negligible (probably falling under other end uses), while the amount being land filled is 17.5%.

Table 1.2: Texas Scrap Tire Usage and Landfill Disposal, 2001 to 2005 [10]

Category	Consumption (Scrap Tire Units*)					Change from 2004 to 2005
	2001	2002	2003	2004	2005	
End Uses						
Tire-Derived Fuel	11,179,401	11,632,968	12,068,845	16,823,282	17,463,316	+4%
LRPUT**	4,639,575	7,847,146	6,696,538	7,269,066	7,068,988	-3%
Crumb Rubber Products	7,485	340,573	1,484,920	1,817,654	1,584,357	-13%
Civil Engineering Projects	5,019,091	3,810,200	1,748,156	806,758	260,146	-68%
Septic Systems	672,146	504,426	213,118	204,791	16,442	-92%
Other End Uses	1,592,197	827,392	966,028	414,802	1,046,902	+152%
End Uses Subtotal	**23,109,895**	**24,962,705**	**23,177,605**	**27,336,353**	**27,440,151**	**+0.4%**
Landfill Disposal	2,338,578	1,037,834	1,201,929	803,649	1,042,701	+30%
Total	**25,448,469**	**26,000,539**	**24,379,534**	**28,140,002**	**28,482,852**	**+1.2%**

* Scrap tire unit. 1 STU = 20 pounds of scrap-tire material. This unit of measurement is used because scrap-tire material can take many different forms.
** LRPUT - Land Reclamation Project Using Tires

Tires in one piece are difficult to landfill because they tend to float to the surface. Stockpiles of scrap tires result in public health, environmental, and aesthetic problems in addition to being fire hazards [2]. Disposing of waste tires is becoming more expensive. Over the years the average tipping fees for disposing of tires have continually increased. This trend is likely to continue as landfill spaces become scarcer.

Tires take up landfill space. Whole tires are banned from many landfills or charged a higher tipping fee than other waste (see Table 1.4); even if they are carefully buried to prevent rising they are very bulky. Shredded tires take up less space, but it is space that could be saved if the tires were utilized as raw material for products or as fuel. So this means whatever the end use of scrap tires, the future trend is to shred the tires first. Any application making use of shredded tires should be economically viable in future- since the tires have to be shred anyway.

Leading applications in civil engineering according to rubber manufacturer's association 2009 report [9] were lightweight fill, drainage layers for landfills and aggregate for septic tank leach fields. For these applications, scrap tires are processed into TDA, with a range of 2 to 12 inches. The driving forces for market growth are the beneficial properties of TDA including light

weight, durability, high permeability, ability to attenuate vibrations, compressibility and good thermal insulating properties.

Table 1.3: Texas Scrap Tire Usage and Landfill Disposal, 2007 [8]

Category	2007 Consumption		
	Pounds	Scrap Tire Units*	Percentage of Total
End Uses			
Land Reclamation	232,734,555	11,636,728	36%
Tire-Derived Fuel	211,311,280	10,565,564	33%
Crumb Rubber	50,917,250	2,545,863	8%
Rubber Mulch	8,309,880	415,494	1.25%
Septic/Leachate Drainage	5,603,280	280,164	.75%
Other End Uses	21,638,121	1,081,906	3.5%
End Uses Subtotal	**530,514,366**	**26,525,719**	**82.5%**
Landfill Disposal	111,844,847	5,592,242	17.5%
Total	**642,359,213**	**32,117,961**	**100%**

* Scrap Tire Unit. 1 STU = 20 pounds of scrap tire material. This unit is used because scrap tire material can take many different forms

However, ASTM D 6270 [12] suggests that it is preferable to use TDA as a landfill in environments with a near neutral pH to reduce leaching of metals (in areas of low pH) and leaching of organics (in areas of high pH). In the past some sites have experienced an exothermic reaction inside tire shred fill and ignition can occur due to the rise in temperature from an exothermic reaction. Initial exothermic reaction could be due to oxidation of exposed steel wires, oxidation of rubber or microbes consuming liquid petroleum products.

Table 1.4: Cost of Land filling [2]

COSTS OF LANDFILLING AUTOMOTIVE WASTE TIRES IN THE UNITED STATES
(In dollars per ton or cents per tire) 1/

	Costs by Region			
	Northeast	Midwest	South	West
Shredded				
Landfill Fee 2/	45	18	16	13
Processing Cost	25	25	25	25
Total	**70**	**43**	**41**	**38**
Whole				
Landfill Fee 3/	108	75	50	35
Processing Cost	0	0	0	0
Total	**108**	**75**	**50**	**35**
Savings Realized by Shredding 4/	**38**	**32**	**9**	**-3**

With the above shortcomings of using TDA as a landfill, more research continues on other applications of this material. One of them is using TDA as crumb in rubber modified asphalt. However as shown in Table 1.1, the cost of production of Crumb Rubber is too high making projects using this product to be expensive or economically unviable.

Table 1.5: Shredded tires and their approximate cost range [4]

Product	Size	Applications	Approx. Cost Range
Coarse	5–10"	Civil Engineering (CE)	$10–$44/ton
Nominal 2"	2–3"	Tire Derived Fuel (TDF), CE	$15–$45/ton
Nominal 1"	<2"	TDF, CE	$20–$65/ton

Table 1.5 shows the cost of production of shredded tires while Table 1.6 shows the cost of shredded tires compared with other construction raw materials. As can be seen, the cost of shredded tires is comparable to other civil engineering raw materials, and since rubber has an added advantage of improving mechanical properties, then it would be preferable to use. In the process, we can be able to utilize a material that is an environmental nuisance to our advantage.

Table 1.6: Cost of shredded tires compared with other construction raw materials [11]

Material	Unit Cost ($/yd^3 in-place 2007)
TDA	$27 to $40
Expanded Polystyrene (EPS) Geofoam®	$50 to $70
Common Borrow	$ 8 to $16
Lightweight Aggregate	$40 to $60

1.2 Objectives of this Research

According to ASTM D6270 [12] the definitions in Table 1.7 are adopted.

Table 1.7: Definition of Tire chips

Definition	Size (mm)	Size (inches)
Granulated or ground rubber	<12 mm	<0.5”
Tire chips	12 to 50 mm	0.5 to 2”
Tire shreds	50 to 305 mm	2 to 12”

Table 1.8: Comparison of Properties of TDA to those mineral aggregates

Property	TDA	Mineral Aggregates
1. Specific gravity, Gs	1.02 to 1.27	2.6 to 2.8
2. Elastic modulus, E	180 psi to 750 psi	6×10^3 psi to 12×10^3 psi
3. Poisson’s ratio, μ,	≈0.5	0.15 and 0.45
4. Water absorption capacity	2 to 4%	2 to 4%
5. Unit weight, γ	40 to 45 lbs/ft^3	100 to 130 lbs/ft^3
6. Void ratio, e	1.5 to 2.5 for uncompacted TDA, and 0.9 to 1.2 for compacted TDA	
7. Porosity (n),	0.60 to 0.70 for uncompacted TDA and from 0.45 to 0.55 for compacted TDA.	

Specific gravity of more than one mean that TDA does not float when submerged in water, which is considered a major advantage over other lightweight fills (e.g., some expanded polystyrene [EPS] Geofoam®) in submerged or flooding applications. Under same stress conditions, TDA will deform much more than mineral aggregates since it has a lower elastic modulus but the material would deform at a constant volume as the Poisson’s ratio for TDA approximately 0.48 [13].

Another significant difference between TDA and mineral aggregates is that individual particles of TDA are more deformable and tend to bend more easily than sand and gravel particles.

Based on the above property observations, it was this research's hypothesis that using TDA as a lightweight aggregate in concrete would improve the ductility of concrete. Another hypothesis was that due to TDA's lower elastic modulus, strength of the final concrete would drop. Part of this drop in strength would be due to poor bonding between the concrete and rubber.

The main questions of this research were to find out by how much TDA or Crumb Rubber can be used in concrete without adverse effect to concrete strength, how ductility would improve by substituting mineral aggregates with TDA and find out the drop in concrete strength due TDA's lower elastic modulus. The role of Interfacial Transition Zone (ITZ) between aggregates and the concrete mortar is examined and its contribution to strength development and possible ways of ITZ improvement suggested. Finally through modeling, a way to predict the expected properties of concrete when substituting mineral aggregates with TDA is provided.

For the use of recycled materials to become widespread in engineering construction projects, the materials must perform properly and be acceptable to the regulating agencies. This research aims to present technical consideration in the use of scrap tires as a Tire Derived Aggregate (TDA) in a concrete mix. The final goal is to provide a clear direction on how much mineral aggregate can be replaced by TDA, how TDA affects concrete properties and how one can predict concrete properties in order to have uniform properties in different mixes/batches.

1.3 Importance of this research

Scrap tires continue to be a nuisance to the environment hence research continues on finding innovative ways of utilizing this material in a more environmentally friendly way [2]. One way is using the material as an aggregate in concrete to substitute for mineral aggregates. However for material to be acceptable as an engineering material, its properties and behavior has to be well understood. The information on TDA is still scarce.

This research aims to provide a clear understanding on the effects of using scrap

tires as an aggregate in concrete. The pros and cons of TDA would be explored, ways of overcoming the shortcomings suggested and a way of predicting concrete properties when using TDA would be provided.

Use of scrap tires is needed from the viewpoint of environmental preservation and effective utilization of resources. Environmental preservation is derived from the fact that unused scrap tires are often disposed in large mono-fill stockpiles that provide the potential for creating undesirable and possibly hazardous conditions, such as increased mosquito breeding, rodent activity, and combustion. To avoid these conditions, it is desirable to reduce the quantity of stockpiled scrap tires through recycling and alternative-use programs. Effective utilization of resources is derived from the fact that recycled scrap tires would replace mineral aggregates which would have otherwise been used.

CHAPTER 2

BACKGROUND STUDY

2.1 Current Applications of Tire Derived Aggregate

Since 1992, when the first civil engineering applications were introduced to the marketplace, the number of available applications has increased dramatically. In addition, the quality of the shred used in these applications has increased as well. Over time, tires shreds have turned into a commodity and are now commonly referred to as Tire-Derived Aggregate, or TDA [9].

Tire derived aggregate (TDA) is an engineered product made by cutting scrap tires into 25 to 300-mm (1 to 12-inch) pieces [14]. The growth of TDA is fueled by many factors among them is the fact that TDA is lightweight (0.8 Mg/m^3), produces low lateral pressures on walls (as little as 1/2 of soil), is a good thermal insulator (8 times better than soil), has a high permeability (greater than 1 cm/s for many applications), and absorbs vibrations. Just as important, use of TDA's special properties can greatly reduce construction costs. For these reasons, TDA needs to be considered to overcome road building challenges [14].

Leading applications for TDA are lightweight fill, drainage layers for landfills and aggregate for septic tank leach fields. For these applications, scrap tires are processed into TDA, with a range of two to 12 inches. Table 2.1 lists the properties of tire rubber used in civil engineering applications.

For the fourth consecutive year, use of tire derived aggregate (TDA) in civil engineering applications has decreased. In 2007, 560 thousand tons of scrap tires were used in civil engineering applications. This is a decrease of 12.5% percent from the 2005 level, when 640 thousand tons of scrap tires were used in civil engineering applications [9]. The short-term

outlook for TDA is dimmed considering that 27 states report no known use of TDA. Opportunities exist to introduce TDA into several key states; especially when/where no other large-scale market currently exists.

Table 2.1: Properties of TDA Used in Civil Engineering Applications [9]

Size	2 to 12 inches
Weight	1/3 to 1/2 weight of soil
Volume	1 cubic yard ≈75 tires
Drainage	10 times better than well graded soil
Insulation	8 times better than gravel
Lateral Foundation Wall Pressure	1/2 that of soil

Some of the current uses of TDA in civil engineering applications are summarized below.

2.1.1 Landfill Applications of TDA

Due to beneficial engineering properties such as high hydraulic conductivity, high internal friction angles (i.e., shear strength), and excellent heat insulation, TDA has become a viable alternative to many traditional landfill system components. TDA has been used in the following landfill components: Landfill gas collection layers; drainage layer in leachate collection systems; drainage layers in landfill covers; leachate flow trenches; landfill protective layers; and daily and intermediate covers. Conventional materials utilized for these transmission layers are granular soils (sands and gravels) or geosynthetics (geonet and geocomposite). Compared to these materials, TDA can be very cost-effective in some projects.

2.1.2 Backfill behind Retaining Walls

TDA has been used as lightweight fill for retaining walls to replace commonly used granular soil backfills. The use of TDA provides some advantages. First, the low unit weight of TDA helps to decrease the lateral earth pressures acting on the retaining wall, thus reducing the cost of the retaining wall. Secondly, for walls founded on weak soils, the low unit weight helps to increase global stability and to avoid failure due to insufficient bearing capacity. Additionally, TDA

is a free-drainage material and provides good frost insulation.

2.1.3 Highway Embankment Fill

TDA is usually used as a lightweight fill in highway embankments. Compared to other lightweight fill materials (e.g., Geofoam®), TDA has proven in various projects to be the material with the lowest cost. The low unit weight of TDA reduces driving forces and hence increases slope stability. TDA also reduces the weight of embankment, thereby reducing settlement if the embankment is on soft soils. When founded on weak soil, TDA helps to avoid failure due to insufficient bearing capacity. Using TDA as lightweight fill has proven to be a good solution for road embankments built on top of soft ground.

Another application of TDA in highway embankment fill is insulation of sub bases and bases from frost penetration in cold climates. Frost penetration beneath roads when uncontrolled can lead to bumpy driving conditions and cracking of pavement. TDA is a good solution to this problem because the thermal conductivity of TDA is significantly lower than that of common soils.

2.1.4 Septic Drainage Media

Conventional septic systems consist of a septic tank and a leach field. The septic tank is a temporary storage for sewer waste, where wastewater is separated from heavy solids and lighter grease or oil. Wastewater then flows through the leach field, which typically is a trench filled with coarse aggregate. Biofilms developed on the surface of the aggregate in the leach field help purify the wastewater. Furthermore, wastewater is distributed into the surrounding soil, where the wastewater seeps in and is then decomposed by bacteria living in the soil. After this process, the sewage returns to the groundwater. TDA can be used as a drainage media in the leach field in a septic system. The functions of the septic leach field drainage media are to provide effective and reliable distribution of the liquid wastewater to the surrounding soil and provide a medium onto which biofilm develops to assist in the removal of oxygen-demanding wastes.

2.1.5 Asphalt Rubber

Asphalt rubber (as produced using the so called wet process) is defined by ASTM D8 as: “a blend of asphalt cement, reclaimed tire rubber, and certain additives in which the rubber component is at least 15% by weight of the total blend and has reacted in the hot asphalt cement sufficiently to cause swelling of the rubber particles” [11]. Asphalt rubber has been used in the United States since the early 1960s. Arizona, California, and Texas are the main users of this technology. Other products often referred to as rubberized asphalt, have also been used.

These products include the “dry process”, where Crumb Rubber is added during the mixing operation and the Crumb Rubber does not fully react with the asphalt. In the “terminal blend process”, the Crumb Rubber is “aggregated” into the asphalt cement at the asphalt plant. The “terminal blend process” typically uses half of the amount of tire rubbers as the wet or dry processes.

The benefits of asphalt rubber include improved resistance to skid, reduced noise levels, improved resistance to rutting and also prevents cracking in new pavements. Asphalt rubber also provides excellent, long-lasting color contrast for striping and marking, reduces reflective cracking in asphalt overlays (i.e., cracks appearing in new, thin overlays that are identical to cracks present in existing pavement) and provides a long-lasting and durable pavement and helps reduce maintenance costs. A 2-in. resurfacing layer constructed with asphalt rubber results in the beneficial use of over 2,000 tires per mile (one lane).

The limitations of these products include odor and air quality problems and more labor requirements. Unit cost is higher than traditional pavement, although the annual cost within the life cycle is lower; and construction cannot occur in cold weather.

2.1.6 Playground Cover

Playground cover made from tire chips offers some advantages because it provides good shock absorption capacity, which helps protect children from injury. TDA in playground covers drains well after rain. TDA is clean and does not attract insects or small animals.

TDA does not decompose and is easy to maintain. As long as the tire chips have been properly cleansed, TDA is non-toxic and safe to children.

2.2 Performance Considerations

As seen above, while shredded tires appear to be an excellent choice for a lightweight fill material, they do have some drawbacks. Generally, the use of shredded tires as a lightweight fill material is a fairly new concept and there is a definite lack of information concerning their use and very limited design standards are available [15]. Recent projects have used trial and error methods for determining the amount and depth of shredded tires to use. The following issues have arisen in civil engineering projects where TDA is used.

2.2.1 Puncture Damage Potential

The wires contained in TDA have created constructability and performance issues. The wires puncture geomembrane liners when TDA is in contact with geomembrane. Contact with belt wire causes scratches and indentations, which may impair the ability of the geomembrane to serve as a primary hydraulic barrier. To overcome this, any geomembrane placed adjacent to a TDA layer should have a separation layer placed between the TDA and the geomembrane to provide protection against puncture.

2.2.2 Stability

TDA must provide sufficient shear strength to resist against global stability failure in slopes and similar applications. In addition, the interface between TDA and other materials especially geosynthetics must have sufficient shear strength to resist potential sliding or pullout.

The stability of TDA is controlled mainly by unit weight and shear strength. TDA has lower unit weight and relatively lower shear strength than granular soil. The mobilized shear strength of TDA depends on the mobilized strain that the system is undergoing. In applications such as landfill covers, where TDA is placed over geosynthetics, the system is subject to down-drag.

2.2.3 Compressibility

In some applications, such as highway embankments and bridge abutments, the compressibility of TDA may influence the serviceability of the project. To reduce settlement, a soil cover with sufficient thickness overlying the TDA fill can be used. An alternate solution is to mix soil and TDA to reduce the compressibility of the backfill. However, adding soil to TDA may increase costs significantly in some projects. As more soil is added to the mix, the beneficial TDA properties as a lightweight aggregate are reduced.

Differential compression of TDA during construction and operation affects the integrity of overlying structures and pavement. Therefore a soil bridging layer is provided. In landfills, if a TDA layer supports a clay liner, cracks due to differential settlement may compromise the hydraulic barrier function of the clay liner. When TDA is used for drainage, the compression of TDA reduces the voids and thereby the hydraulic conductivity.

2.2.4 Clogging

TDA clogging decreases its drainage capacity causing a buildup of pore water pressure. If the pore pressure buildup is in a slope, the higher pore pressure may lead to slope instability. In landfill applications such as leachate collection layers, clogging may cause buildup of hydraulic head on top of the liner system, which increases the leakage potential of landfill leachate. Clogging can be caused by biochemical or physical processes.

Biochemical Clogging occurs in environments rich in microbes. Biological reactions cause inorganic constituents (e.g., calcium carbonate) to deposit reducing the pore space. Physical Clogging occurs due to the fact that TDA has larger voids than most soils used for backfill. Physical clogging then occurs as sediments build up over time within the voids of TDA fill.

2.2.5 Internal Heating and Combustibility Potential

Internal heating is a major concern for TDA fills and stockpiles. As metal wires of TDA oxidize due to corrosion and/or exothermic reactions, heat is generated. Under extreme conditions when the heat generation rate is faster than the dissipation rate, combustion of TDA

can result if internal temperatures reach the auto-ignition point of approximately 550° to 650°F (260-340°C).

Reported cases of fire due to TDA exothermic reaction include a road embankment in Ilwaco, Washington (January, 1996), a road embankment in Garfield County, Washington (January, 1996), and a retaining wall in Glenwood Canyon, Colorado (summer, 1995) [11].

Factors that facilitate this internal heating process include temperature, water pH, nutrient sources (for microbial action), and the availability of oxygen and moisture. In addition, the relatively high insulation capacity of TDA, hinders dissipation of generated internal heat, and further increases the heating potential. Internal heating potential is also influenced by TDA particle size: smaller TDA particle sizes are generally more susceptible to combustion than larger TDA particles. Oxidation is more pronounced for small TDA particles because they have a larger cut-face surface area per unit mass.

ASTM D 6270 [12] provides guidelines to minimize the internal heating potential of a TDA layer.

2.2.6 Environmental Considerations

The potential release of contaminants from TDA fills may pose an environmental risk to public health if not properly addressed.

Test results have showed that the presence of TDA had a negligible effect on the concentration of metals such as arsenic (As), barium (Ba), cadmium (Cd), chromium (Cr), copper (Cu), and lead (Pb) relative to primary drinking water standards. However, concentrations of other metals related to secondary drinking water standards, such as iron (Fe) and manganese (Mn), were encountered at elevated levels [11]. Because secondary standards are based on aesthetic factors (e.g., color, odor, and taste) and not on health concerns, the release of manganese and iron is not a critical concern. However, aesthetic concerns should be evaluated if TDA is to be placed below the groundwater table (ASTM D 6270).

Results have shown that trace levels of a few volatile and semi-volatile organics were

found in tap water taken directly from TDA filled trenches [11]. These water containments include benzene, chloroethane, cis-1,2-dichloroethene, and aniline. Minnesota Pollution Control Agency (MPCA) has shown that tire shreds may leach out heavy metals when subject to highly acidic solutions with a pH of 3.5 [15].

2.2.7 Constructability

The use of TDA fill may present some difficulties during construction. For example, when an overlying soil layer is to be constructed, the elastic compression and rebound of the TDA fill may make the soil layer difficult to compact. In landfill applications, a compacted clay liner directly above a TDA layer would not be feasible because the high compressibility of TDA may lead to cracks. This problem may be avoided if a soil-bridging layer is added between the clay liner and the TDA layer.

When a geomembrane is to be placed on top of TDA fill, the relatively large deformations induced by construction activities may impede the placement of the geomembrane or disrupt liner-seaming activities where a firm, stable foundation is required.

2.2.8 Public Perception

The general public still considers using shredded tires for fill material as just another way of burying waste. The public may oppose projects using waste tires even if projects are deemed environmentally safe. Overall, more research must be conducted on the engineering and environmental aspects of this "new" material in order for it to have an impact as an alternative construction material [15].

2.3 Current Understanding on Research on use of TDA in Concrete

Petr et al [7] in US Patent Number “US 2005/0096412 Al” claims of an invention where rubber aggregate of predetermined shape (either a square, zigzag, triangle, cross, rectangle, square, octagon) and smooth surface replaces mineral aggregate of between 0.01 to 35%. Size of rubber aggregate is 95% passing 1-inch sieve and final compression strength of about 3000 PSI. However the author of the patent does not explain how use of rubber aggregate affects the properties of concrete either positively or negatively.

Aiello [16] investigated the properties of various concrete mixtures at fresh and hardened state obtained by a partial substitution of coarse and fine aggregate with different volume percentages of waste tires rubber particles, having the same dimensions of the replaced aggregate. The size range of the rubber particles used was between 10 mm and 25 mm. The rubberized concrete mixtures were found to have a lower unit weight compared to plain concrete and good workability. Compressive and flexural tests indicated a larger reduction of mechanical properties of rubcrete when replacing coarse aggregate rather than fine aggregate. On the other hand, the post-cracking behavior of rubberized concrete was positively affected by the substitution of coarse aggregate with rubber shreds, showing a good energy absorption and ductility. With 50% and 75% by volume of coarse aggregate replacement, presented, respectively, a decrease in compressive strength of about 54% and 62%, compared to the control mixture. Whereas with 50% and 75% by volume of fine aggregate substitution, showed, respectively, a compressive strength decay of about 28% and 37%, compared to the control mixture.

Eldin [17] examined compressive and tensile strengths of rubberized concrete. He notes that rubberized concrete did not perform as well as normal concrete under repeated freeze-thaw cycles. It exhibited lower compressive and tensile strength than that of normal concrete but unlike normal concrete, rubberized concrete had the ability to absorb a large amount of plastic energy under compressive and tensile loads. It did not demonstrate the typical brittle failure, but rather a

ductile, plastic failure mode.

Emiroğlu [18] produced rubber filled concretes by replacing the normal aggregates with rubber aggregates (5%, 10%, 15% and 20%) by volume respectively. The three point bending tests were conducted on 100 x 100 x 500 mm beam specimens to determine deflection amount of the beams. It was observed that by increasing rubber content in the concrete, the conformity of the relationship between experimental results and empirical equation results for elasticity modulus were decreased.

Ghaly [19] investigated the possibility of using fine rubber particles in concrete mixtures. The study was to establish the effect of the addition of crumb rubber, size between 1 and 2 mm, as replacement of a portion of fine aggregates (sand), on the strength of concrete. Rubber was added to concrete in quantities of 5%, 10%, and 15% by volume of the mixture. Three different water/cement ratios were used: 0.47, 0.54, and 0.61. Test results gathered in this research project indicated that the addition of Crumb Rubber to concrete resulted in a reduced strength as compared with that of conventional concrete. The compressive stress of the concrete decreased with the increase of the rubber content in the mix.

Güneyisi [20] investigated mechanical properties of rubberized concretes with and without silica fume. Two types of tire rubber, Crumb Rubber and tire chips, were used as fine and coarse aggregate, respectively, in the production of rubberized concrete mixtures which were obtained by partially replacing the aggregate with rubber. Six designated rubber contents varying from 2.5% to 50% by total aggregate volume were used. The concretes with silica fume were produced by partial substitution of cement with silica fume at varying amounts of 5–20%. Test results indicated that there was a large reduction in the strength and modulus values with the increase in rubber content. However, the addition of silica fume into the matrix improved the mechanical properties of the rubberized concretes and diminished the rate of strength loss. Results also revealed that a rubber content of as high as 25% by total aggregate volume might be practically used to produce rubberized concretes with compressive strength of 16–32 MPa.

Huang [21] prepared and tested cylindrical rubberized concrete samples and ordinary concrete samples for basic physical/mechanical properties. It was found that rubberized concrete has very high toughness. However, its strength decreases significantly as the rubber content increases. The rubber chips used had dimensions of 25.4×25.4×5 mm. With 15% of coarse aggregate replaced by rubber chips, the compressive strength was reduced by 45%, and the indirect tensile strength was reduced by 23%.

Khaloo [22] investigated the feasibility of using elastic and flexible tire–rubber particles as aggregate in concrete. Tire–rubber particles composed of tire chips, crumb rubber, and a combination of tire chips and crumb rubber, were used to replace mineral aggregates in concrete. The rubber particles had Sieve residue on mesh 60 (0.25mm) of 80%. These particles were used to replace 12.5%, 25%, 37.5%, and 50% of the total mineral aggregate's volume in concrete. The fresh rubberized concrete exhibited lower unit weight and acceptable workability compared to plain concrete. The results of a uniaxial compressive strain control test conducted on hardened concrete specimens indicate large reductions in the strength and tangential modulus of elasticity. A significant decrease in the brittle behavior of concrete with increasing rubber content is also demonstrated. Unlike plain concrete, the failure state in rubberized concrete occurs gently and uniformly, and does not cause any separation in the specimen.

Khatib [23] developed an experimental program in which two types of tire rubber (fine Crumb Rubber and coarse tire chips) were used in Portland cement concrete (PCC) mixtures. Rubberized PCC mixes were developed by partially replacing the aggregate with rubber and tested for compressive and flexural strength in accordance to ASTM standards. Tire chips were elongated particles that ranged in size from about 10 to 50 mm (0.4 to 1.9 in.) Results show that rubberized PCC mixes can be made and are workable to a certain degree with the tire rubber content being as much as 57% of the total aggregate volume. However, strength results show that large reductions in strength would prohibit the use of such high rubber content. It is suggested that rubber contents should not exceed 20% of the total aggregate volume.

Li [24] explored the use of steel reinforced Crumb Rubber concrete as seismic structural materials with high energy-consuming capacity. The study of structural properties through the pseudo-static test of pillar and the cross-section bending experiments of the beam showed that the steel reinforced Crumb Rubber concrete has good ductility and energy-consuming capacity compared with the ordinary concrete therefore suitable for high seismic requirements structure.

Pelisser [25] investigated the potential use of recycled tire rubbers in cement matrices. Concrete formulations were produced with the replacement of 10% sand aggregate by recycled tire rubber using conventional rubber and rubber modified with alkaline activation and silica fume addition to improve the mechanical properties. The recycled rubber (below 4.8 mm mesh) was washed with sodium hydroxide (1M NaOH) to increase the hydrophilicity of the rubber particle surface. Further, silica fume (microsilica) was added (15% mass fraction) to the recycled rubber as a surface modifier. The mixture was then mixed with the plasticizer (lignosulfonate). The water/cement ratio (or composition) and the testing age were used as additional variables.

The concrete characterization was performed by testing the compressive strength, elastic modulus, density and microstructure (SEM). The recycled tire rubber proved to be an excellent aggregate to use in the concrete. It was observed that its compressive strength was reduced by only 14% (28 days), in comparison to the conventional concrete, reaching 48 MPa for the mixture with higher resistance. The concrete compositions were found to be lighter and a reduced interface was observed between the rubber and cement matrix after the chemical treatment. The rubberized concrete can support construction sustainability, minimize the consumption of natural resources by using an industrial residue and produce a material with special features.

Schimizze [26] evaluated two rubberized concrete mixes to obtain an indication of the loss of strength and increase in flexibility caused by the addition of 5% rubber by weight. Strength lost was about 50% for both mixes, which could be acceptable for some of the low strength applications. Flexibility increased in both mixes. The increase was 25 percent with the addition of coarse rubber and over 50 percent with the addition of fine rubber.

Siddique [27] reports that there is approximately 85% reduction in compressive strength and 50% reduction in splitting tensile strength when coarse aggregate is fully replaced by coarse Crumb Rubber chips. However, a reduction of about 65% in compressive strength and up to 50% in splitting tensile strength is observed when fine aggregate is fully replaced by fine crumb rubber. Both of these mixtures demonstrate a ductile failure and have the ability to absorb a large amount of energy under compressive and tensile loads.

Son [28] investigated the efficiency of waste tire rubber-filled concrete to improve the deformability and energy absorption capacity of Reinforced Concrete columns by considering different concrete compressive strength, size of waste tire rubber particles and rubber content. Twelve column specimens were tested using concrete of compressive strength 24 and 28 MPa mixed with 0.6 and 1 mm tire rubber particles. They found out that using waste tire rubber-filled concrete leads to a slightly lower compressive strength and modulus of elasticity, but the curvature ductility can increase up to 90%. They concluded that this type of concrete can offer good energy dissipation capacity and ductility, which makes it suitable for seismic applications.

Topçu and Bilir [29] studied the usage of ground elastic wastes such as rubber in Self Compacted Concrete (SCC). Rubber replaced aggregates at the contents of 60, 120 and 180kg/m3 in SCC by weight. Different viscosity agents were used to see the effects on the properties of Rubberized SCC (RSCC). Fly ash was used as filler material. The slump–flow, V-funnel, compressive strength, high temperature and freezing–thawing resistances of RSCC were compared to the properties of ordinary SCC. They observed that increase in Rubber Aggregate content leads to increase in fresh properties of RSCC such as workability because of the existence of viscosity agents in mixtures but decreases the hardened properties such as compressive strength and durability.

Topçu and Demir [30] studied durability of mortar and concrete, including aggregate of discarded car tires under environmental conditions like freeze-thaw, seawater, and high temperature. Concrete specimens were produced with a cement dosage of 300, a 0.5 water-

cement ratio, and 0, 10, 20, and 30% rubber aggregate in volume, where the grain size was 1–4 mm instead of fine aggregate. They concluded that in the regions where the environmental conditions are not harsh, use of concrete produced with 10% rubber aggregate is appropriate as it is economical and an effective way of recycling the discarded tires.

Toutanji [31] investigated the effect of replacement of mineral coarse aggregate by rubber tire aggregate. He used four different volume contents of rubber tire chips: 25, 50, 75 and 100%. Shredded rubber tires used had a maximum size of 12.7 mm (l/2 in) and a specific gravity of about O.61.The incorporation of these rubber tire chips in concrete exhibited a reduction in compressive and flexural strengths; the reduction in compressive strength was approximately twice the reduction of the flexural strength. The specimens which contained rubber tire aggregate exhibited ductile failure and underwent significant displacement before fracture. The toughness of flexural specimens was evaluated for plain and rubber tire concrete specimens. The test revealed that high toughness was displayed by specimens containing rubber tire chips as compared to control specimens. Slump measurements showed that workability decreased with introduction of rubber.

Yang {{3036 Yang,Linhu 2010;}} added Crumb Rubber into reinforced concrete (RC) and found that it changed the stress-strain relationship of concrete improving the sectional ductility of reinforced concrete (RC) beam. Their results showed that Crumb Rubber improves the ductility of Crumb Rubber Concrete beam significantly.

Zheng {{3113 Zheng,L. 2008;}} investigated the effect of rubber types and rubber content on strength and deformation properties of concrete. The tire-chip group of rubber had particles that ranged in size from about 15 to 4 mm, with the steel belt wires included and extended. Rubber replacements of 15, 30, and 45% by the volume of the coarse aggregate were used. Their experimental results revealed that strength and modulus elasticity of rubberized concrete decreased with the increasing amount of rubber content. The average cylinder compressive strength of the normal concrete at 28 days was determined to be 38.8 MPa. The strength of

rubberized concrete at the content of 15, 30, and 45% decreased to 30.1, 21.0, and 18.1 MPa, with the decrease of 22.3, 45.8, and 53.3% respectively. Compressive strength and modulus of elasticity of crushed rubberized concrete were lower than that of ground rubberized concrete. Brittleness index values of rubberized concrete were lower than that of normal concrete, which means that rubberized concrete had higher ductility performance than that of normal concrete.

Other uses of rubber from tires are in asphalt. Akisetty [32] investigated the mixture performance characteristics of rubberized warm asphalt mixtures, and their correlation with binder properties, through a series of laboratory tests (e.g., viscosity, dynamic shear rheometer (DSR), and bending beam rheometer (BBR)) conducted on the binders, and obtaining the indirect tensile strength, rutting resistance, and resilient modulus of various mixtures. The results of the experiments indicated that the use of Crumb Rubber can effectively improve the engineering properties of these mixes at lower mixing and compacting temperatures.

However, none of the studies have elucidated in any detail the beneficial aspects of TDA and the mechanism by which the properties of TDA reinforced concrete differ from traditional concrete. In this study we hope to detail the properties of concrete where some of the coarse aggregate (rock) is replaced with TDA and where some of the fine aggregate (sand) is replaced by Crumb Rubber.

CHAPTER 3

RAW MATERIALS AND PROCEDURE

This chapter discusses the raw materials used in the optimal mix design and the mixing and testing procedures adopted in this study.

3.1 Raw Materials

3.1.1 Portland Cement

Commercially available high-early strength Type III Portland cement meeting ASTM C 150 was used in this study. A specific gravity of 3.15 was assumed for the purpose of mix proportioning. The fineness on 325 mesh (45 µm sieve) was found to be 98% passing and the Blaine was 540 m^2/kg.

3.1.2 Coarse Aggregates

There were two different types of coarse aggregates used in this study. The major coarse aggregate was provided by Hanson Pipe and Precast in Grand Prairie, Texas. Table 3.1 provides the sieve analysis of this aggregate compared to ASTM C 33 requirements. The second coarse aggregate used in this study was Tire Derived Aggregate (TDA). Table 3.2 provides the sieve analysis of TDA. TDA was sourced from Fast Tires in Arlington, Texas and Granutech-Saturn Systems in Grand Prairie, TX.

Maximum size of coarse aggregate used in concrete has a bearing on economy. Usually more water and cement is required for small-size aggregates than large sizes. Generally, for a given water-cement ratio, the amount of cement required decreases as the maximum size of coarse aggregate increases. The maximum size of aggregate that can be used generally depends on the size and shape of the concrete member and the amount and distribution of reinforcing steel.

The maximum size of aggregate particles generally should not exceed one fifth of the narrowest dimension of concrete member or three-fourths the clear spacing between reinforcing bars or one-third the depth of slabs.

Table 3.1: Sieve Analysis of Coarse Aggregates from Hanson Pipe and Precast

	Grading Requirements for coarse aggregates (ASTM C33 Size No. 57)		Percent Passing Coarse Aggregates from Hanson
Sieve Size	Low	High	
1 ½" (37.5 mm)		100	100%
1" (25 mm)	95	100	99.8%
¾' (19 mm)			93.0%
5/8" (15.8 mm)			79.1%
½" (12.5 mm)	25	60	
3/8" (9.5 mm)	0	15	22.2%
#4 (4.75 mm)	0	5	2.1%

Table 3.2: Sieve Analysis of TDA

Sieve Size	Percent Passing TDA
2" (50 mm)	100.0%
1 ½" (37.5 mm)	88.7%
1" (25 mm)	45.0%
¾' (19 mm)	20.6%
5/8" (12.5 mm)	15.1%
3/8" (9.5 mm)	9.2%
#4 (4.75 mm)	5.5%

3.1.3 Fine Aggregates

The fine aggregates used in the design was also provided by Hanson Pipe and Precast in Grand Prairie, TX. The sieve analysis is given in Table 3.3. The amount of fine aggregate passing the No. 50 and No. 100 sieves affects workability, surface texture and bleeding of concrete. Most specifications allow 10% to 30% to pass the No.50 sieve [33].

Other requirements for fine aggregates stipulated in ASTM C 33 are that the fine aggregate must not have more than 45% retained between any two consecutive standard sieves and the fineness modulus must be not less than 2.3 nor more than 3.1, nor vary more than 0.2 from the typical value of the aggregate source.

Table 3.3: Sieve Analysis of Fine Aggregate

	Grading Requirements for fine aggregates (ASTM C33)		Percent Passing
Sieve Size	Low	High	
#4 (4.75 mm)	95	100	100.0%
#8 (2.36 mm)	80	100	97.3%
#16 (1.18 mm)	50	85	40.7%
#30 (600µm)	25	60	8.0%

The fineness modulus (FM) of either fine or coarse aggregates according to ASTM 125 is obtained by adding the cumulative percentages by weight retained on each of a specified series of sieves and dividing the sum by 100 [33]. FM is an index of fineness of aggregates- the higher the FM, the coarser the aggregate. FM is fine aggregate is useful in estimating proportions of fine and coarse aggregates in concrete mixtures.

3.1.4 Silica Fume

The silica fume used in this study was compacted silica fume sourced from Fritz-Pak Corporation in Mesquite, TX. It is a pozzolanic material which is composed of highly refined silicon dioxide in the non-crystalline form. Silica Fume was expected to chemically react with the calcium hydroxide released by the hydration of Portland cement to form compounds possessing superior cementitious properties. This ultra-fine material will better fill voids between cement particles and result in a very dense concrete with higher compressive strengths and extremely low permeability.

Silica Fume is recommended for all types of concrete where improved concrete performance with reduced permeability is required to reduce the effect of corrosive chemicals, such as deicing salts, on structural steel. Silica Fume is also recommended where higher density and ultimate strengths are desired.

3.1.5 Mixing Water

The water used for mixing was tap water. The unit weight of water was assumed to be 62.4 lbs/ft^3 (1000kg/m^3).

3.2 Experimental Procedure

In order to establish the maximum amount of TDA that can be used to replace coarse aggregates without significantly compromising the strength of the concrete, several batches of concrete were made using different amounts of TDA and tested for compressive strength.

The concrete proportioning was done following the Absolute Volume Method as described by Portland Cement Association [33]. The 28-day compressive strength of over 4500 psi (31 MPA) was targeted while the Portland cement content was based upon water/cement (w/c) ratio of between 0.55 and 0.60. The actual batch compositions in terms of weight are shown in Table 3.4 for TDA whose size was 100% passing 2 in (50.8 mm) sieve and TDA size was 100% passing 1 in (25.4 mm) sieve. Table 3.5 shows the batch numbers, designation and description that would be used.

In order to incorporate Crumb Rubber into the mix, a specific amount by weight of fine aggregate was removed and replaced with an equal volume of crumb rubber, keeping all other factors constant. Two different quantities of fine aggregate were replaced, i.e. 7.5% and 15%. In order to further improve concrete properties, silica fume was added to some batches. The actual batch compositions in terms of weight and batch designations when Crumb Rubber was used are shown in Table 3.6.

Table 3.4: Mix proportions for various concrete batches prepared for testing compressive strength to determine amount of TDA to be used.

	Batch Number											
Component (lb)	1	2	3	4	5	6	7	8	9	10	11	12
Cement	92.5	92.5	92.5	92.5	92.5	92.5	92.5	74.0	92.5	92.5	92.5	92.5
Silica Fume								18.5	18.5	18.5	18.5	
Rock (Coarse Aggregates)	393.6		326.7	354.3	354.3	354.3	354.3	354.3	354.3	364.1	364.1	364.1
Sand (Fine Aggregates)	259.2	259.2	259.2	259.2	259.2	259.2	259.2	259.2	259.2	259.2	259.2	259.2
Water	51.2	51.2	51.2	51.2	51.2	51.2	51.2	51.2	51.2	51.2	51.2	51.2
TDA		118.8	24.3	14.3	14.3	14.3	14.3	14.3	14.3	10.3	10.3	10.3
2- Part Epoxy							√					
NaOH					√	√						
Total	796	522	754	771	771	771	771	771	790	796	796	777

Table 3.5: Batch Number, Designation and Description

Batch Number	Designation	Description
1	Control-0% TDA	Control Mix Design- No TDA used
2	100% TDA -2"	100% Replacement of Coarse Aggregate with TDA of size 2"
3	17% TDA -2"	17% Replacement of Coarse Aggregate with TDA of size 2"
4	10% TDA -2"	10% Replacement of Coarse Aggregate with TDA of size 2"
5	10% TDA -2"- NaOH Sol	10% Replacement of Coarse Aggregate with TDA of size 2". TDA dissolved in NaOH solution and both TDA and NaOH solution included in batch
6	7.5% TDA -1"- NaOH	10% Replacement of Coarse Aggregate with TDA of size 2". TDA dissolved in NaOH solution for 24 hours but solution not included in the batch
7	10% TDA -2"- Epoxy	10% Replacement of Coarse Aggregate with TDA of size 2". TDA treated with 2-part epoxy before mixing.
8	10% TDA -2"-SF-R	10% of Coarse Aggregate replaced with an equal volume of TDA size 2" and 20% of cement replaced with Silica Fume
9	10% TDA -2"-SF-A	10% of Coarse Aggregate replaced with an equal volume of TDA size 2" and Silica Fume equal to 20% of cement added to the mix
10	7.5% TDA -2"-SF-A	7.5% of Coarse Aggregate replaced with an equal volume of TDA size 2" and Silica Fume equal to 20% of cement added to the mix
11	7.5% TDA -1"-SF-A	7.5% of Coarse Aggregate replaced with an equal volume of TDA size 1" and Silica Fume equal to 20% of cement added to the mix
12	7.5% TDA -1"	7.5% of Coarse Aggregate replaced with an equal volume of TDA size 1"

Table 3.6: Mix Compositions for various batches per cubic yard when Crumb Rubber was used

Description of Type of Concrete	Control	7.5% Fine Aggregate Replaced With Crumb Rubber	15% Fine Aggregate Replaced With Crumb Rubber	Control With addition of Silica Fume	7.5% Fine Aggregate Replaced With Crumb Rubber With Addition of Silica Fume	7.5% Fine Aggregate Replaced with Crumb Rubber and 7.5% Coarse Aggregate Replaced with TDA
Designation	0%Crumb	7.5%Crumb	15%Crumb	0%Crumb-SF	7.5%Crumb-SF	7.5%Crumb+7.5%TDA
Cement (LB)	470	470	470	470	470	470
Silica Fume (LB)				59	57	
Coarse Aggregate (LB)	2000	2000	2000	2000	2000	1850
Fine Aggregate (LB)	1317	1218	1119	1317	1218	1218
Water (LB)	260	260	260	315	314	260
Crumb Rubber (LB)		41	70		42	36
TDA (LB)						55
Total	4047	3989	3919	4138	4079	3802
Water/Cementitious material Ratio	0.55	0.55	0.55	0.60	0.60	0.55
Slump , inches (mm)	1 (25.4)	1 ½ (38.1)	1 ¼ (31.2)	2 (50.4)	3 (76.2)	1 ½ (38.1)

The moisture content of the aggregates was assumed to be Saturated Surface Dry (SSD), that is, neither absorbing water from nor contributing water to the concrete mixture. Therefore no adjustment was made to the weight of aggregates required, based on the amount of absorbed and free water present in the Mix Design Procedures.

The batches were prepared and cured following ASTM Designation C192 [34]. The American Concrete Institute recommends two methods for proportioning a concrete mix design: (1) by mass when using the S.I. System or by weight when using the U.S. Standard System, and (2) the volumetric method which is the one chosen for this study. Volumetric method is considered the more accurate of the two.

Before starting the rotation of the drum, the mixer (Multiquip Inc, Model MC-94P, 9 cu ft) was charged with the coarse aggregates and about one quarter of the mixing water. Then the mixer was started and fine aggregate, cement, and remaining required mixing water was added in that order. TDA was charged at the same time with coarse aggregates.

The Mixer was then operated for 5 minutes after all of the ingredients had been added, followed by a brief rest period to confirm if the mixture was workable then run for an additional 2 min. At the completion of mixing, the concrete was deposited in a wheel barrow, remixed by shovel until it appeared uniform. Then slump test was carried out following ASTM C143 [35].

The moulds used were 6in diameter and 12in long (150 mm by 300 mm) plastic cylinders and 20in x 6 in x 6 in (510mm x150 mm x 150mm) rigid steel forms. The cylinders were filled with three lifts of freshly mixed concrete, tamping each lift 25 times with the tamping rod and tapping each lift lightly with a mallet 10 to 15 times. The excess concrete was struck off and finished to a smooth surface with a steel or wooden trowel. The cylinders were used to test for compressive strength following ASTM C39 ([36] and splitting tensile test following ASTM C496 ([37]. The splitting tensile test set-up is shown in Figure 3.1. The 20in x 6 in x 6 in (510mm x150 mm x 150mm) concrete beams were used to test for flexural strength with loading at the third points following ASTM C78 [38] whose set up is shown in Figure 3.2.

The molded cylinders were left covered at room temperature for about 24 hours after which the moulds were removed and then the cylinders transferred to the curing room set at a temperature of 80°F (26°C) and relative humidity of approximately 95-100%. One set of three cylinders or beams was tested after 7 days and another set of three after 28 days.

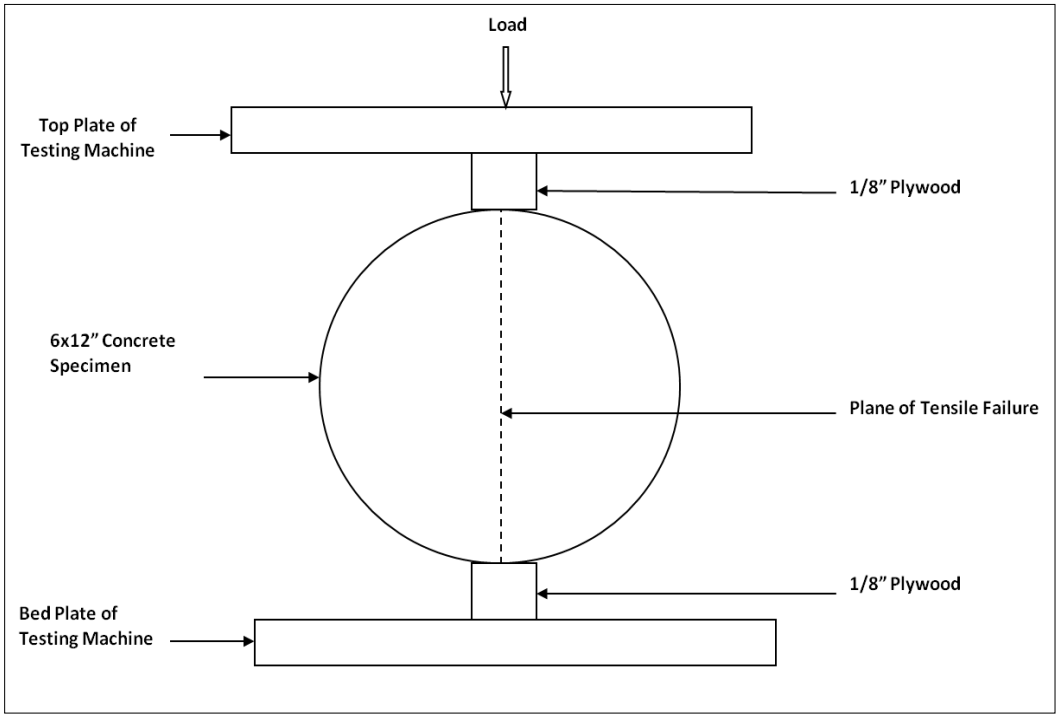

Figure 3.1: Splitting Tensile Test set up (ASTM C496)

During the ASTM C78 test (Figure 3.2), the Load (P) was collected and the Modulus of Rupture (MR) was calculated based on Equation (3.1). The MR represents the flexural strength of the beam.

$$MR = \frac{PL}{bd^2} \qquad (3.1)$$

Where L = Supported length of the beam (18 in).

b = Average width of the specimen (6 in).

d = Average depth of the specimen (6 in).

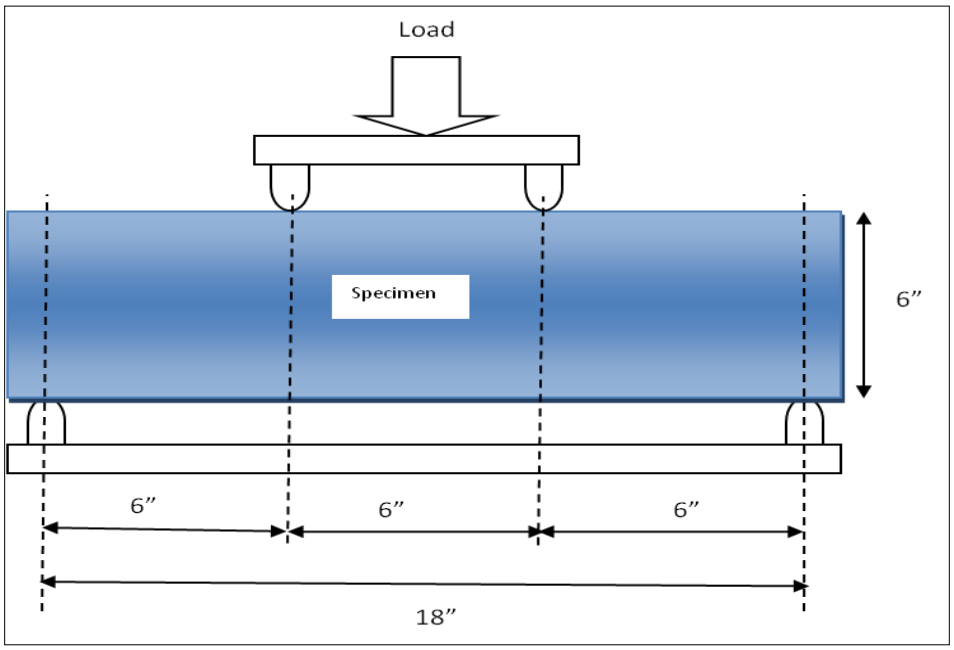

Figure 3.2: Flexural Strength Test of a Concrete Beam Set up (ASTM C78)

Similarly, for ASTM C496 (Figure 3.1), the Load (P) was collected and splitting tensile strength (T) of cylindrical concrete specimens was calculated based on Equation (3.2).

$$T = \frac{2P}{\pi LD} \qquad (3.2)$$

Where L = Length of the cylindrical specimen (12 in) and d = Diameter of the specimen (6 in).

Both ASTM C78 and ASTM C496 are indirect methods of obtaining tensile strength of a concrete specimen.

ASTM C39 test method was followed for compression tests where the applied load was measured using a load cell and displacement was measured using two LVDTs all of which were connected to a computer system. The computer system included a Vishay Scanner, Model 5100B and a Laptop computer with Strainsmart5000 software. The two LVDT were attached on a tailored cylinder which was screwed to the body of the concrete cylinder to measure displacement

of the concrete directly as shown in Figure 3.3 . The LVDT used were Omega's LD621-5 with a Range of 0 to 10 mm (0 to 0.4").

The data collected was load (lb) and displacement in inches from each LVDT. In all the calculations of strain, the average displacement from the two LVDTs was used. Compressive strength was measured either by 500 KIP (2.2 Meganewton) Compression Machine or 400 KIP (1.8 Meganewton) Tensile/Compression Machine.

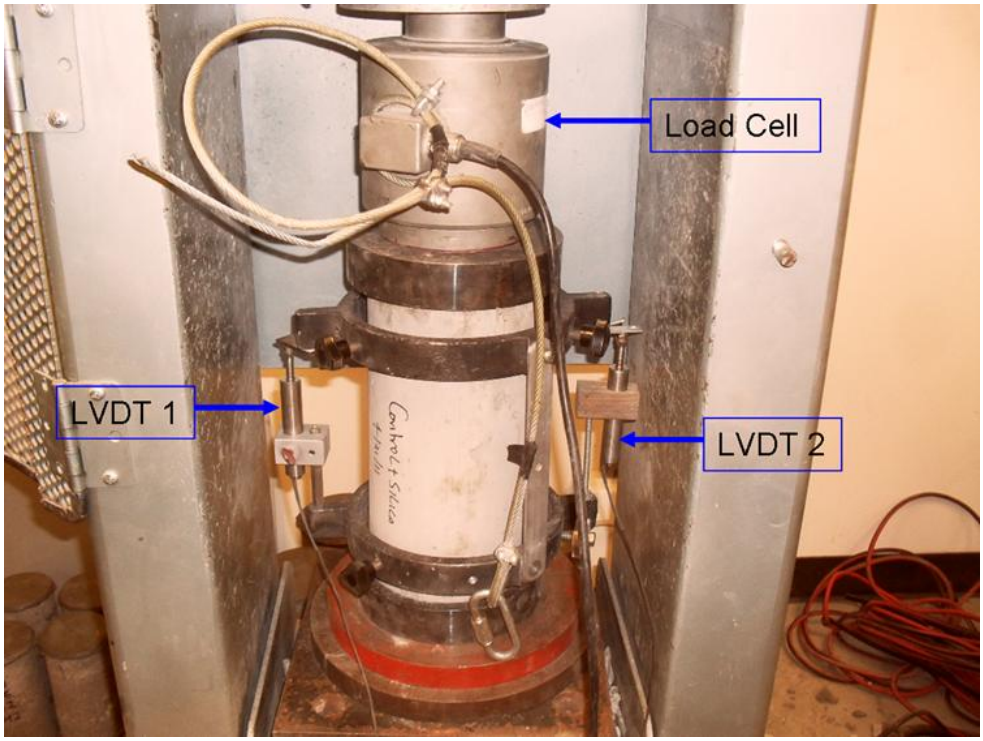

Figure 3.3: Compressive Strength Test Set-Up (ASTM C39)

The splitting tensile test followed the ASTM C496 and flexural strength followed ASTM C78, the applied load was measured using a load cell and displacement of the testing machine head was measured using Novotechnik position transducers (TR 100) with a range of 0-100 mm. The 400 KIP (1.8 meganewton) Tensile/Compression Machine was used in the splitting tensile test (ASTM C496) and 60 KIP (0.27 Meganewton) Tensile/Compression Machine was used in the flexural strength test (ASTM C78).

Two different sizes of TDA were used. Those that 100% passed a 2" (≈50 mm) sieve and those that 100% passed a 1" (≈25.4 mm) sieve. The TDA particle distribution is shown in Figure 3.4 in comparison with coarse aggregates that were used. The initial consideration of size of TDA was mainly based on cost. The particle size distribution of Crumb Rubber is compared to fine aggregate in Figure 3.5.

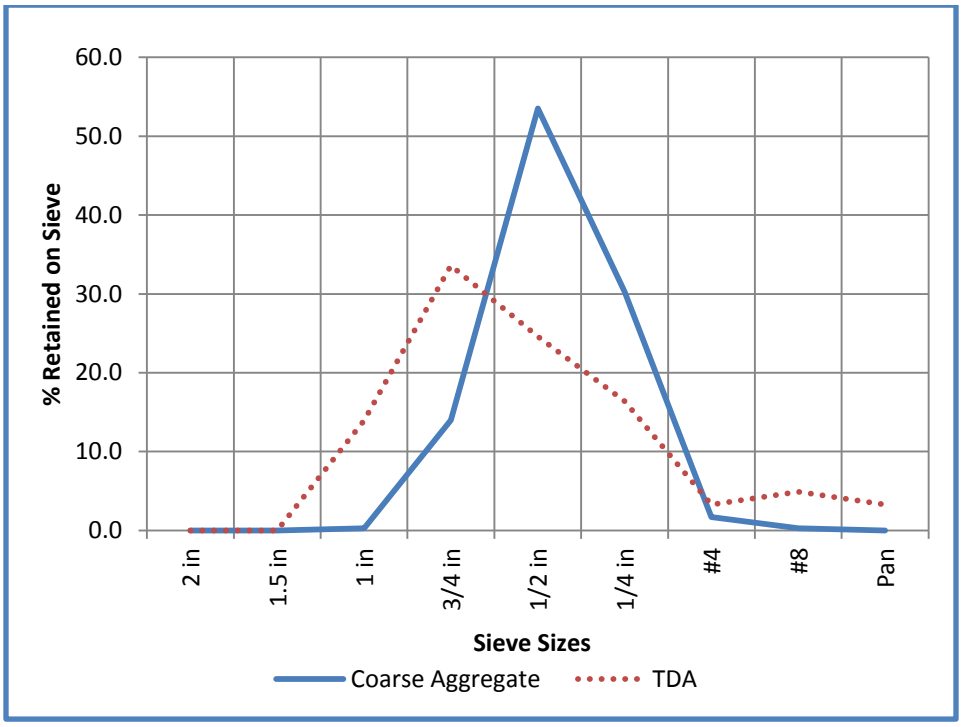

Figure 3.4: Coarse Aggregate and TDA Particle Distribution Comparison

A control batch (batch with no TDA) was first prepared. The compressive strength of this batch was used to compare the properties of concrete where TDA replaced some or all of the coarse aggregates. All process factors in TDA batches are held constant except for the replacement of coarse aggregates (rock) with an equal volume of TDA. The different amounts of coarse aggregates replaced with an equal amount of TDA (by volume) were 100%, 17%, 10% and 7.5%.

In order to improve strength of the concrete with TDA, several additives were evaluated to improve the bond between the TDA and concrete components. Earlier studies had suggested

that treatment with NaOH enhanced bonding with concrete [5] and hence was one of the methods attempted. The second method involved using a 2-part epoxy with the hope that this would improve bonding between TDA and concrete and the last method attempted was the incorporation of silica fume which has been shown to improve the strength of concrete [39]. Silica fume was use in two ways, first it was used to replace 20% cement and later an amount equal to 20% of cement was added to the concrete without replacing any cement. The results are shown in Figure 4.1.

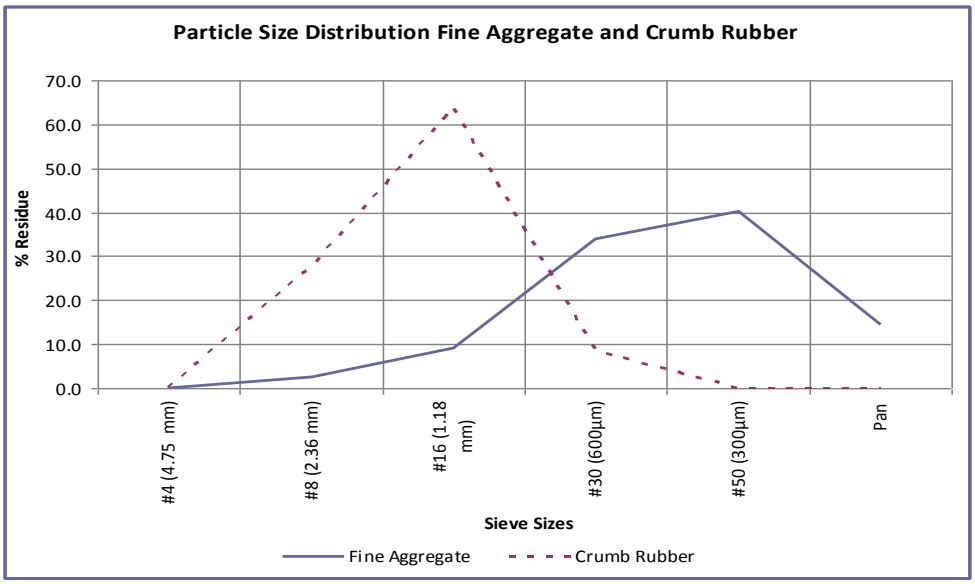

Figure 3.5: Particle Size Distribution for Fine Aggregate and Crumb Rubber

NaOH was used in two ways. At first, a third of the total water required was set aside and used to prepare a 1-Molar NaOH solution where the TDA was immersed in the solution for 30 minutes prior to introduction of both the solution and the TDA to the mixer. When this method did not yield good results as shown in Figure 4.1, a second method was attempted. Here, 1-Molar NaOH solution was prepared and TDA was immersed in the solution for 24 hours after which the TDA was introduced to the mixer while still wet but the NaOH solution was discarded. The rest of the procedure remained the same as described earlier.

When the two part epoxy was used, TDA was placed in a container and the two parts of epoxy were added to it, mixed and then introduced to the mixer immediately well before the epoxy started to set. The epoxy used was PC Products, PC-Concrete 600 ml Concrete Bonding Agent. The rest of the procedure was then followed as described in the earlier section.

Pull-out tests were also performed based on ASTM 234. The purpose was to determine the bond strength between concrete and deformed steel reinforcing bars due to the adhesion of the paste to the steel, the friction between the steel and the concrete, and the bearing of the concrete against the lugs of the deformed steel bars. The direct pull-out is used to test the bond strength of reinforcing rods in concrete. ASTM 234 recommends using the direct pull-out test for determining the bond strength developed between the concrete and reinforcing steel. The moulds used in this experiment were the 6 in x 12 in (150 mm x 300 mm) cylinders and #4 steel bars.

The direct pull-out test method consisted of a #4 steel bar embedded through a cylindrical concrete specimen. The specimens had the steel bar embedded at the depth of 4 in [101.6 mm] of the full length of the cylindrical specimen (12 inches [300 mm]). The concrete was constrained and the steel rod was pulled from one end of the specimen. The bond strength (stress) of the concrete is determined from the force (P) applied to the re-bars divided by the interfacial contact area of the re-bar bonded region as shown in Equation (3.3)

The performance of the concrete with Crumb Rubber or TDA is compared to conventional concrete in terms of compressive strength, tensile strength, failure patterns, and energy absorption during loading to failure and workability.

$$\text{Bond Stress (psi)} = \frac{P}{\pi dL} \qquad (3.3)$$

Where: Length of RE-bar Embedment (L) = 4 in.

Nominal Diameter of RE-bar (d) = 0.5 in.

Bond Area between the Concrete and the RE-bar = πdL = 6.286 in^2

CHAPTER 4

EFFECT OF TIRE DERIVED AGGREGATE IN CONCRETE

4.1 Workability

Workability is defined in terms of the amount of mechanical work or energy required to produce full compaction of the concrete without segregation [1]. Workability also refers to concrete consistency, flowability, mobility, pumpability, compactibility, finishability and harshness.

Workability of a freshly mixed concrete was evaluated through slump measurement as outlined in ASTM C143 [35]. The slump test is considered to be a measure of the shear resistance of concrete to flowing under its own weight. Table 4.1 shows slump measurements for the different batches that were prepared.

Table 4.1: Slump Measurements Based on ASTM C143

	Water/Cementious Ratio	Slump (in)	Slump (mm)
Control-0% TDA	0.55	½	12.7
7.5% TDA -2"-SF-A	0.55	¼	6.4
7.5% TDA -1"- NaOH	0.55	1 ½	38.1
Control-0% TDA	0.60	2 ¼	57.2
7.5% TDA -1"	0.60	3 ½	88.9
7.5% TDA -1"-SF-A	0.60	2	50.8

Incorporation of TDA into concrete results in an increase of the slump by an average of 1 inch at the same water/cement ratio when compared to the control. Higher slump implies better workability when shaping fresh concrete into desired shapes during construction. Aiello and Leuzzi [16] made the same observations of improved workability when they investigated the properties of various concrete mixtures at fresh and hardened state obtained by a partial substitution of coarse and fine aggregate with different volume percentages of waste tires rubber particles, having the same dimensions of the replaced aggregate. The size range of the rubber particles they used was between 10 mm and 25 mm. Topçu and Bilir [29] made similar

observation of improved workability with introduction of rubber into concrete. However, Toutanji [31] recorded slump measurements showing that workability decreased with introduction of rubber.

It was found out that one should consider silica fume as a cementitious material in calculating amount of water required when silica fume is incorporated in concrete if the same workability is to be achieved in the absence of either a water reducer or superplasticizers. This conclusion is from the observed reduction in slump with the introduction of silica fume (Table 4.1).

At low doses of 3 percent or less, silica fume serves to liquefy the concrete by fitting in between the cement grains due to their small size that they displace water, which becomes free to help with the flowability of the concrete. In effect, it becomes its own water reducer. But when you add more and more silica fume, up to the neighborhood of 5 percent of cementitious material, the surface area of the silica fume begins to outweigh its water displacement function, and surface forces begin to have a strong effect, and water reducer, or superplasticizer, or both must be added to overcome the need for more water [40].

4.2 Compressive Strength

Strength is defined as a measure of the stress required to fracture a material. Figure 4.1 is a summary of compressive strength of various batches with different amounts of TDA in comparison with regular concrete (control) both at 7 days and 28 days. When all the coarse aggregate is replaced with TDA (100% TDA -2"), the TDA concrete developed only 8% of the strength of that of the control concrete at 7 days. This was a very drastic drop and it was concluded that only very little amount of TDA can be used as a substitute for coarse aggregates. These results are consistent with Siddique and Naik [27] who had also reported approximately a 85% reduction in compressive strength when coarse aggregate is fully replaced by coarse Crumb Rubber chips.

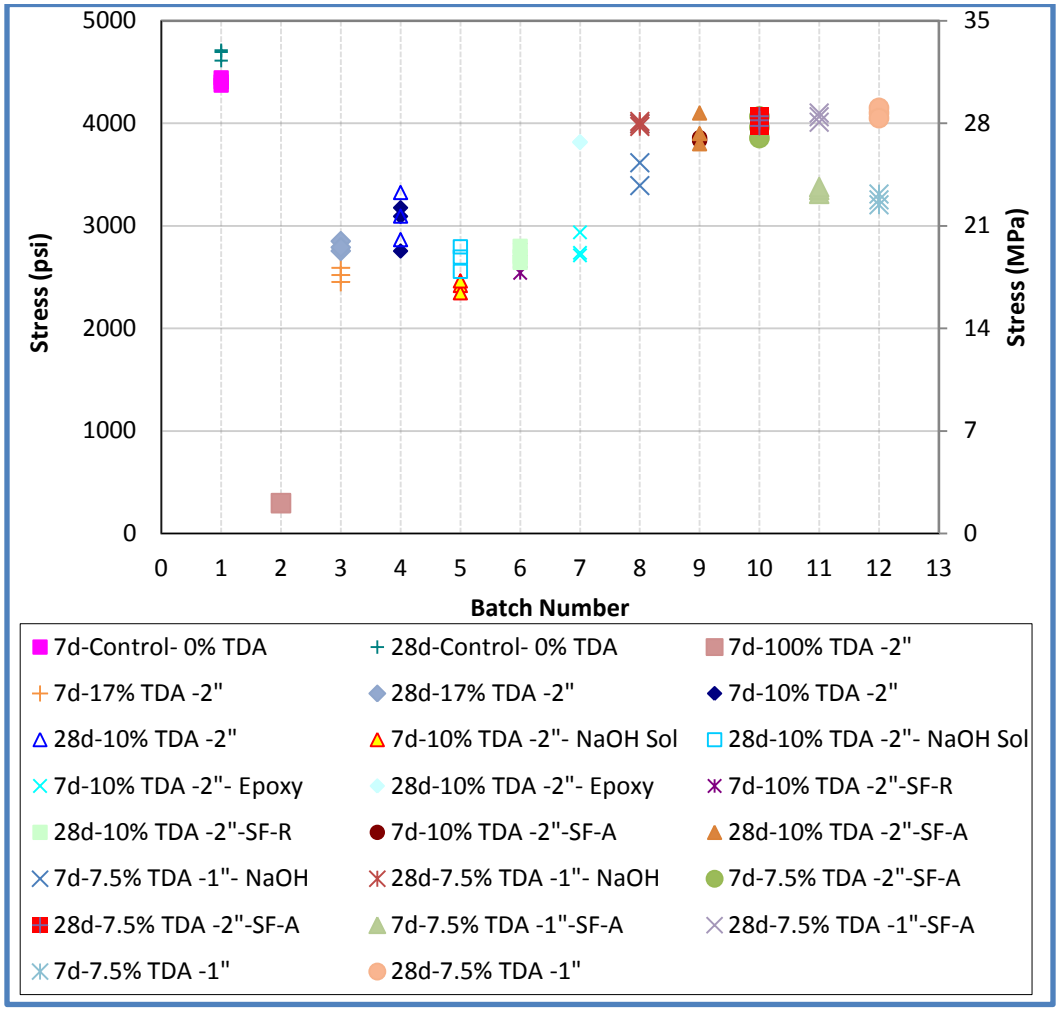

Figure 4.1: Summary of Compressive Test Results with loading up to concrete failure at 7 days and 28 days. The batch designation is as shown in Table 3.5.

Replacing 17% of coarse aggregates (17% TDA -2") with an equal volume of TDA, all other factors remaining constant saw a 45% drop in strength at 7 days and 40% drop at 28 days in comparison with the control concrete. This drop was still considered large and therefore unacceptable. It was then decided to drop the quantity of TDA further in order to improve on the strength. These results confirm those of Huang et al [21] who recorded a 45% compressive strength reduction when 15% of coarse aggregate were replaced by rubber chips.

When 10% of coarse aggregate (10% TDA -2") was replaced with an equal volume of TDA, there was a slight mitigation of the properties, with a drop of 28.6% and 33.8 % at 7-day

and 28-day respectively when compared to the control batch (Control-0% TDA). This drop in compression strength is still high but it was deemed that it would be impractical to further reduce the amount of TDA. At this point ways of improving concrete strength were sought.

Also shown in Figure 4.1 is a summary of compressive strength when NaOH solution, epoxy and silica fume were incorporated into concrete containing TDA. NaOH treatment of rubber before introduction of TDA and NaOH solution (10% TDA -2"- NaOH Sol) into the concrete did not improve the bonding between the concrete constituents and the rubber chips and in fact the overall compressive strength declined when compared with the samples with an equal amount of TDA but with no NaOH treatment as seen from Figure 4.1.

This is the opposite of results obtained by Pelisser et al [25] and Segre et al [5] whose results indicated that NaOH increases rubber particle's surface hydrophilicity hence improving bonding between the rubber and concrete. However, when the TDA was treated with NaOH solution before being added to the mixer but the solution discarded (7.5% TDA -1"- NaOH) saw the strength of the concrete being equal to the that with equal amount of TDA but no treatment with NaOH (7.5% TDA -1").

Possible negative effect of NaOH could have been increased solubility of gypsum in the cement leading to flash set in the concrete. NaOH addition may also result in undesirable morphology and non-uniformity of hydration products in the pastes, thus reducing cement strength. Addition of NaOH generally decreases ettringite formation [41]. Ettringite is a hydration product formed through the reaction of tricalcium aluminate (C_3A) and gypsum in the presence of water. Formation of ettringite slows down the hydration of C_3A by creating a diffusion barrier around C_3A therefore allowing for more time for tricalcium silicate (C_3S) to hydrate. C_3S is the cement compound that is responsible for strength development.

After 7 days of curing the 2-part epoxy did not result in improvement of strength but had a significant impact after 28 days. The 28 day strength was 18% less compared to the control batch. This showed that the epoxy improved the TDA concrete by about 23% when compared to

TDA concrete without Epoxy at 28 days. Since no improvement was noted at 7 days (early strength) when using epoxy, this method was considered unattractive.

Replacing part of cement with silica fume did not have any positive effect on strength as seen from Figure 4.1 (10% TDA -2"-SF-R) but addition of silica fume (7.5% TDA -2"-SF-A) into batch had a positive effect on concrete strength. At 10% coarse aggregate replacement with TDA and addition of silica fume equal to 20% of cement, the drop in strength was 12.4% at 7 days and 16.5% at 28 days compared to the control batch. Pelisser et al [25] observed that compressive strength was reduced by 14% at 28 days, in comparison to the conventional concrete when the replacement of 10% sand aggregate by recycled tire rubber using conventional rubber and rubber modified with alkaline activation and silica fume addition to improve the mechanical properties. Zheng et al [42] found a 22.3% decrease in strength with 15% Rubber replacements by the volume of the coarse aggregate at 28 days. However, these results are a big improvement from the results recorded by Schimizze et al [26]. Schimizze et al record a strength loss of about 50% by the addition of 5% rubber by weight.

The overall compressive strength of about 3900 psi (≈27 MPa) was also deemed acceptable and falls within the range of structural concretes. Mindness et al [1] give a range of structural concretes to be 17-63 MPa (2465 -9135 psi). The results of improved strength when using silica fume agrees with Güneyisi et al [20] who showed that the addition of silica fume into the matrix improved the mechanical properties of the rubberized concretes and diminished the rate of strength loss.

Silica Fume (SF) functions in a concrete as a highly efficient pozzolan, that is, it reacts chemically with the calcium hydroxide produced by the hydration of the Portland cement to form calcium silicate hydrates (C-S-H) which bind the concrete together. Silica Fume is highly reactive due to the high proportion of non-crystalline SiO_2 and the large surface area [39].

Silica fume can be used in concrete in two ways: as an addition (generally 8–15% by mass of cement), to enhance properties of the fresh and/or hardened concrete or as a partial

cement replacement (5–10% by mass of cement) to maintain the 28-day compressive strength at lower cement content (with associated environmental benefits) while reducing the heat of hydration, and improving durability [39]. From the results in Figure 4.1 the former would be preferred when using TDA.

The functions of silica fume in Portland cement concrete are twofold, both physical and chemical in nature. Physically, there are three major attributes for silica fume. Because the silica fume particles are much, much smaller than the cement particles — with a surface area in the neighborhood of 20,000 m^2/kg - they can "pack" between the cement particles and provide a finer pore structure. This property is particularly important because it is likely that TDA could be increasing the void content due to poor bonding to the concrete resulting in the low strength in concretes with TDA. The final strength of the concrete is in a large part a function of the amount of compaction, a small increase in void content (or decrease in relative density) will lead to a large decrease in strength. In the early stages of hydration, silica fume can help accelerate the hydration process, because its tiny particles provide nucleation sites for hydration.

In the nucleation process, a silica fume particle provides a site on which material in solution can "nucleate" or "center," which helps the material precipitate sooner than it might otherwise do. And once it precipitates, the concentration of that material in solution is reduced, which tends to get more material into solution from elsewhere, speeding the process. Silica fume can dramatically reduce bleeding as it introduces a lot of surface area into the mix, which in turn helps hold the water in place.

Chemically, if time and moisture are allowed to do their job, silica fume has a very strong pozzolanic reaction, so that when the cement grains hydrate and generate calcium hydroxide, the silica fume will react with that and create more calcium silicate hydrate. In this instance, more space is filled up within the concrete, which gives much more strength, and improves resistance to intrusion from a number of factors. These benefits include radically reduced permeability to water, and reduced diffusivity to chloride ions.

A further reduction of quantity of TDA to 7.5% replacement had only a marginal effect even with incorporation of silica fume into the batch as seen from the results in Figure 4.1. The results elucidate that the batch with TDA developed 87.6% of the control batch strength at 28 days. At 7 days, the batch with TDA showed 8.5% reduction in compressive strength compared with the control. This was only a 3.4% improvement from the batch where 10% coarse aggregate was replaced with TDA.

From these results it was concluded that small amounts of TDA with a maximum size of 2 inches in the range of 7.5-10% can be used to replace coarse aggregates in concrete whose compressive strength is about 4000 psi (28 MPA). To achieve this compressive strength, strength enhancing materials like silica fume would need to be used. This recommendation is about half of what Khatib and Bayomy [23] recommend. Khatib and Bayomy recommend that rubber contents should not exceed 20% of the total aggregate volume.

However, if the size of TDA is reduced, the results in Figure 4.1 show that one can achieve a compressive strength of up to 4000 psi without using strength enhancing materials like silica fume. The choice of TDA size would then depend on cost considerations i.e. the cost of further reduction of TDA size versus the cost of the strength enhancing materials.

4.3 Concrete Ductility

Apart from the positive environmental effect of using TDA as a lightweight replacement for mineral aggregates, it was hoped that TDA would improve some other properties of concrete like ductility. Rubber which is the source of TDA under same stress conditions would deform much more than mineral aggregates since it has a lower elastic modulus but the material would deform at almost constant volume as the Poisson's ratio for TDA is approximately 0.48 [13]. Another significant difference between TDA and mineral aggregates is that individual particles of TDA are more deformable and tend to bend more easily than sand and gravel particles.

At high stress level, the strain no longer remains proportional to the applied stress, and it becomes permanent i.e. it would not be reversed if the specimen is unloaded. This strain is called

plastic or inelastic strain. The amount of inelastic strain that can occur before failure is a measure of the ductility of the material. Typically under compression, concrete appears to show inelastic strain at fracture of the order of 2 $x10^{-3}$ [43].

Two concretes (7.5%TDA -1" and Control-0%TDA) are compared in Figure 4.2 using stress-strain curves. In Figure 4.2 the batch with no TDA is labeled Control-0%TDA 1/2/3 and the batch in which TDA replaced 7.5% of coarse aggregates is labeled 7.5%TDA -1" 1/2/3. On an average, the deformation the concrete with TDA can sustain before failure is higher than those without TDA even though they fail at slightly lower strength. Zheng et al [42], Toutanji [31], Aiello and Leuzzi [16], Khaloo et al [22] and Eldin and Senouci, [17] made a similar observation. The concrete with TDA exhibits improved post-cracking behavior, showing a good energy absorption and ductility and the concrete with TDA did not demonstrate the typical brittle failure, but rather a ductile, plastic failure mode.

Figure 4.3 has the same stress-strain comparison between the control batch (Control-0% TDA) and TDA batch but this time with addition of Silica Fume (7.5% TDA -1"-SF-A). Silica fume is noted to have improved the consistency of TDA concrete and its strength but appears to have had a negative effect on the amount of strain the concrete can sustain before failure.

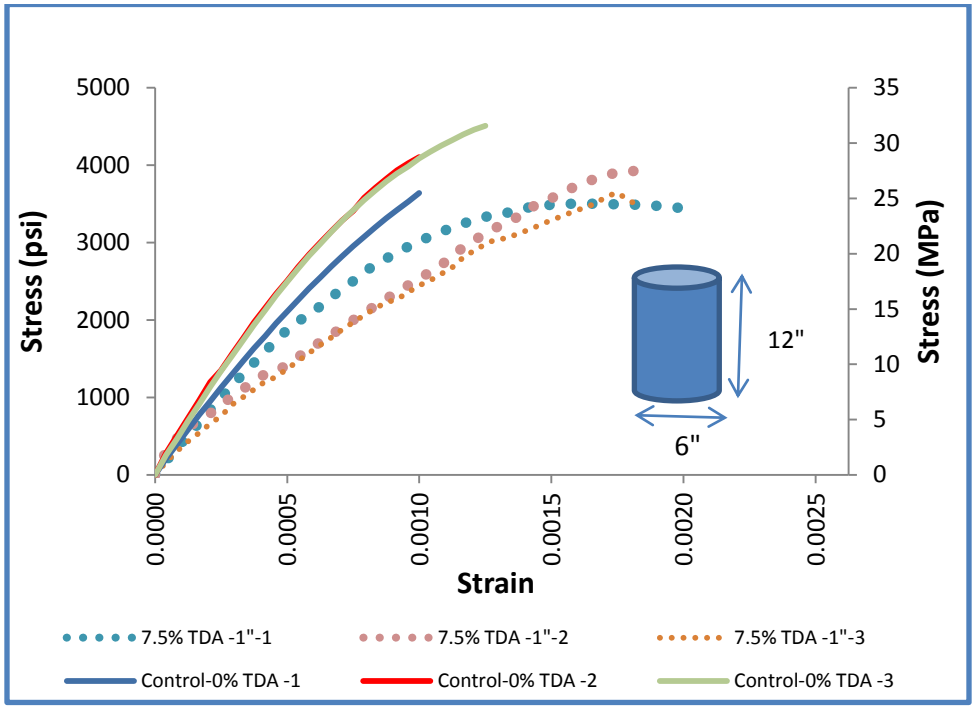

Figure 4.2: Stress vs. Strain Comparison between Control Concrete and TDA Concrete at 28 days

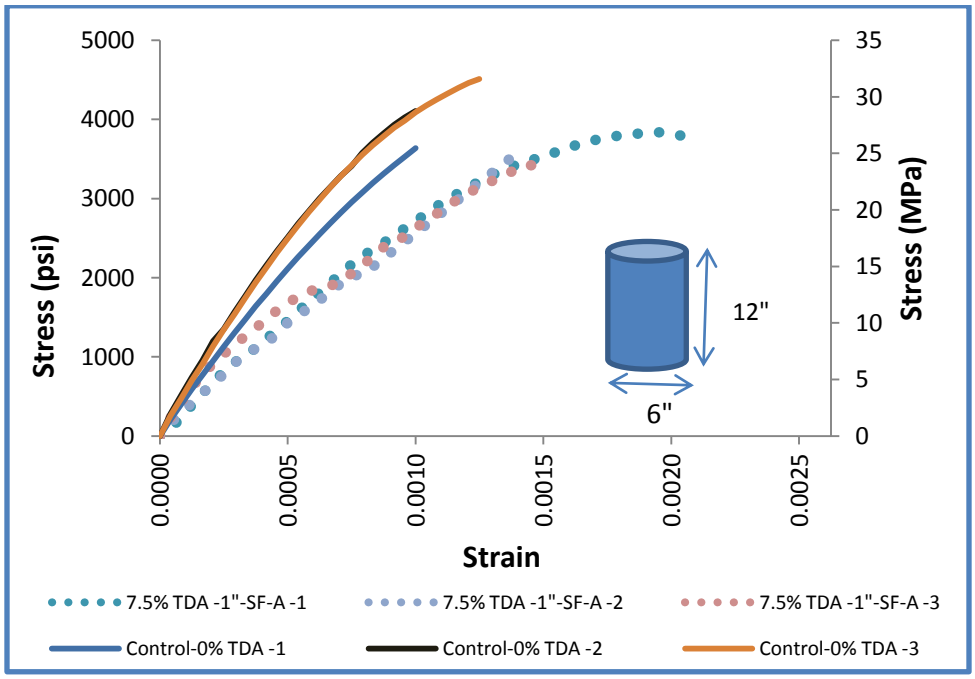

Figure 4.3: Stress vs. Strain Comparison between Control Concrete and TDA Concrete with Silica Fume at 28 days.

4.4 Concrete Toughness

The energy required to break the material, the product of force and distance, is represented by the area under the curve of the stress-strain plot. The term toughness is a measure of this energy.

Calculation of area under the curves in Figure 4.2 and Figure 4.3 is summarized in Table 4.2. TDA is shown to improve concrete toughness but the effect is diminished if silica fume is used. Huang et al [21] and Toutanji [31] also found that rubberized concrete had very high toughness when they replaced coarse aggregate with rubber chips.

4.5 Modulus of Elasticity

The modulus of elasticity is defined as the ratio between the stress and the reversible strain. It is a measure of stiffness of a component. The elastic modulus of concrete in compression varies from 14 x 10^3 to 40 x 10^3 MPa (2 x10^6 to 6 x10^6 psi) [43]. The significance of the elastic limit in structural design lies in the fact that it represents the maximum allowable stress before the material undergoes permanent deformation. The elastic modulus of the material influences the rigidity of the design.

However, due to concrete non-linearity, three methods are used to compute the modulus giving rise to three types of moduli. These are the tangent modulus given by the slope of a line drawn tangent to the stress-strain (σ-ε) curve at any point on the curve, secant modulus given by the slope of a line drawn from the origin to a point on the curve corresponding to a 40% stress at failure load and chord modulus given by the slope of a line drawn between two points on the σ-ε curve. The chord modulus was used in the calculations by shifting the base from the origin to correct the slight concavity observed at the beginning of the σ-ε curve up to a point about 40% of the stress at failure. Table 4.2 summarizes the computed results for elastic modulus.

Table 4.2: Calculated Elastic Modulus, Splitting Tensile Strength, Flexural Strength, Peak Bond Stress and calculated area under stress-strain plots for the Control and TDA concrete with and without silica fume

	Elastic Modulus , psi (MPa)		
Component	Control-0% TDA	7.5% TDA -1"	7.5% TDA -1"-SF-A
At 28 days	3.35E+06 (2.31E+04)	2.72E+06 (1.88E+04)	2.69E+06 (1.85E+04)
At 7 days	2.69E+06 (1.85E+04)	2.37E+06 (1.63+04)	2.13E+06 (1.85E+04)
	Splitting Tensile Strength , psi (MPa)		
At 28 days	466 (3.2) ±7.9%	525 (3.6) ±7.2%	
At 7 days	466 (3.2) ±17%	431 (2.97) ±6%	
	Flexural Strength (Modulus of Rupture) , psi (MPa)		
At 28 days	570 (3.93) ±10.7%	535 (3.69) ±2.7%	480 (3.31) ±6.9%
At 7 days	602 (4.2) ±10%	550 (3.8) ±7%	464 (3.2) ±12%
	Pull-Out Test Peak Bond Stress , psi (MPa)		
At 28 days	1929 (13.3) ±12.3%	1890 (13.0) ±14.3%	
	Calculated Area under stress-strain plots representing concrete toughness		
At 28 days	75.7±31%	215±29%	154±15%

From Table 4.2 it is found that use of TDA in concrete would lower the elastic modulus of concrete by about 20%. Güneyisi et al [20] also in their study indicated that there is a large reduction in the strength and modulus values with the increase in rubber content in concrete. A steep slope of the stress-strain curve, thus a high modulus of elasticity means that a greater force is required to stretch bonds hence higher binding energy. A lower modulus of elasticity in concrete containing TDA could then signify low binding energy (weak bonds) between TDA particles and the rest of the concrete components. It could also mean a higher porosity in concrete with TDA.

However if a stress of 3000 psi is applied to each material, the concrete without TDA deforms elastically to a maximum of 0.001 in./in. while the concrete with TDA would deform

elastically to a minimum of 0.00125 in./in. as shown Figure 4.2 and Figure 4.3 Therefore concrete with TDA would deform elastically 20% more compared with concrete without TDA.

4.6 Behavior of Concrete under Uniaxial Compression

Generally, the stress-strain curve shows a linear –elastic behavior up to about 30% of the ultimate strength, f'c, because under the short-term loading the micro-cracks in the interfacial transition zone remain undisturbed. For stresses above this point, the curve shows a gradual increase in curvature up to about 0.75 f'_c to 0.9 f'_c then it bends sharply (almost becoming flat at the top) and finally, descends until the specimen is fractured [43].

Concrete contains void spaces of various sizes and shapes in the matrix and microcracks at the interfacial zone therefore failure modes vary with the type stress. In uniaxial compression, as stress increases, cracks are initiated within the matrix; their number and size increases progressively. Eventually cracks in the matrix and the interfacial transition zone (shear-bond cracks) eventually join up, and generally a failure surface develops at about 20° to 30° from the direction of the load. Figure 4.4 show failure modes for control concrete (Control-0%TDA). Generally the fracture line is straight and runs through the specimen.

However, as seen from Figure 4.5, TDA concrete (7.5%TDA -1") fracture line can be up to 45° from the direction of the load, not straight and does not run through the specimen. This may explain why the TDA concrete does not have a brittle failure like the control concrete in Figure 4.4. Khaloo et al [22] also demonstrated a significant decrease in the brittle behavior of concrete with increasing rubber content and unlike plain concrete, the failure state in rubberized concrete occurred gently and uniformly, and did not cause any separation in the specimen.

The difference between the two concretes was the amount of course aggregates. One had part of coarse aggregates replaced by TDA. The difference in behavior of the two concretes is thought to have been caused by changes in the interfacial transition zone characteristics due to the different size, shape and surface texture of the aggregate particles therefore affecting the concrete strength and failure modes. It is also believed that due to the smooth surface of TDA

particles, a weak physical bond between TDA particle and the hydrated cement particle is formed which is responsible for the lower strength of TDA containing concrete.

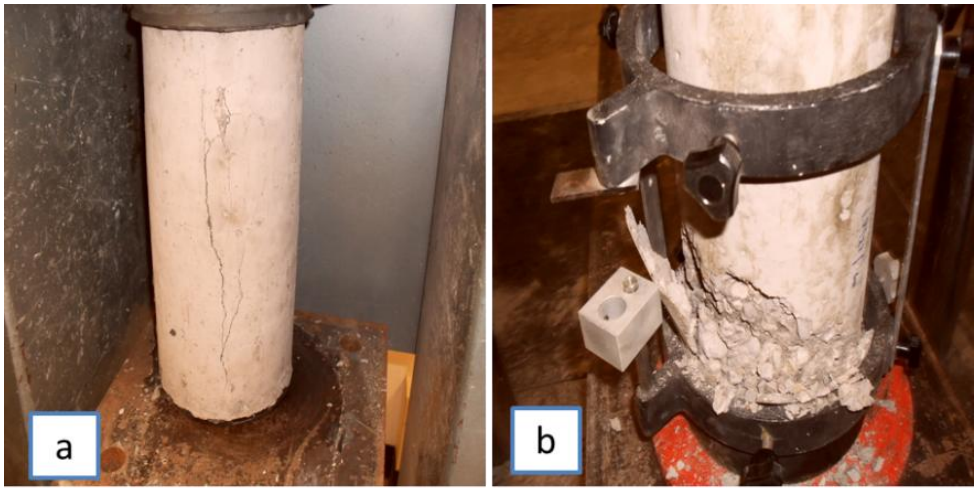

Figure 4.4: Control-0% TDA Concrete failure patterns. (a) The fracture line was generally parallel to the loading direction (b) failure was catastrophic.

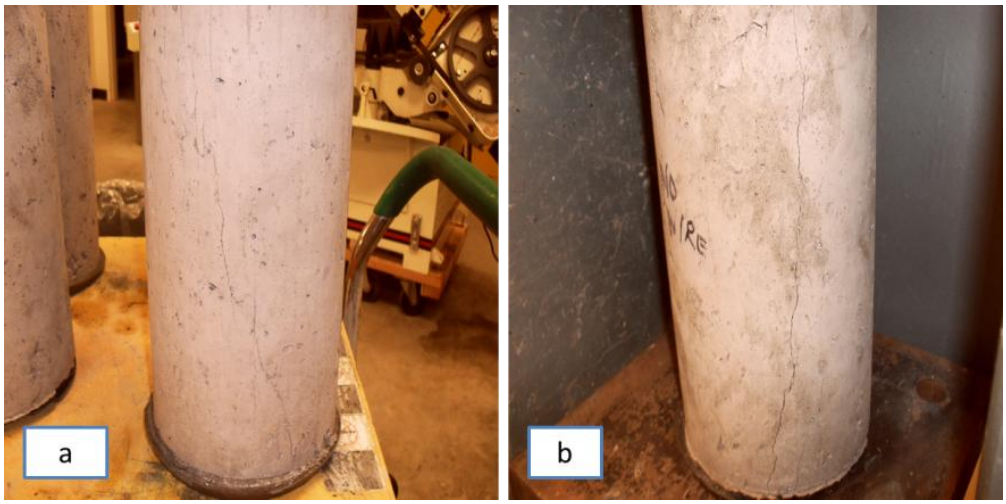

Figure 4.5: 7.5% TDA -1" Concrete Failure Patterns.(a) The fracture line was generally at an angle to the loading direction (b) Failure was not catastrophic

Two characteristics of aggregates have an important influence on proportioning concrete mixtures. These are grading (particle size distribution) and nature of the particle (shape, porosity, surface texture). The aggregates are predominantly responsible for the unit weight, elastic modulus and dimensional stability of the concrete. These properties of concrete depend to a large

extent on the bulk density and strength of the aggregate, which in turn are determined by physical rather than chemical characteristics of the aggregate. Grading is important for attaining an economical mixture because it affects the amount of concrete that can be made with a given amount of cement and water.

4.7 Splitting Tensile Strength of Cylindrical Concrete

Table 4.2 summarizes the results for splitting tensile strength. From the results it seen that the average splitting strength for the control batch was 466 psi (3.2 MPa) while the batch with 7.5% of coarse aggregates replaced with an equal volume of TDA was 525 psi (3.6 MPa). This represents 12.7% improvement in splitting tensile strength at 28 days.

Another important consideration in the testing of concrete mixes is the percent a particular strength parameter compares to the 28-day design compressive strength, f ′c. The standard by which all concrete strengths are compared is that of f ′c for the identical mix, cured under the identical conditions, and at the same age. For the two batches, the control batch developed an average of 10.4% of f ′c while the batch with 7.5% of coarse aggregates replaced with an equal volume of TDA developed 13.1% of f ′c. f ′c was taken to be 4500 psi (≈31 MPa) for control concrete and 4000 psi for TDA concrete.

At 7-days (early strength), the average splitting strength for the control batch was also 466 psi (3.2 MPa) while the batch with 7.5% of coarse aggregates replaced with an equal volume of TDA was 431 psi (3.0 MPa). This represented 7.6% drop in splitting tensile strength for the batch with TDA compared with the control batch at 7 days. Generally, splitting tensile strength is used in the design of structural lightweight concrete members to evaluate the shear resistance provided by concrete and to determine the development length of reinforcement. From the results at 28 days, it was concluded that in this respect, the TDA concrete would perform satisfactorily or superior to the control concrete in the long time.

As seen from Figure 4.6, the control concrete (Control-0% TDA) developed a single fracture line which ran through the specimen while the TDA concrete (7.5% TDA -1") developed

multiple fracture lines which were not joined as loading was increased probably due to the presence to TDA particles between the fracture lines. This may explain the superior performance noted for TDA concrete in terms of ultimate splitting tensile test.

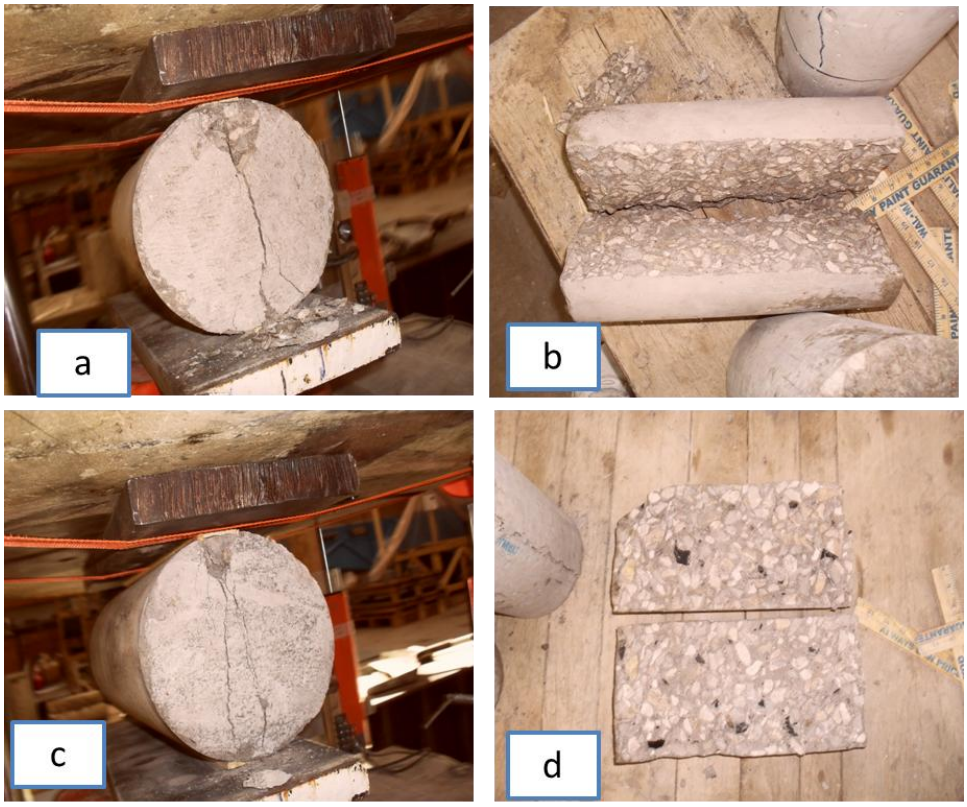

Figure 4.6: (a) and (b) Failure Pattern for Control-0% TDA. Single fracture line cutting through the specimen is noted. (c) 7.5% TDA -1" during splitting tensile test showing multiple fracture lines. (d) Distribution of TDA in the 7.5% TDA -1" concrete.

4.8 Flexural Strength (Modulus of Rupture) of a Concrete Beam

Table 4.2 summarizes the results for the flexural strength of a concrete beam with loading at the third point at 7 and 28 days after casting.

The tests at 28 days of flexural strength of a concrete beam with loading at the third points show the Control Concrete (Control-0% TDA) having an average modulus of rupture of 570 psi (3.93 MPa) while the batch with 7.5% of coarse aggregate replaced with TDA (7.5% TDA -1"-SF-A) having a modulus of rupture of 480 psi (3.31 MPa) for the batch which included silica fume, while the batch which did not include silica fume (7.5% TDA -1") developed a modulus of

rupture of 535 psi (3.69 MPa). This represented a drop of 15.8% and 6.1% for TDA concrete with and without silica fume respectively. At 7 days, this was drop was 22.9% and 8.6% drop from the control batch respectively.

Figure 4.7 show the fracture lines for TDA concrete and control concrete during flexure test respectively. The fracture line for control concrete was found to be straight (follow the loading direction) and the specimen failed completely into two halves. The TDA concrete fracture line did not follow the loading direction and the specimen did not fail completely into two halves. This was found to be due to the cracks not being able to cut through the TDA particles. This could be an advantage in structures in avoiding catastrophic failures.

A plot of Modulus of Rupture (psi/MPa) against displacement (in/mm) is shown in Figure 4.8 comparing the control concrete and TDA concrete. The displacement for TDA concrete is average 50% higher than the control concrete even though the modulus of rupture is low. This is a good indication of improved concrete ductility.

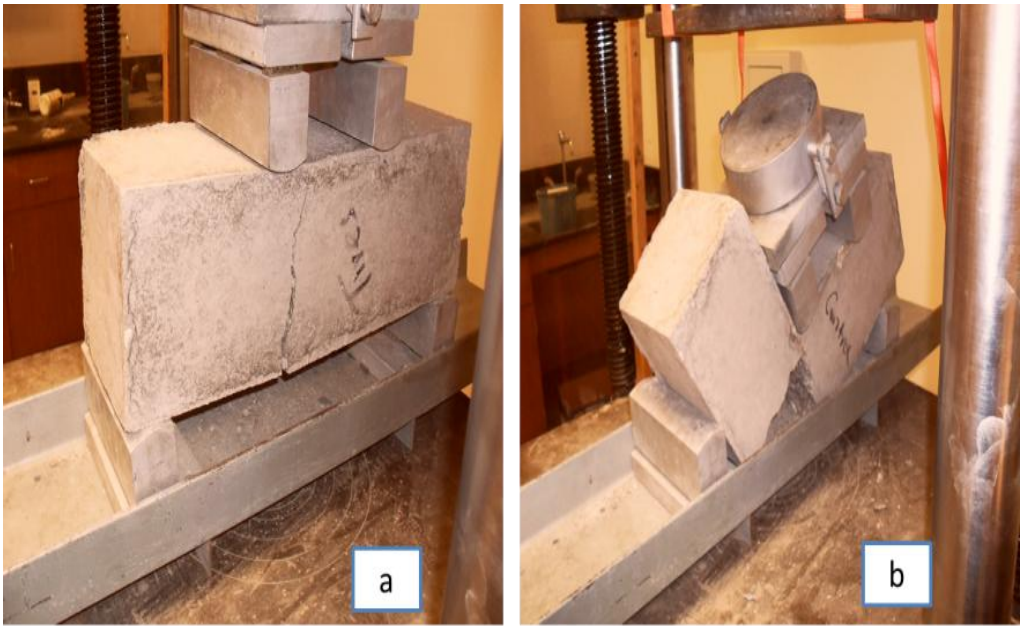

Figure 4.7: (a) Failure pattern for 7.5% TDA -1" concrete beam. The beam did not fail into 2 halves and fracture line was not parallel to loading direction (b) Failure pattern for Control-0% TDA concrete beam. The beam failed into 2 halves and fracture line was parallel to loading direction.

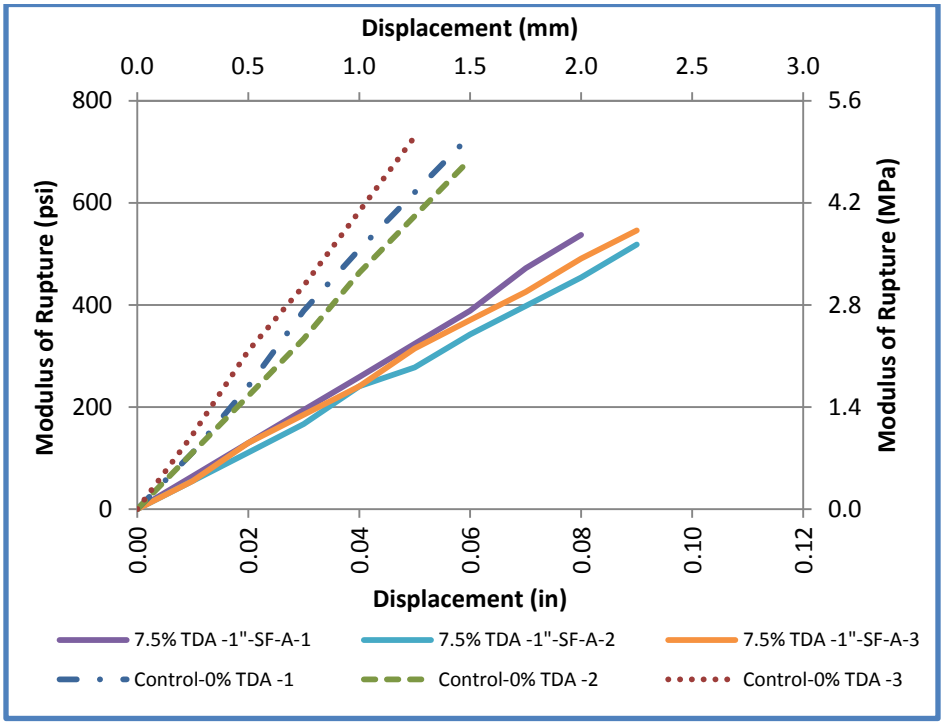

Figure 4.8: Comparison of Modulus of Rupture between the control concrete (Control-0% TDA) and TDA concrete with silica fume (7.5% TDA -1"-SF-A)

4.9 Pull-Out Test

The calculated peak bond stress results from the pull-out test are as shown in Table 4.2. Overall there was a difference of 2% between the averages of the control specimen and the specimen with TDA. This difference is small and can be considered to be within experimental error. This implies that using TDA in concrete would not affect negatively the bond strength of reinforcing rods in concrete. Observation of failure patterns in Figure 4.9 for control concrete and TDA concrete show that TDA would prevent widening of cracks and hence prohibit catastrophic failure.

A plot of the bond stress against rebar slip is shown in the Figure 4.10 for the two types of concrete. Average re-bar slip for the four control concrete specimen is 0.29 in (7.4mm) while that of TDA is 0.39 in (9.9mm) representing an increase of 37%. Since the calculated bond strength represent the adhesion of the paste to the steel, the friction between the steel and the

concrete, and the bearing of the concrete against the lugs of the deformed steel bars it therefore means that TDA would lower these properties hence the increased re-bar slip.

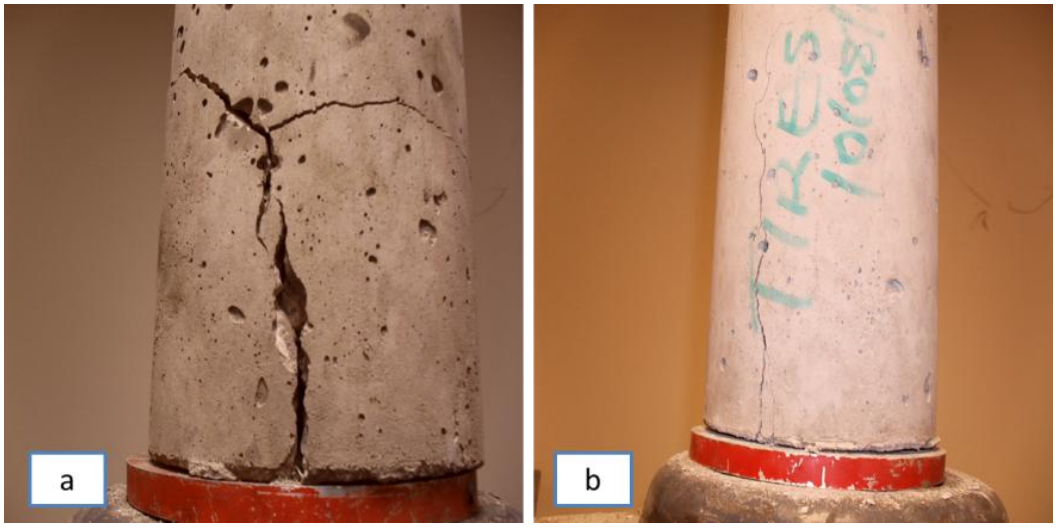

Figure 4.9: (a) Failure Pattern for Control-0% TDA concrete (b) 7.5% TDA -1" Concrete Failure Pattern during pull-out test. Wide and multiple cracks are noted in the Control-0% TDA concrete while a single crack forms in 7.5% TDA -1" concrete.

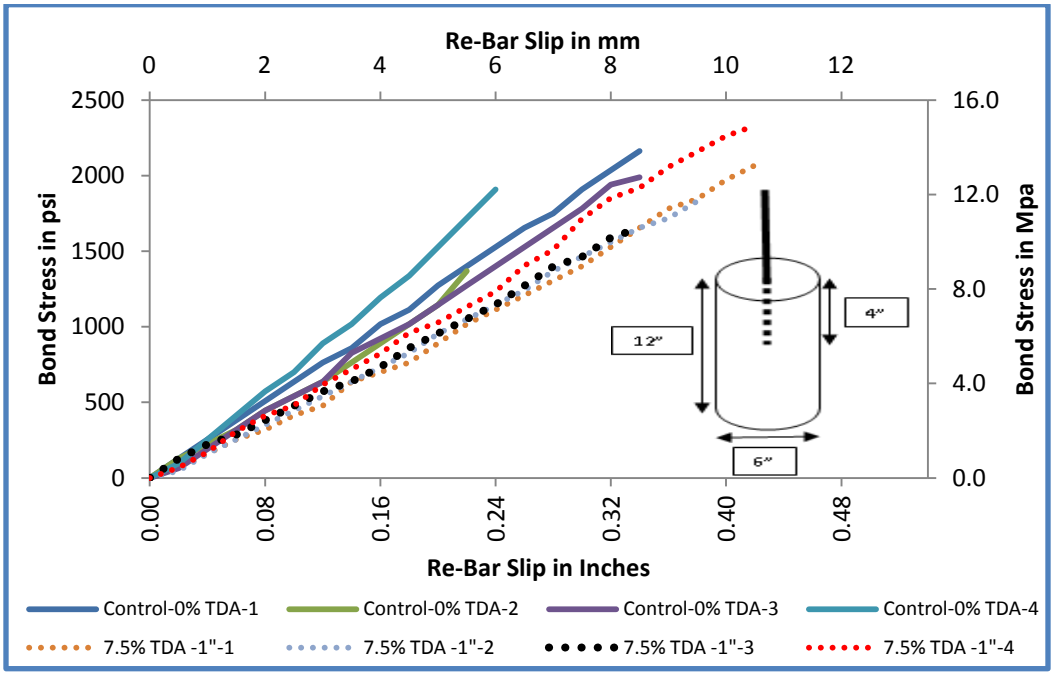

Figure 4.10: Comparison of Bond stress against Re-Bar slip for Control-0% TDA and 7.5% TDA -1" at 28 days.

4.10 Conclusion

Small amounts of waste tires (TDA) in the range of 7.5% to 10% can be used in concrete with a target compressive strength of up to 4000 psi but strength enhancing materials like silica fume need to be used. As TDA increase, the compressive strength drops. At 7.5% of TDA replacing coarse aggregates, this drop is found to be averagely 10% compared to the control concrete if silica fume is added into the mixture. However, this amount of strength can also be achieved without using strength enhancing materials (silica fume) if the top TDA size is lowered from 2 in to 1 in.

Using TDA to substitute for mineral aggregates lowers the modulus of elasticity of concrete by about 20% but increases the concrete toughness and ductility. However silica fume, as much as it increases compressive strength and consistency, has a negative effect to ductility. Workability of fresh concrete with TDA is slightly better as it has a slump of averagely 1 in. higher compared to the control concrete. However if a stress of 3000 psi is applied to each material, the concrete without TDA deforms elastically to a maximum of 0.001 in./in. while the concrete with TDA would deform elastically to a minimum of 0.00125 in./in. Therefore concrete with TDA would deform elastically 20% more compared with concrete without TDA.

TDA lowers the modulus of rupture of concrete but it increases displacement up to 50% (improved concrete deformation) during loading. The splitting tensile strength improves by 12.7% with introduction of TDA into concrete. The bond strength of the TDA concrete is not significantly different from that of the control concrete but TDA improves post cracking behavior of the concrete as noted from the pull-out tests.

CHAPTER 5

EFFECT OF CRUMB RUBBER IN CONCRETE

5.1 Workability

Workability of a freshly mixed concrete was evaluated through slump measurement as outlined in ASTM C143 [35]. Table 5.1 shows results of slump measurements for the different batches that were prepared at the same water/cement ratio. For the batches that contained silica fume, the silica fume was considered a cementitious material and included in calculating the total water requirement.

The results show that Crumb Rubber improves concrete workability slightly since the slump recorded was higher by between ¼" to ½" compared to the control concrete (0%Crumb). Khaloo [22] also reports that fresh rubberized concrete exhibited lower unit weight and acceptable workability compared to plain concrete when rubber particles that had Sieve residue on mesh 60 (0.25mm) of 80% were used to replace 12.5%, 25%, 37.5%, and 50% of the total mineral aggregate's volume in concrete.

The slump test is considered to be a measure of the shear resistance of concrete to flowing under its own weight. Therefore the amount of mechanical work or energy required to produce full compaction of the concrete containing Crumb Rubber without segregation would be less as compared to the control concrete. It also implies that the concrete with Crumb Rubber would be more consistent, easy to flow, pump and compact when shaping the fresh concrete into desired shapes during construction.

5.2 Compressive Strength

Average compressive strength tests results for the 6in x 12in (150 mm x 300 mm) concrete cylinders based on ASTM C39 are shown in Table 5.2. Figure 5.1 shows the variability of compressive strength within specimens of the same batch and comparisons between different batches.

The results Table 5.2 shows that up to 15% of fine aggregates can be replaced with an equal volume of Crumb Rubber in a concrete mix without affecting the compressive strength of the concrete. Addition of silica fume to the control concrete would improve the compressive strength by 16% at 7 days and 10% at 28 days. However addition of both Silica Fume and Crumb Rubber improves the concrete strength by 22% at 7 days and 20% at 28 days. Keeping the Silica Fume constant, the Crumb Rubber improves the strength by 5% at 7 days and 9% at 28 days.

In conclusion, Crumb Rubber can be used as a light aggregate substitute for the fine aggregates in concrete. Up to 15% of fine aggregate can be replaced without any loss in strength by Crumb Rubber and the resulting concrete would have better damage tolerance properties as shown in Figure 5.2 and Figure 5.3. Topçu and Demir [30] in their study with concrete specimens where 0, 10, 20, and 30% rubber aggregate in volume, with the grain size of 1–4 mm replaced fine aggregate concluded that in the regions where the environmental conditions are not harsh, use of concrete produced with 10% rubber aggregate is appropriate as it is economical and an effective way of recycling the discarded tires.

However, Khaloo [22] reports reductions in the strength and tangential modulus of elasticity when he used rubber particles with Sieve residue on mesh 60 (0.25mm) of 80% to replace 12.5%, 25%, 37.5%, and 50% of the total mineral aggregate's volume in concrete in a uniaxial compressive strain control test conducted on hardened concrete specimens.

Table 5.1: Slump measurements for the different batches with crumb rubber

Description of Type of Concrete	Control	7.5% Fine Aggregate Replaced With Crumb Rubber	15% Fine Aggregate Replaced With Crumb Rubber	Control With addition of Silica Fume	7.5% Fine Aggregate Replaced With Crumb Rubber With Addition of Silica Fume	7.5% Fine Aggregate Replaced with Crumb Rubber and 7.5% Coarse Aggregate Replaced with TDA
Designation	0%Crumb	7.5%Crumb	15%Crumb	0%Crumb-SF	7.5%Crumb-SF	7.5%Crumb+7.5%TDA
Water/Cementitious material Ratio	0.55	0.55	0.55	0.60	0.60	0.55
Slump , inches (mm)	1 (25.4)	1 ½ (38.1)	1 ¼ (31.2)	2 (50.4)	3 (76.2)	1 ½ (38.1)

Table 5.2: Compressive Results Summary

	0%Crumb	7.5%Crumb	15%Crumb	0%Crumb-SF	7.5%Crumb-SF	7.5%Crumb+7.5%TDA
	psi (MPa)	psi (MPa)	psi (MPa)	psi (MPa)	psi (MPa)	psi (MPa)
7 Day Average Strength (psi)	4018 (27.7)	4184 (28.8)	4129 (28.5)	4672 (32.2)	4883 (33.7)	3200
28 Day Average Strength (psi)	4613 (31.8)	4890 (33.7)	4615 (31.8)	5096 (35.1)	5530 (38.1)	4108

Table 5.3: Modulus of Toughness and Modulus of Elasticity for different types of concrete

	0%Crumb-SF	7.5%Crumb-SF	0%Crumb	7.5%Crumb	15%Crumb
	psi (MPa)	psi (MPa)	psi (MPa)	psi (MPa)	psi (MPa)
Modulus of Toughness	210 (1.45)	323 (2.23)	110 (0.76)	173 (1.19)	126 (0.87)
Modulus of Elasticity	3,665,000 (25,269)	2,410,000 (16,616)	3,245,000 (22,373)	2,897,000 (19,975)	3,610,000 (24,890)

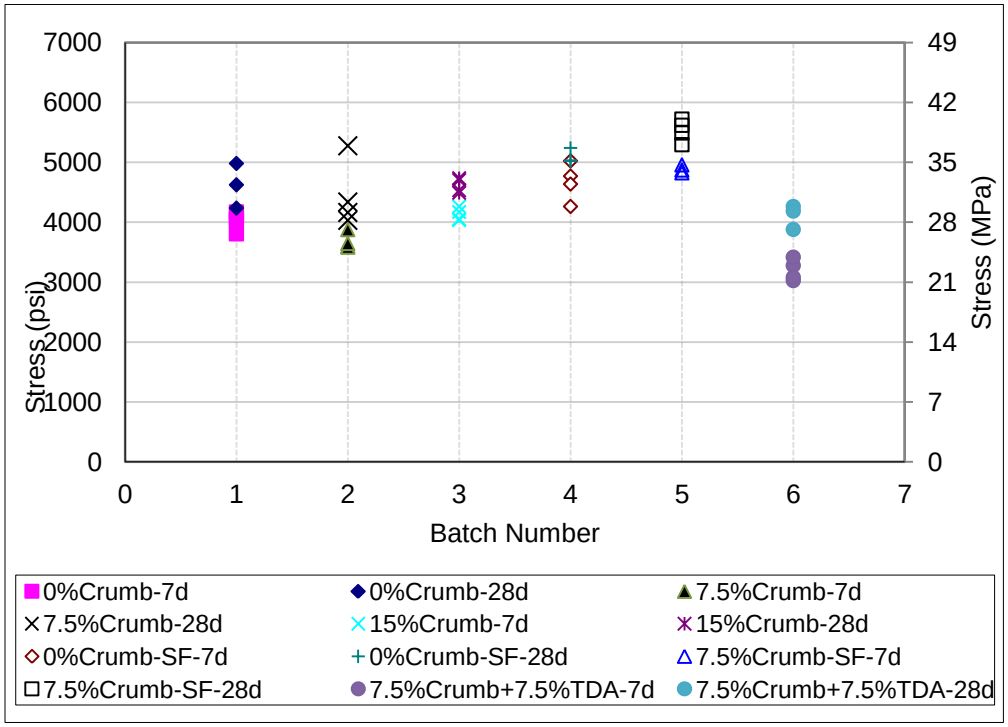

Figure 5.1: Compressive Results Distribution within various specimens in a batch

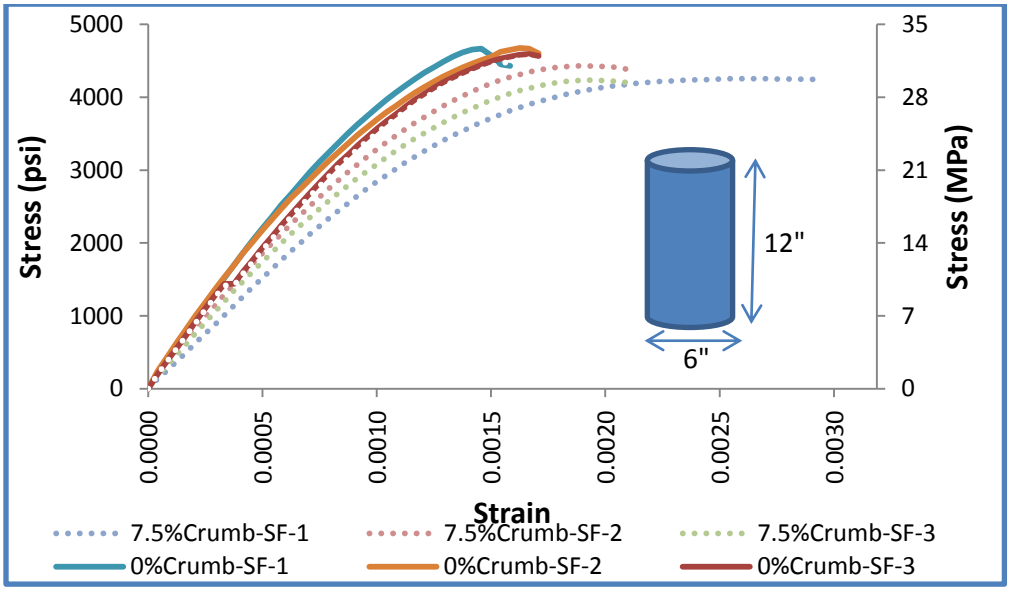

Figure 5.2: Stress vs. Strain Comparison for concrete with 7.5% Crumb with Silica Fume and Control with Silica Fume.

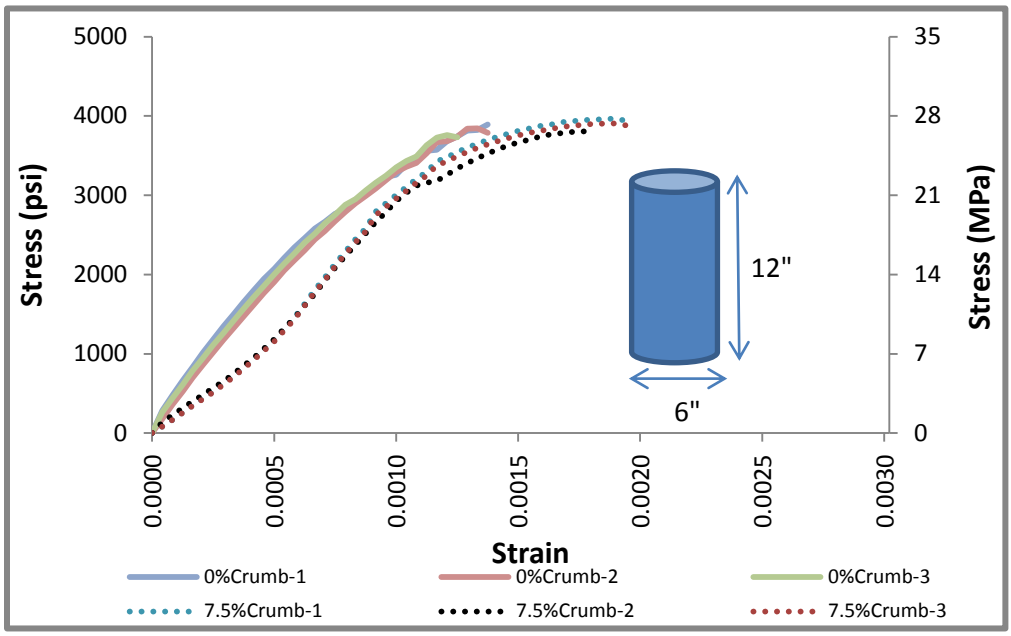

Figure 5.3: Stress vs. Strain Comparison for Control Concrete (0%Crumb) and concrete with 7.5% of fine aggregate replaced by Crumb Rubber (7.5%Crumb).

Ghaly [19] also reports that addition of Crumb Rubber to concrete resulted in a reduced strength as compared with that of conventional concrete and the compressive stress of the concrete decreased with the increase of the rubber content in the mix. In his study Ghaly, added Crumb Rubber in quantities of 5%, 10%, and 15% by volume of the mixture, size between 1 and 2 mm, as replacement of a portion of fine aggregates (sand).

Finally, Güneyisi [20] also reports test results indicating that there is a large reduction in the strength and modulus values with the increase in rubber content and the addition of silica fume into the matrix improved the mechanical properties of the rubberized concretes and diminishes the rate of strength loss.

5.3 Concrete Ductility

Ductility is a measure of the amount of inelastic strain that can occur before failure of a material. Ductility can be quantified by the fracture strain, which is the engineering strain at which a test specimen fractures. Typically under compression, concrete appears to show inelastic strain at fracture of the order of 2 $x10^{-3}$ [43]. Figure 5.2 is a comparison of the stress- strain curves for

control concrete (0%Crumb-SF) and concrete with 7.5% of fine aggregate replaced with Crumb Rubber (7.5%Crumb-SF). Figure 5.3 compares control concrete (0%Crumb) and concrete with 7.5% of fine aggregate replaced with Crumb Rubber (15%Crumb) while Figure 5.4 compares control concrete (0%Crumb) and concrete with 15% of fine aggregate replaced with Crumb Rubber (15%Crumb).

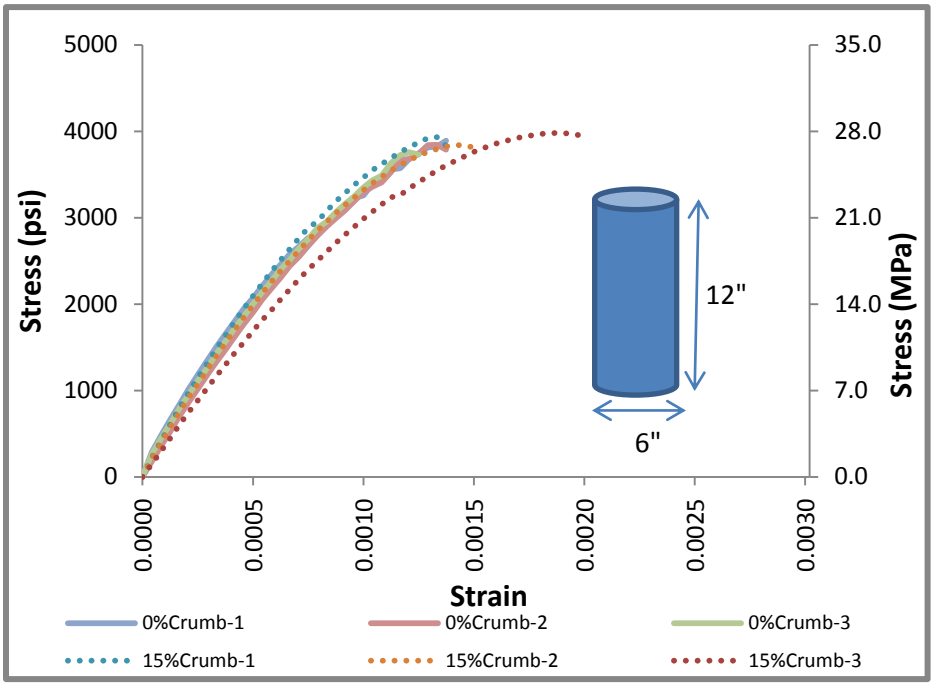

Figure 5.4: Stress vs. Strain Comparison for Control Concrete (0%Crumb) and concrete with 15% of fine aggregate replaced by Crumb Rubber (15%Crumb).

Control concrete has an average strain of 0.0015 at failure while the concrete with 7.5% replacement of fine aggregate by Crumb Rubber has an average strain of 0.0020 at failure. The ultimate failure stress for both concretes (control concrete and concrete with crumb rubber) does not vary by more than 5%. Adding Crumb Rubber to the concrete mixture would increase the strain at failure by about 33% with negligible loss of compressive strength. Strain being a measure of material deformation, it then shows the concrete with Crumb Rubber would experience more deformation before the concrete fails. However the deformation decreases with

increase in quantity of Crumb Rubber used. At 15% replacement, the control concrete and Crumb Rubber concrete strains are averagely equal.

The curves for Crumb Rubber concrete in Figure 5.2 and Figure 5.3 exhibit good energy absorption and ductility as the concrete does not experience the typical brittle failure, but rather a ductile, plastic failure mode. As seen in Figure 5.5, the concrete containing Crumb Rubber does not have excessive cracks running through the concrete. The absence of the cracks running through the concrete explains the increased damage tolerance observed in the stress- strain curves for concrete with Crumb Rubber in Figure 5.2 and Figure 5.3.

Figure 5.5: Fracture of control concrete and concrete with 7.5% Fine aggregate replaced with crumb rubber. From the pictures it is seen that concrete with Crumb Rubber does not have cracks running through the concrete

Khaloo [22] also reports a significant decrease in the brittle behavior of concrete with increasing rubber content (rubber particles with Sieve residue on mesh 60 (0.25mm) of 80%) and unlike plain concrete, the failure state in rubberized concrete occurs gently and uniformly, and does not cause any separation in the specimen.

Yang {{3036 Yang,Linhu 2010;}} while adding Crumb Rubber into reinforced concrete (RC) also found out that the stress-strain relationship of concrete was changed showing improved

sectional ductility of reinforced concrete (RC) beam and ductility of Crumb Rubber Concrete beam was significantly improved.

5.4 Concrete Toughness

Toughness is the amount of strain energy required to break a material and is represented by the area under the curve of the stress-strain plot. The area under the stress-strain curve up to a given value of strain is the total mechanical energy per unit volume consumed by the material in straining it to that value. Calculated average of area under the curves up to fracture in Figure 5.2, Figure 5.3 and Figure 5.4 is summarized in the Table 5.3 and this is termed the Modulus of Toughness with units of pressure (psi or N/m^2) or strain energy per unit volume (Nm/m^3).

At 7.5% replacement, Crumb Rubber improves the Modulus of Toughness by 54% while at 15% the Modulus of Toughness for Crumb Rubber concrete is 15% higher than the control concrete. Therefore addition of Crumb Rubber into the concrete would improve concrete toughness. The high Moduli of Toughness exhibited by Crumb Rubber concrete signify the concrete would show good impact resistance.

5.5 Modulus of Elasticity

The Modulus of Elasticity is the ratio between the stress and the reversible strain. It is a measure of stiffness of a component. The elastic modulus of concrete in compression varies from 14×10^3 to 40×10^3 MPa (2×10^6 to 6×10^6 psi) [43]. The significance of the elastic limit in structural design lies in the fact that it represents the maximum allowable stress before the material undergoes permanent deformation. The elastic modulus of the material influences the rigidity of the design.

In this study, the slope of a line drawn between two points on the stress-strain (σ-ε) curve was calculated. The slope is the young modulus (Modulus of elasticity). The Modulus obtained in this method is also referred as the chord modulus. The base was shifted from the origin to correct the slight concavity observed at the beginning of the σ-ε curve up to a point about 40% of the stress at failure.

Table 5.3 summarizes the computed results for elastic modulus. It is shown that at 15% Crumb Rubber replacement, the concrete with Crumb Rubber has the modulus of elasticity which is 11% higher than the control. However when comparing the two concretes with silica fume, the Crumb Rubber modified concrete has an elastic modulus which is 34% less when compared with the control which also contains silica fume. Silica fume has been shown to increase compressive strength (Table 5.2) and as seen in Figure 5.6 it also increases the modulus of elasticity. Generally, the modulus of elasticity increases with increasing strength.

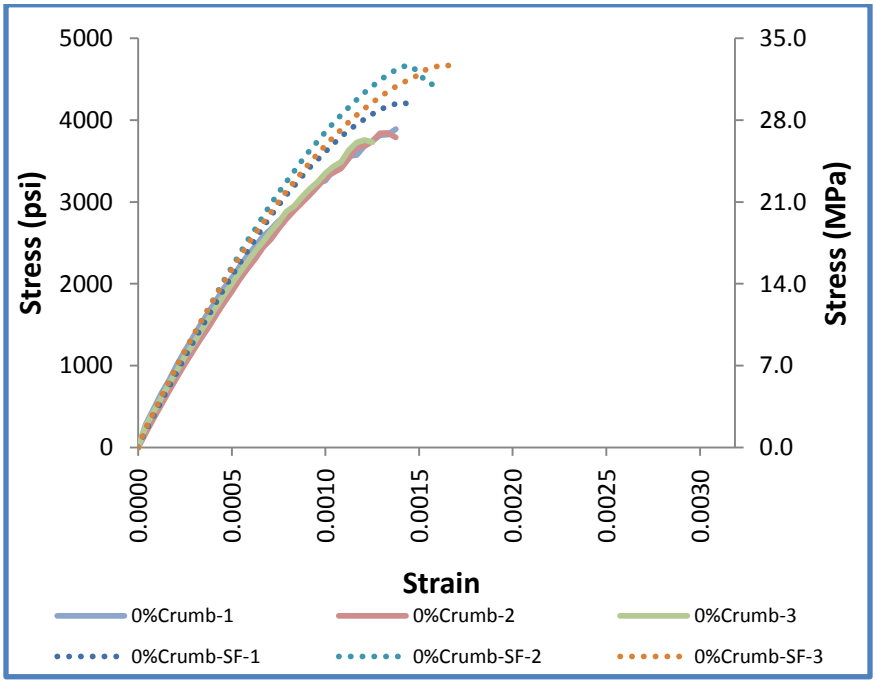

Figure 5.6: Stress- strain curves showing the effect of Silica Fume in concrete.
Note the increase in compressive strength and shift in slope (Modulus of elasticity)

5.6 Splitting Tensile Strength of Cylindrical Concrete

The splitting tensile test is an indirect evaluation of direct tensile strength of concrete. Table 5.4 is a summary of the results for splitting tensile strength for different quantities of crumb rubber. It is seen that splitting tensile strength decreases with an increase in quantity of Crumb Rubber used.

Table 5.4: Splitting Tensile Strength of different types of concrete with varying amount of crumb rubber

	Peak Splitting Tensile Strength		
	0%Crumb psi (MPa)	7.5%Crumb psi (MPa)	15%Crumb psi (MPa)
Average Tensile strength at 28 days	415 (3.1)	370 (2.5)	309 (2.1)

However, the standard by which all concrete strengths are compared is that of 28-day design compressive strength, f ′c for the identical mix, cured under the identical conditions, and at the same age therefore percent of splitting strength is compared to the 28-day f ′c. For the two batches, the control batch developed an average of 8.1% of f ′c while both batches with Crumb Rubber developed splitting strength equivalent to 6.7% of f ′c. The values of f ′c are as shown in Table 5.2.

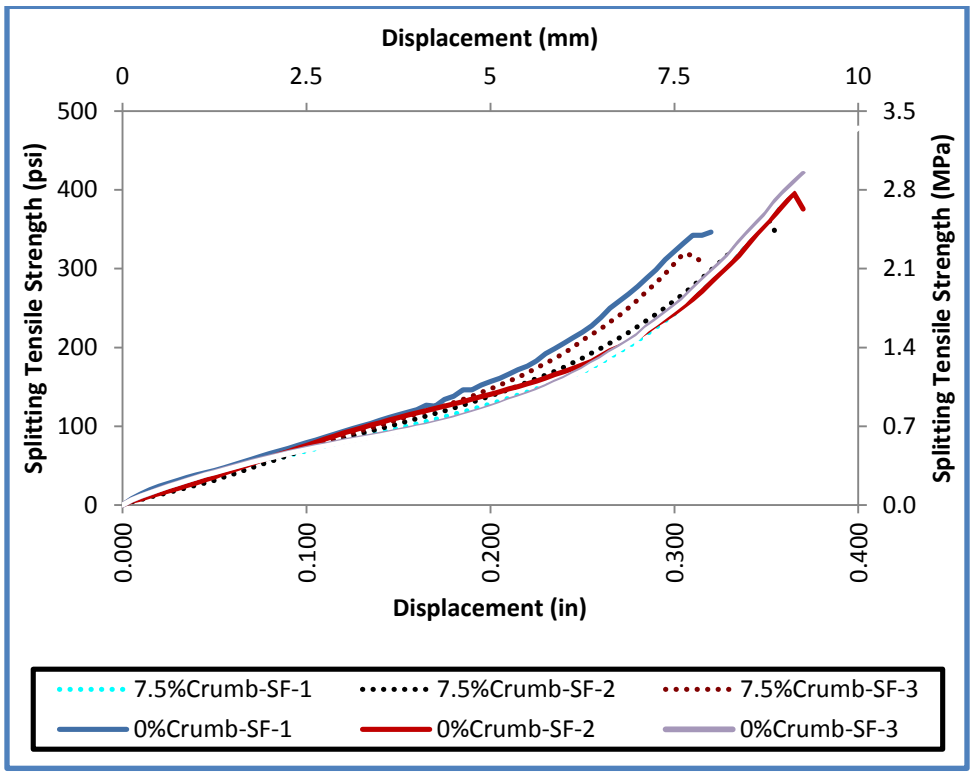

Figure 5.7: Splitting Tensile Strength vs. Displacement Comparison between Control Concrete and Concrete with 7.5% Fine Aggregates replaced by Crumb Rubber

Figure 5.7 shows the stress-displacement plot for the control concrete (one without crumb rubber) and one that had 7.5% of fine aggregate replaced with crumb rubber. Both batches contained Silica Fume. It is seen that the maximum displacement for the two concretes is almost equal. However, the concrete with Crumb Rubber showed more uniformity during loading as can be seen from the curves' variability.

5.7 Flexural Strength (Modulus of Rupture) of a Concrete Beam

Table 5.5 summarizes the results for Four Point loading of a concrete beam (ASTM C78) at 7 and 28 days after casting. Flexural strength is expressed in terms of Modulus of Rupture, which is the maximum stress at rupture.

Table 5.5: Flexural strength (Modulus of Rupture) for various types of concretes

	Modulus of Rupture, psi (MPa)				
	0%Crumb	0%Crumb-SF	7.5%Crumb	7.5%Crumb-SF	15%Crumb
7 Days	624 (4.31)	549 (3.79)	557 (3.84)	517 (3.57)	545 (3.76)
28 Days	717 (4.94)	595 (4.10)	640 (4.41)	610 (4.21)	614 (4.24)

Addition of Silica Fume was found to increase compressive strength by 16% at 7 days and 10% at 28 days. However, it was found as shown in Table 5.5 that it has a negative effect on flexural strength. A drop of in flexural strength 12% and 17% at 7 days and 28 days respectively was noticed with addition of Silica Fume. Crumb Rubber addition to the concrete also lowers the modulus of rupture by an average of 12%.

One relationship that has been developed by the American Concrete Institute (ACI) [1] to relate flexural and compressive strengths is shown in Equation (5.1),

$$f_r' = \alpha\sqrt{f_c'}, \qquad where\ \alpha = 7.5 \tag{5.1}$$

Where: $f_r' is\ flexural\ strength\ and\ f_c'\ is\ the\ compressive\ strength$

From experimental data, the flexural strength and compressive strength information has been collected and the two have been used to calculate the proportionality factor, α, in the ACI equation above for various types of concrete. The results for the factor α, is shown in the Figure

5.8. It can be concluded that for different concretes, if the flexural strength is between 500-650 psi, the factor α, would range from 7 to 10.

A plot of Modulus of Rupture (psi) against displacement (in) is shown in Figure 5.10 comparing the control concrete, concrete with 7.5% and 15% of fine aggregate replaced with crumb rubber. It is observed that Crumb Rubber does not have an effect on displacement or deformation of the concrete beam since the maximum displacement for all the concretes is averagely the same.

Generally as seen from Figure 5.9, the concrete beam failure for both concrete with and without Crumb Rubber was similar with both having a straight fracture line and beam dividing into two almost equal halves.

From the flexural results, it is observed that Crumb Rubber would lower the Modulus of Rupture (maximum flexural strength), would have no effect on the maximum deformation the concrete beam would sustain and would not affect the way the concrete would fail (fracture). Since Modulus of Rupture is a measure of concrete ductility, it therefore concluded that Crumb Rubber does not improve concrete ductility.

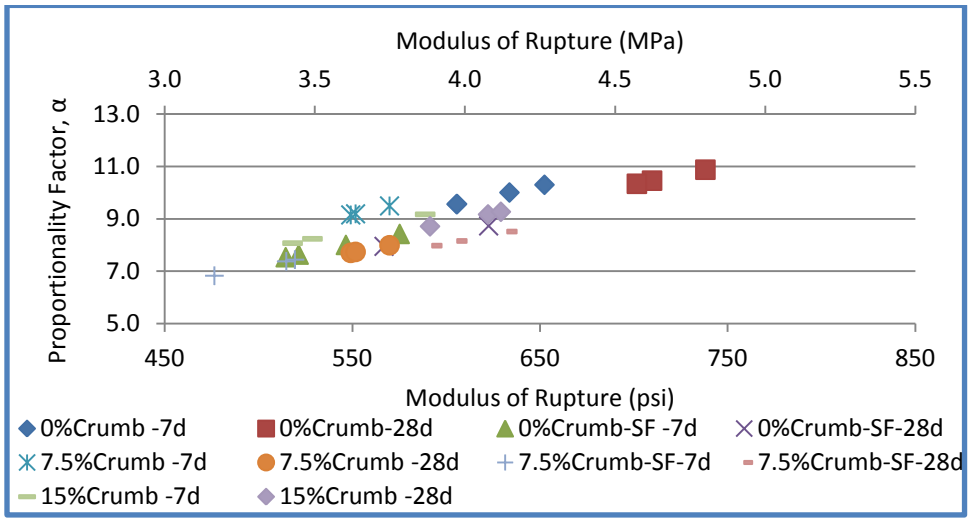

Figure 5.8: Proportionality factor relating flexural strength to compressive strength of various concretes

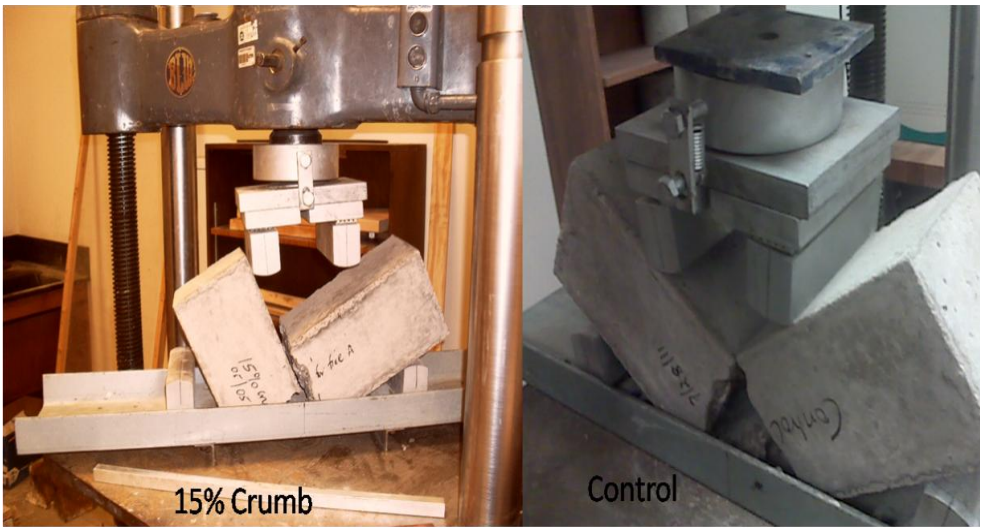

Figure 5.9: Fracture Pattern for control concrete and concrete with Crumb Rubber

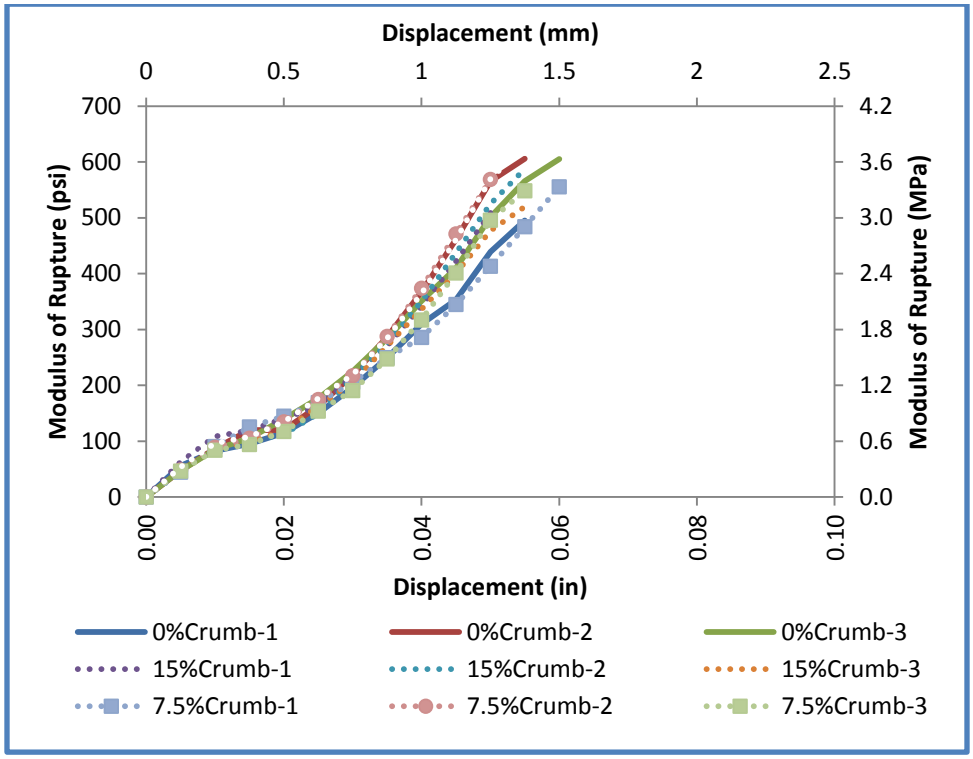

Figure 5.10: Modulus of Rupture of control concrete and concrete with 7.5% and 15% of Fine aggregates replaced with crumb rubber

5.8 Conclusion

It has been shown that up to 15% of fine aggregates can be replaced with an equal volume of Crumb Rubber in a concrete mix without affecting the compressive strength of the concrete. Keeping the Silica Fume constant, the Crumb Rubber improves compressive strength by 5% at 7 days and 9% at 28 days.

Crumb Rubber improves concrete workability slightly since the slump was higher by between ¼" to ½". Adding Crumb Rubber to the concrete mixture would increase the strain at failure by about 33% with negligible loss of compressive strength. Strain being a measure of material deformation, it then shows the concrete with Crumb Rubber would experience more deformation before the concrete fails during compressive loading. However the deformation decreases with increase in quantity of Crumb Rubber used. At 15% replacement, the control concrete and Crumb Rubber concrete strains are averagely equal.

Crumb Rubber concrete exhibits good energy absorption and ductility as the concrete does not experience the typical brittle failure, but rather a ductile, plastic failure mode. At 7.5% replacement, Crumb Rubber improves the Modulus of Toughness by 54% while at 15% the Modulus of Toughness for Crumb Rubber concrete is 15% higher than the control concrete. Therefore addition of Crumb Rubber into the concrete would improve concrete toughness and impact resistance

It is shown that at 15% Crumb Rubber replacement, the concrete with Crumb Rubber has the modulus of elasticity which is 11% higher than the control. However when comparing the two concretes with silica fume, the Crumb Rubber modified concrete has an elastic modulus which is 34% less when compared with the control which also contains silica fume.

However, Crumb Rubber lowers the splitting tensile strength with an increase in quantity of Crumb Rubber used. Crumb Rubber addition to the concrete also lowers the modulus of rupture by an average of 12%.

CHAPTER 6

CONCRETE MICROSTRUCTURE

Concrete is a composite material, however many of its characteristics do not follow the laws of mixtures. For instance, under compressive loading both the aggregate and the hydrated cement paste, if separately tested, would fail elastically, whereas concrete itself shows inelastic behavior before fracture [43]. Likewise, strength of concrete is usually much lower than the individual strength of the two components. Such anomalies in the behavior of concrete can be explained on the basis of its microstructure, especially the important role of the Interfacial Transition Zone (ITZ) between coarse aggregate and the cement paste.

The gross elements of the microstructure of a material can readily be seen from a cross section of the material, whereas the finer elements are usually resolved with the help of a microscope. Microstructure characterization and chemical composition of mortars and aggregates was done by scanning electron microscopy (SEM) and energy dispersive X-ray spectroscopy (EDX) analyses. SEM is useful for the topographic study. Since incident beam can be focused in very small areas, as small as sub-microns, use of SEM in conjunction with x-ray analysis provides quite useful information of materials microstructure. This technique is normally called the Energy Dispersion X-Ray (EDX) technique.

The EDX is a fast method of determining the atomic composition although the outcome of an EDX analysis is semi-quantitative and the values provide the mutual ratio of the selected atoms. It is not an absolute quantitative measurement of the composition, since not all types of atoms are considered. Identification of the components of sand was done using X-Ray diffraction (Powder Method).

Concrete microstructure is heterogeneous and complex and microstructure-property relationship in concrete are not fully developed [43]. However, knowledge of the microstructure

and the properties of each individual components of concrete and their relationship to each other is useful for exercising control on the properties. The strength of the concrete is determined by the characteristics of the mortar, coarse aggregate, and the interface between them.

6.1 Concrete Microstructure Complexities

From examination of a cross section of the Control Concrete (without TDA or Crumb Rubber) in Figure 6.1, the two phases that can easily be distinguished are the aggregate particles of varying size and shape, and the binding medium composed of an incoherent mass of the hydrated cement paste (mortar). However, when Tire Derived Aggregate (TDA and Crumb Rubber) are added to the batch, a third phase that is easily distinguishable as black spots is seen as shown in Crumb Rubber and TDA Concrete in Figure 6.1. This third phase is rubber which is bound to the rest of the concrete with or within the hydrated cement paste.

Figure 6.1: Cross-Sectional view of various types of concretes showing different concrete phases.

At the macroscopic level therefore, Control Concrete is a two-phase material, consisting of aggregate particles dispersed in a matrix of cement paste while TDA Concrete and Crumb

Rubber Concrete is a three-phase material consisting of aggregate and rubber particles dispersed in a matrix of cement paste.

At the microscopic level, the aggregate phase and hydrated cement matrix phase are neither homogeneously distributed with respect to each other, nor are they themselves homogeneous as seen from Figure 6.2. As seen from Figure 6.2 (a), the density and composition within the phase varies across the microstructure. The porosity also varies within the microstructure as seen from Figure 6.2 (b). Variation of density and porosity within the structure would induce variability in response of concrete to applied stress. For example, the modulus of elasticity of cement paste is approximately proportional to the cube root of porosity while it varies directly with density [1]. Within the mortar, the cause of adhesion between the aggregate particles and the hydration products is the van der Waals force of attraction therefore strength of the concrete, especially that of the Interfacial Transition Zone (ITZ) depends on the volume and size of voids present [43].

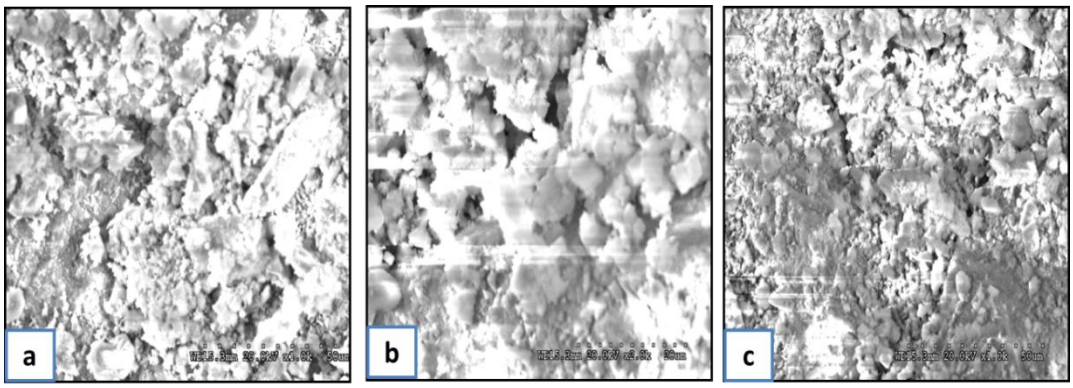

Figure 6.2: (a) Homogeneity within the hydrated cement paste (b) Distribution and porosity within the hydrated cement matrix (c) Micro- cracks within the hydrated cement matrix

Within the microstructure, there exist microcracks which are also responsible for the poor strength of the concrete. Microcracks can exist in the cement matrix (Figure 6.2 (c)), ITZ (Figure 6.3 (a)) or even on the aggregate themselves (Figure 6.4). The amount of microcracks would depend on the aggregate size and grading, cement content, water-cement ratio, degree of

consolidation of fresh concrete, curing conditions, environmental humidity, and thermal history of the concrete [43].

Concrete mixture containing poorly graded aggregate is more prone to segregation during consolidation of fresh concrete thus water films form around the aggregate. The larger the aggregate size, the thicker the water film hence the ITZ formed would be susceptible to cracking when subjected to tensile stresses. TDA has a disadvantage in this respect for being poorly graded and difficult to grade.

The microstructure of hydrated cement paste in the vicinity of large aggregate particles is usually different from the microstructure of bulk paste or mortar in the system as can be seen from Figure 6.3 (a) and Figure 6.4. This region is referred to as the Interfacial Transition Zone (ITZ). The ITZ can be identified by the concentration of oriented calcium hydroxide crystals in the vicinity of the aggregate [1]. Calcium hydroxide (CH) also known as Portlandite is visible as white spots in the cement matrix in Figure 6.5.

The common features of the ITZ are the enhanced porosity and the reduction of unreacted cement near the surface of the aggregate [1]. This is due to the inability of the cement particles to pack efficiently around the aggregate, raising the water/cement ration at the interface, which further increases localized bleeding.

The ITZ is observed in Figure 6.3 (a) to have broken bridges, voids and microcracks. The ITZ thickness is not uniform and can be absent in some sections of the surface. Due to a high volume of voids and microcracks, the ITZ becomes the weakest link of the chain hence the strength limiting phase in concrete. Due to the ITZ the concrete would fail at a lower stress level than the strength of either of the two main components- aggregate and hydrated cement paste- because it would take lower energy levels to extend the cracks already existing in the ITZ.

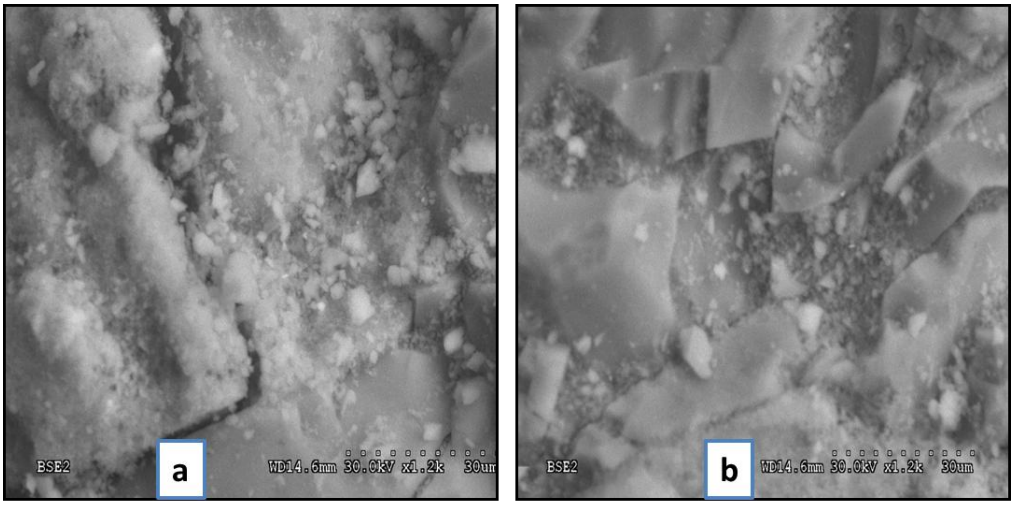

Figure 6.3: (a) Interfacial Transition Zone (ITZ) in concrete and microcracks within the ITZ (b) Monosulfoaluminate crystals formed within the ITZ

The design and attainment of a high strength concrete mixture is therefore made possible by reducing porosity, inhomogeneity and microcracks in the hydrated cement paste and ITZ. Addition of Silica Fume which is a fine pozzolanic material leads to a reduction of the size and quantity of crystalline compounds like calcium hydroxide which consequently reduce the thickness of the ITZ. Crystals of calcium hydroxide or ettringite readily form within the free surface close to the surface of the aggregate [1]. Obstruction by calcium hydroxide crystals may impede complete hydration of cement particles.

The fineness of silica fume also makes it very effective in eliminating bleeding and segregation. In hot, dry weather, bleed water evaporates more quickly than the bleeding rates, which lead to formation of plastic shrinkage cracks. However, silica fume makes the concrete sticky and more difficult to finish and very susceptible to plastic shrinkage cracking.

Within the ITZ, monosulfoaluminate clusters form as irregular plates as seen from Figure 6.3 (b). Monosulfoaluminate is the final product formed after the conversion of ettringite. Ettringite usually grows in capillary pores between cement grains and frequently filling in cracks or voids of mature concretes. This implies a high water-cement ratio (water films) in the vicinity of

the coarse aggregate therefore forming a more porous framework than in the bulk cement paste or mortar mix.

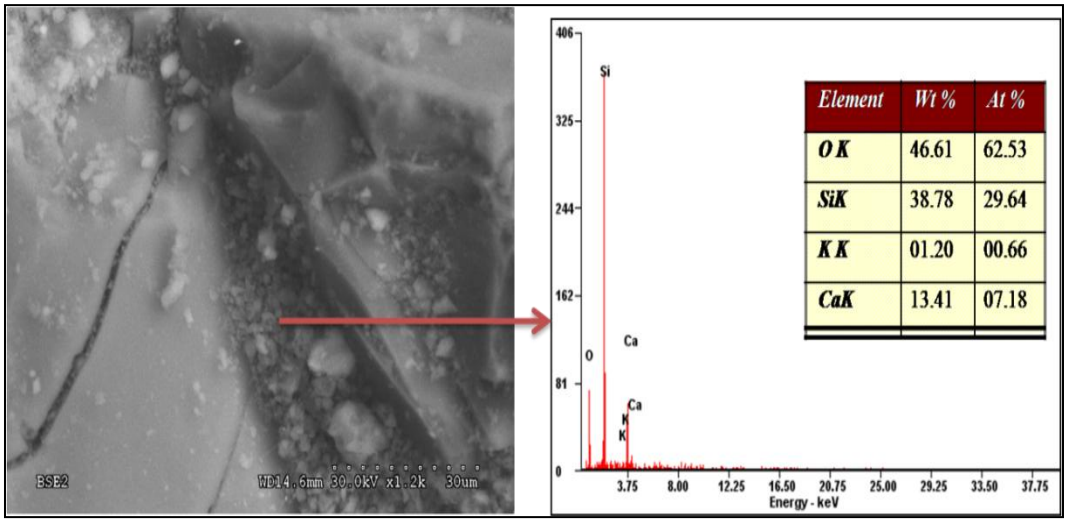

Figure 6.4: Interfacial Transition Zone (ITZ) in concrete and microcracks on the Aggregate phase.

6.2 Microstructure of Aggregate phase

The aggregate phase is predominantly responsible for the unit weight, elastic modulus and dimensional stability of concrete. These properties of concrete depend to a large extent on the bulk density and strength of the aggregates, which in turn are determined by physical characteristics (volume, size, and distribution of pores) rather than chemical characteristics (mineralogical composition) of the aggregate. In addition to porosity, the shape and texture of the coarse aggregate also affect the properties of concrete.

The larger the size of aggregate in concrete and the higher the proportion of elongated and flat particles, the greater will be the tendency for water films to accumulate next to the aggregate face thus weakening the ITZ. As seen from Figure 6.5 and Figure 6.6, the size and distribution of pores across the concrete surface varies widely. Compressive strength and elastic modulus are related to density of the concrete and one factor that affects the density is porosity.

Figure 6.7 (a) shows the bond between the cement paste and the Tire Derived Aggregate (TDA) particle. The interface is shown to be distinct from the rest of the cement paste. The TDA

particle is known to be flat and of lower density compared to the rest of the concrete phases hence susceptible to segregation. Segregation is the separation of components of fresh concrete resulting in non-uniform mix. This may explain the observed variability of properties of concrete when TDA is added to the mix. Increased segregation is observed when the particle shape changes from smooth, well-rounded particles to odd-shaped, rough particles [1].

The physical nature of the response of concrete in compression can be described in terms of microcracks. Figure 6.7 (b) shows microcracks on the aggregate phase. Some of these internal cracks and flaws exist even before loads are applied. These are the bond microcracks. Some of these are beneath large aggregate particles due to segregation and bleeding. As stress on the concrete is increased, the bond microcracking increases while cracks in the mortar begin to form. At approximately 70% of the compressive strength bond cracks bridge with mortar cracks on the aggregate particles leading to concrete failure.

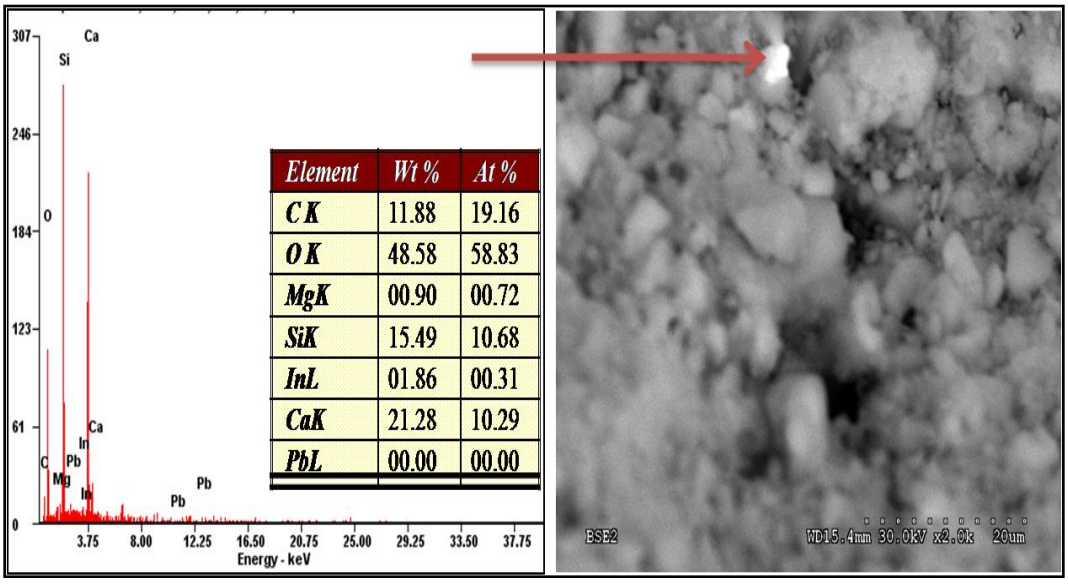

Element	Wt %	At %
CK	11.88	19.16
OK	48.58	58.83
MgK	00.90	00.72
SiK	15.49	10.68
InL	01.86	00.31
CaK	21.28	10.29
PbL	00.00	00.00

Figure 6.5: Pores within the concrete microstructure

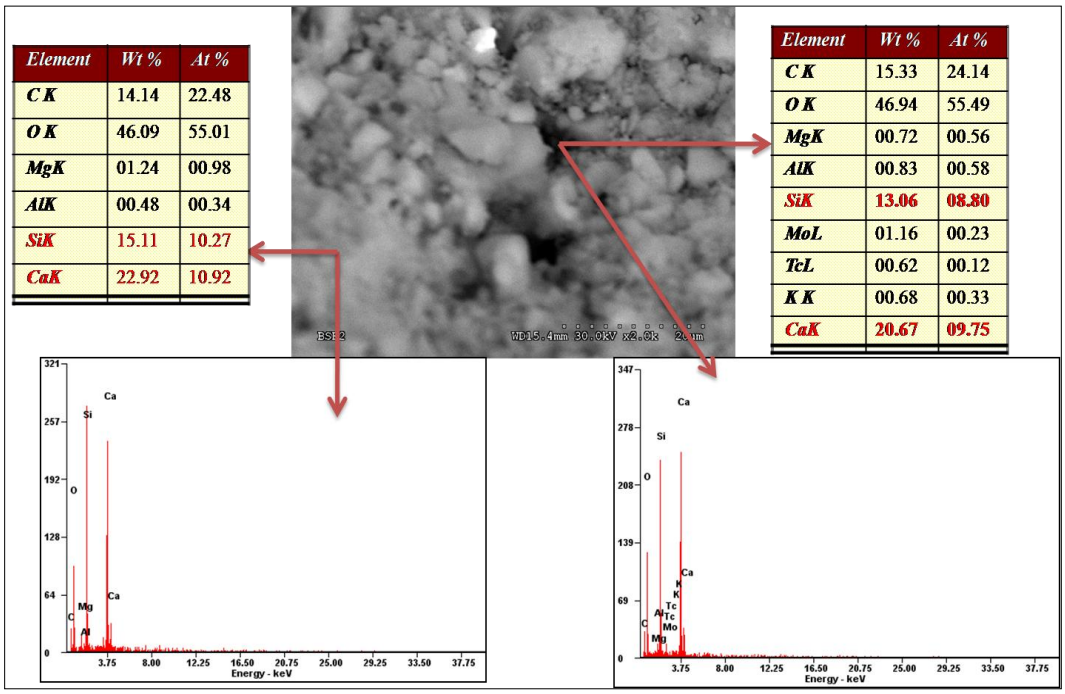

Figure 6.6: Chemistry Pores within the concrete microstructure

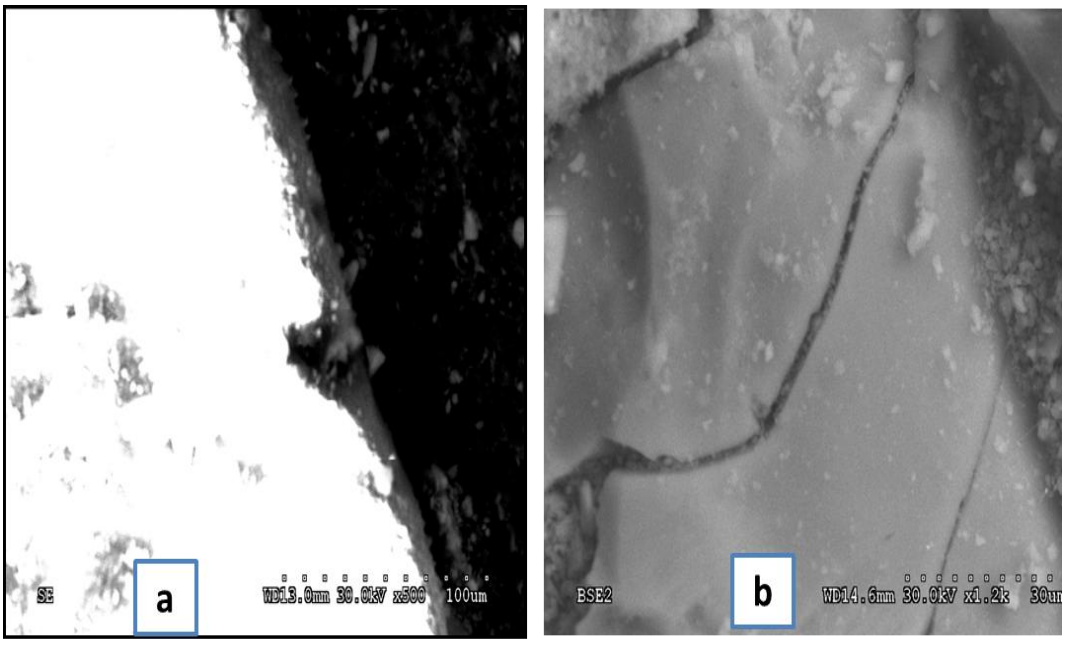

Figure 6.7: (a) Interface between the hydrated paste and TDA particle
(b) Microcracks within the Aggregate particle

6.3 Microstructure of the Hydrated Cement Paste (Mortar)

The hydration process of Portland cement consists of simultaneously occurring reactions of the anhydrous compounds with water since the cement is a heterogeneous mixture of several compounds. All compounds however do not hydrate at the same rate. The aluminates hydrate faster than the silicates and are the ones responsible for the stiffening (loss of consistency) and setting (solidification) characteristics of Portland cement paste. The silicates make up to 75% of ordinary Portland cement and play a dominant role in determining the hardening (rate of strength development) characteristics.

Hydration of aluminates (C_3A and C_4AF) in the presence of gypsum crystallizes into short prismatic needles referred to as ettringite or hexagonal plates known as monosulfate. The reactions of the aluminates are shown in Equation (6.1) and in Equation (6.2). The product formed depends on the concentration of aluminate and sulfate ions in solution. High sulfate/aluminate ratio in solution leads to hydration of ettringite. After depletion of sulfate ions from solution ettringite is converted to monosulfate phase which is the final product of hydration of Portland cements containing up to 5% of C_3A. Cements low in C_3S but high C_4AF are much more resistant to sulfate attack.

$$C_3A + 3C\bar{S}H_2 + 26H \rightarrow C_6A\bar{S}_3H_{32} \quad (6.1)$$

$$C_4AF + 3C\bar{S}H_2 + 21H \rightarrow C_6(A,F)\bar{S}_3H_{32} + (F,A)H_3 \quad (6.2)$$

$$C_3S + 11H \rightarrow C_3S_2H_8 + 3CH \quad (6.3)$$

$$C_2S + 9H \rightarrow C_3S_2H_8 + CH \quad (6.4)$$

Silicates (C3S and C2S) in Portland cement hydrate to produce a family of calcium silicate hydrates which are structurally similar but vary widely in calcium/silica ratio and the content of chemically combined water. The hydration reactions for silicates are shown in Equation (6.3) and Equation (6.4). As seen from Figure 6.8, the calcium silicate hydrate (C-S-H) is poorly crystalline and forms as a porous solid.

Microstructural inhomogeneities as seen from Figure 6.8 (a) and (b), Figure 6.9 and Figure 6.10 can lead to serious effects on strength and other related mechanical properties because these properties are controlled by the microstructural extremes, not by the average microstructure. Because of this, attention should be paid to rheological properties of freshly mixed paste that may influence the microstructure of the hardened paste. Some of factors that may lead to heterogeneous microstructure are local variations of water-cement ratio and flocculation of cement paste.

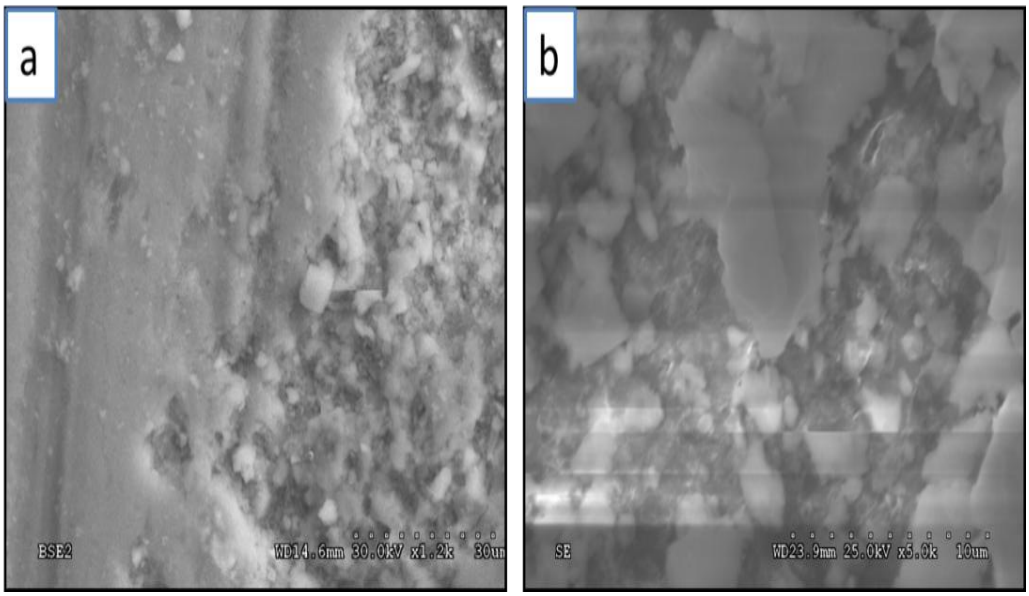

Figure 6.8: Form and structure of the Hydrated Cement Paste Calcium Silicate Hydrate Both (a) and (b) show variations within the cement paste.

Microcracks also exist within the hydrated cement paste system as seen from Figure 6.11 (a). When load is applied to the concrete, these microcracks would increase and propagate within the matrix and join up with the cracks in the interfacial transition zone leading material failure. The rapid propagation of microcracks under applied stress is responsible for the low tensile strength of concrete. The ITZ also exist between the fine aggregate (sand) and the hydrated cement paste as seen from Figure 6.11 (b).

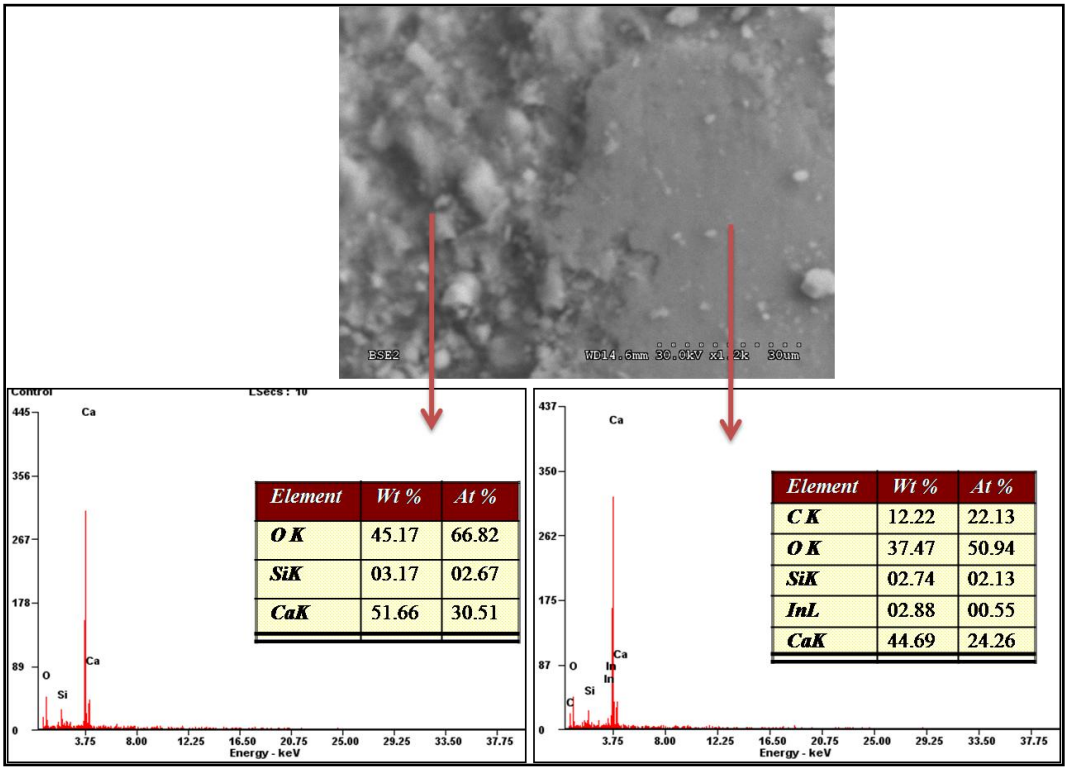

Figure 6.9: Variation of chemistry within the concrete mortar.

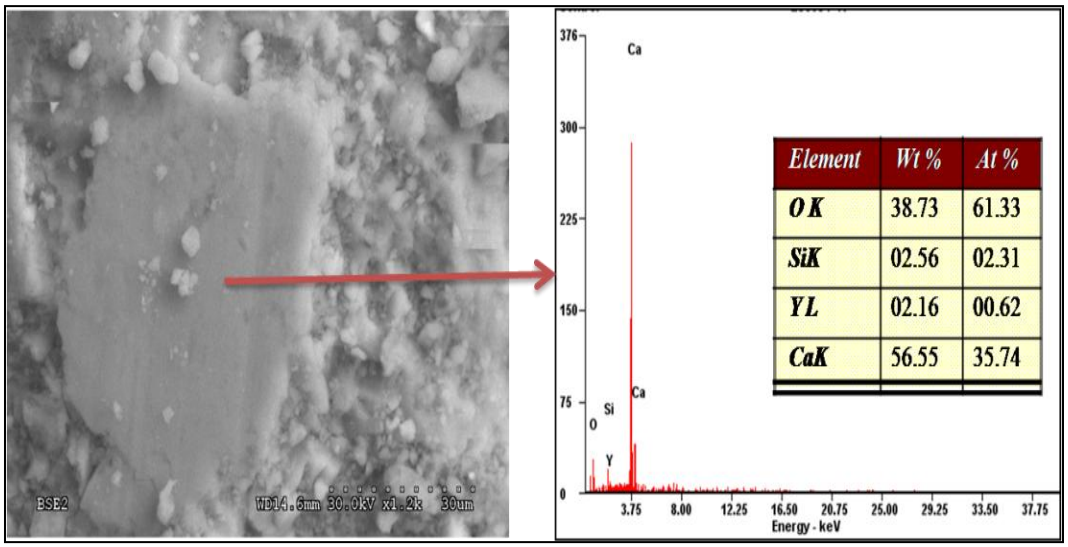

Figure 6.10: Chemistry of grains

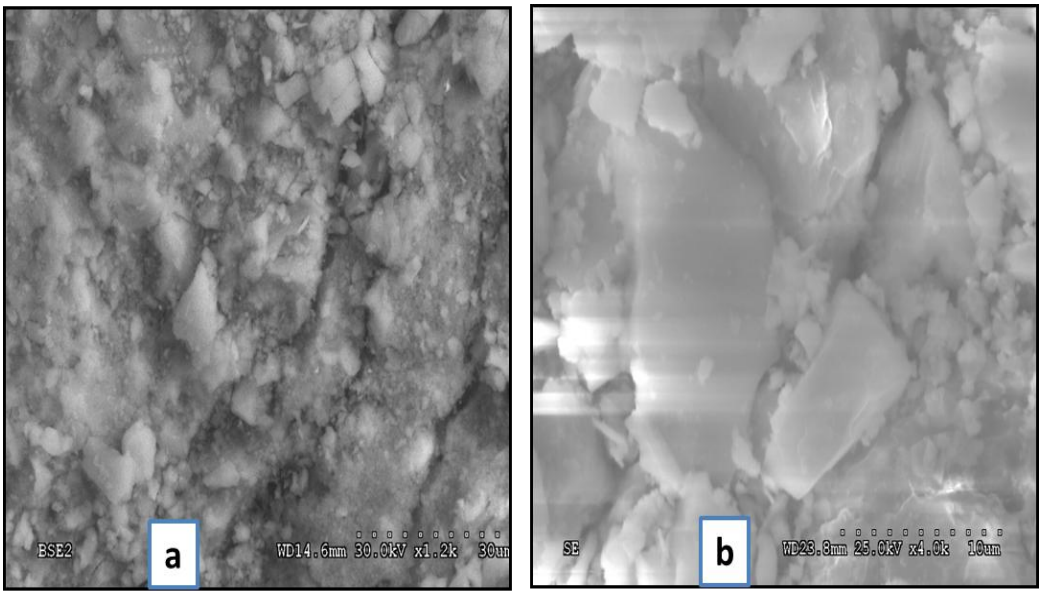

Figure 6.11: (a) Microcracking in the Hydrated Cement paste (b) Bonding within the Hydrated Cement Paste

6.4 Interfacial Transition Zone (ITZ) in Concrete

At any given cement content, water-cement ratio, and age of hydration, cement mortar will always be stronger than the corresponding concrete. The strength of concrete goes down as the coarse aggregate size increases. This is due to the behavior of the ITZ that exists between large particles of aggregate and the hydrated cement paste. It is estimated that the ITZ makes up 20-40% of the total volume of the Cementious matrix in a typical concrete [1].

The larger the maximum size of aggregate in concrete with well-graded aggregate, the less volume there is to fill with paste and the less aggregate surface there is to coat with paste; thus less water and cement is needed. This can be economically beneficial if strength and workability is not reduced. Reducing water content leads to increased compressive and flexural strength, lower permeability, thus increased watertightness and lower absorption, better bond between successive layers, less volume change from wetting and drying and reduced shrinkage cracking tendencies. However large particles tend to produce more microcracks in the ITZ between the coarse aggregate and the cement paste.

The strength of the interfacial transition zone at any point depends on the volume and size of voids. At the ITZ, there is a higher porosity (and hence a lower density) as seen from Figure 6.12 (a). The pores are generally larger than those found in the bulk paste. In practice, low void contents are achieved by using smoothly graded coarse aggregates wit suitable proportions of graded sand.

Another factor responsible for the poor strength of the ITZ in concrete is the presence of microcracks as shown in Figure 6.12 (b) and Figure 6.12 (c). Amount of microcracks depend on factors like aggregate size and grading, cement content, water-cement ratio, degree of consolidation of fresh concrete, curing conditions, environmental humidity, and thermal history of concrete.

TDA has a small thickness relative to its two other dimensions and generally flat. Mehta and Monteiro [43] recommend that the use of elongated, blade-shaped aggregate should be limited to a maximum of 15% by mass of total aggregate. This is in line with results of this study which found that only very limited amount of TDA in the range of 7.5% to 10% can be used in concrete. TDA also has a smooth surface texture. Rougher texture helps in the formation of a stronger physical bond between the cement paste and the aggregate [43]. This explains why concrete with TDA has a low strength compared with conventional concrete without TDA i.e. a weak bond is formed between the smooth surfaces of TDA and the cement paste.

Due to a higher concentration of voids and microcracks in the ITZ, the ITZ becomes the weakest link of the chain and is considered as the strength-limiting phase in concrete. It is because of the presence of the ITZ that concrete fails at lower stress level than the strength of either of the two main components. It does not take very high energy levels to extend the cracks already existing in the ITZ, even at 50% of the ultimate strength; higher incremental strains may be obtained per unit of applied stress. This explains the phenomenon that the components of concrete (aggregate and hydrated cement paste or mortar) usually remain elastic until fracture in uniaxial compression test, whereas concrete itself shows inelastic behavior.

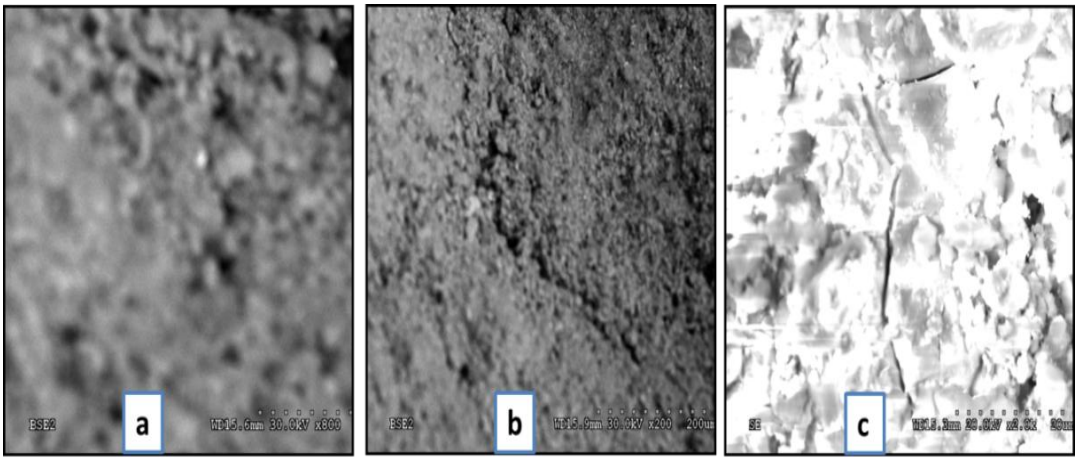

Figure 6.12: (a) Variation of volume and size of pores (voids) in the ITZ (b) Microcracks and pores variation as one approaches the ITZ (c) Microcracks and pores around the Aggregate phase.

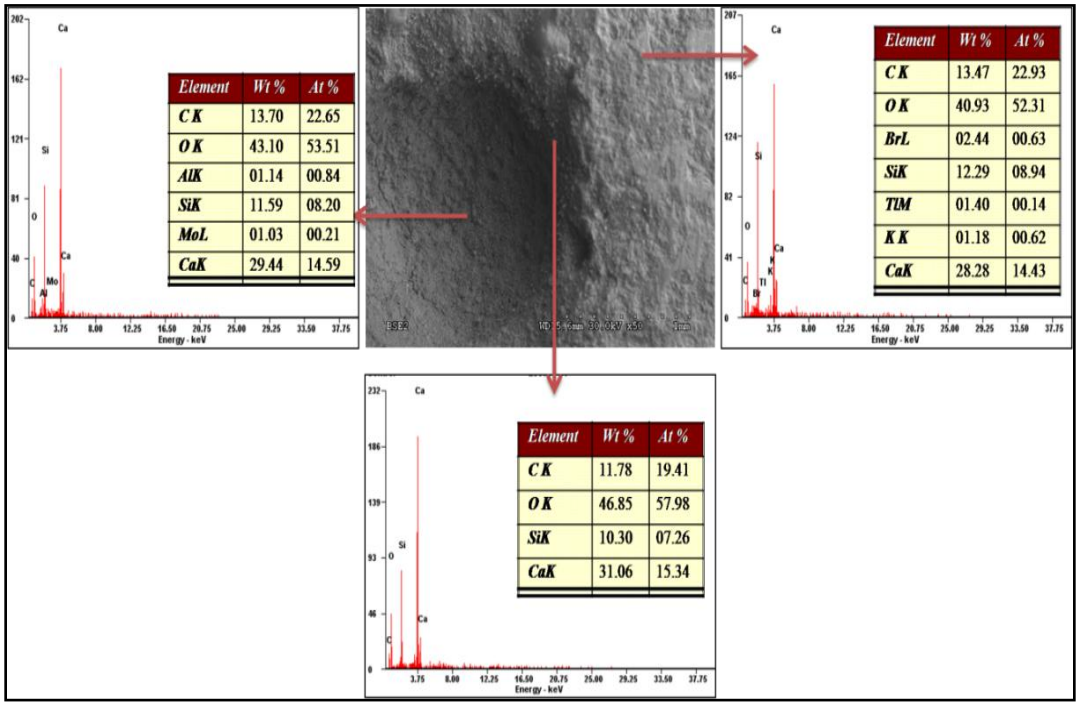

Figure 6.13: Variation of chemistry in the Mortar

The microstructure of the ITZ, especially the volume of voids and microcracks present, has a great influence on the stiffness or the elastic modulus of concrete. In ordinary concretes, the ITZ has less crack resistance than either the aggregate or the hydrated cement paste and so fracture occurs preferentially in the ITZ.

The most effective ways of improving the ITZ, hence strength of concrete is by addition of 10-15% of silica fume by weight of cement [1]. Silica fume is good in several ways. First, it eliminates many of the larger pores in the ITZ making the structure more homogenous. Secondly, it eliminates the growth of calcium hydroxide or transforms calcium hydroxide to C-S-H by pozzolanic reaction and lastly it has a filler effect that modifies the rheological properties of fresh concrete in such a way as to reduce internal bleeding, thus enhancing the paste-aggregate bond. However, modest increases in strength attributable to better paste-aggregate bonding are largely offset by increasing brittleness of the resulting materials. This same conclusion was arrived at in Section 5.7 where addition of Silica Fume was found to increase compressive strength but had a negative effect on flexural strength. A drop of in flexural strength 12% and 17% at 7 days and 28 days respectively was noted with addition of Silica Fume into a concrete batch.

6.5 X-Ray Diffraction

Atoms are arranged periodically on a lattice, and the rays scattered by them have definite phase relations. Phase relations are such that destructive interference occurs in most directions of scattering, but in a few directions constructive interference takes place and diffracted beams are formed. The two essentials of X-Ray Diffraction are a wave motion capable of interference (x-rays) and a set of periodically arranged scattering centers (the atoms of a crystal).

Two powder samples were tested in theta - 2theta (θ-2θ) powder diffraction configuration using the Siemens D500 (2-axis) X-Ray diffractometer. For this project, acquisition conditions were 40 kV, 30mA, and all scans were run from 2º to 90º 2-theta, with a continuous step size of 0.066. The anode used in the machine was copper. Typically, x-rays emitted by copper have a wavelength of λ= 1.54060 Å ([44] for K-α_1 line. Cullity [45] gives a wavelength of λ=1.54051 Å for K-α_1 line. An average of λ=1.54056 Å was used.

The diffractometer is fully computer-controlled using Windows-based software MDI Datascan and the user had access to Jade5 software for data reduction and analysis. Jade5

program include algorithms for search-matching, quantitative analysis, profile fitting, calculating XRD patterns from known or approximated crystal data, and the determination of crystallite size.

The two samples tested were sand (fine aggregate) and concrete which was crashed to form a powder. The diffraction pattern for the two samples is shown in Figure 6.14 and Figure 6.15. The curve of scattered intensity vs. 2θ for a crystalline solid is almost zero everywhere except at certain angles where high sharp maxima occur: These are the diffracted beams. However, from the curves in Figure 6.14 and Figure 6.15, there is a noted scattering that shows no maxima, but merely a regular decrease of intensity with increase in scattering angle. This kind of diffraction is from monoatomic gases, which have no structural periodicity but atoms are arranged perfectly at random and their relative position change constantly with time.

The diffraction patterns for sand and concrete was analyzed by the Jade5 software database. The sand peaks matched the peaks for quartz (silicon dioxide, SiO_2) but no match was found for the concrete peaks in the database.

Bragg's law, shown in Equation (6.5), provides a relationship between the angle between the diffracted beam and the transmitted beam (2θ), also known as the diffraction angle, wavelength of the radiation (λ) and the interplanar spacing, d, of various planes in a crystal that cause constructive reinforcement. In this case x-rays of known wavelength were used and the diffraction angle (2θ) was measured in order to determine the spacing, d, of various planes in the crystals of the samples. When an X-ray spectrometer is used with x-rays of known wavelength to determine the unknown spacing of crystal planes, it is known as diffractometer.

$$\lambda = 2dsin\theta \tag{6.5}$$

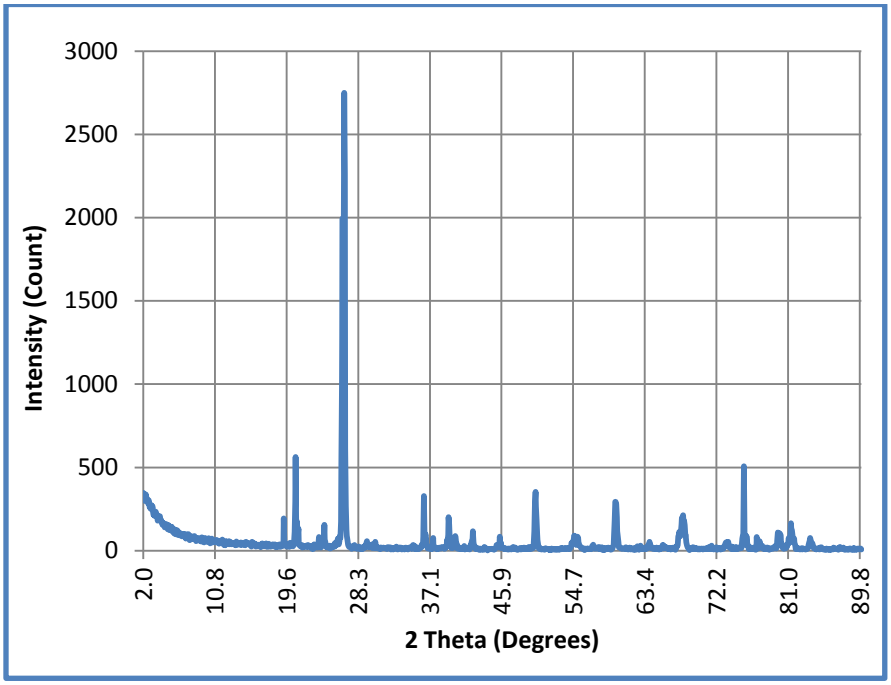

Figure 6.14: Diffraction curve for Sand

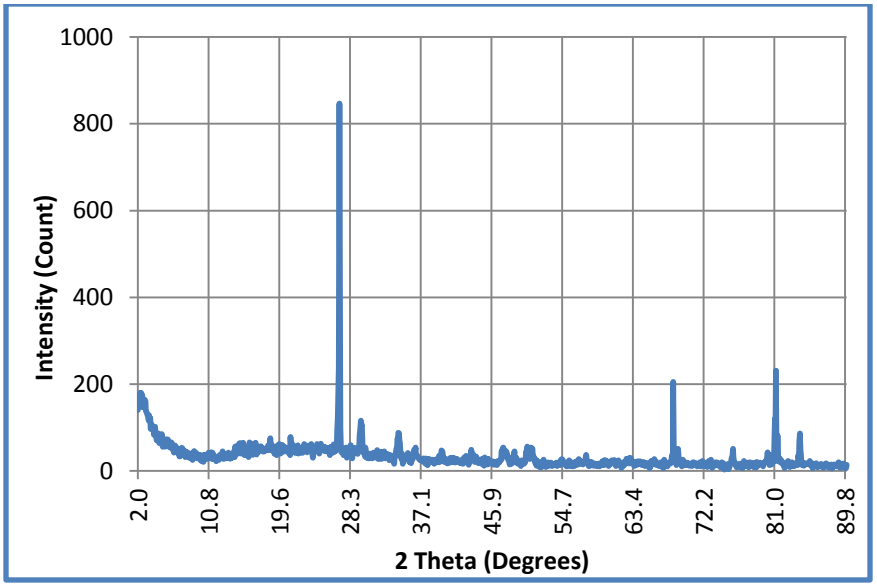

Figure 6.15: Diffraction curve for concrete powder

Diffraction occurs whenever the Bragg law (Equation (6.5)) is satisfied. For Powder method, λ is fixed and θ is varied. The crystals to be examined were reduced to a fine powder and placed in a beam of monochromatic x-rays. When materials are prepared in the form of a fine

powder, there are always at least some powder particles whose planes (hkl) are oriented at the proper θ angle to satisfy Bragg's law. Each particle of a powder is a tiny crystal oriented at random with respect to the incident beam. The result is that every set of lattice planes will be capable of reflection. The powder method is the only method that can be employed when a single crystal specimen is not available [45].

The powder method is especially suited for determining lattice with high precision and for the identification of phases, whether they occur alone or in mixtures such as polyphase alloys, corrosion products, refractories and rocks. The usual monochromatic beam is one containing a strong Kα component superimposed on a continuous spectrum.

Since we know the wavelength of the X-rays, we can determine the interplanar spacing and eventually, the identity of the planes that cause the diffraction. Interplanar spacing is the distance between two adjacent parallel planes of atoms with the same Miller indices. The interplanar spacing in hexagonal materials is given by Equation (6.6).

$$\frac{1}{{d_{hkl}}^2} = \frac{4}{3}\left(\frac{h^2 + hk + k^2}{{a_0}^2}\right) + \frac{l^2}{c^2} \qquad (6.6)$$

Where a_o and c are the lattice parameters and h, k and l represent the miller indices of adjacent planes being considered.

Analysis of the diffraction curve for sand using Jade5 program gave possible planes (hkl) from which the diffraction pattern occurred. Also using the Bragg's equation, the interplanar spacing can be calculated. The interplanar spacing and planes from which diffraction occurred is summarized in the Table 6.1.

Knowing d, the interplanar spacing and the specific plane from which the diffraction occurred, we can calculate the lattice parameters using Equation (6.6). The results for selected angles are shown in Table 6.2.

The lattice parameter is found to be approximately 4.9 Å which is consistent with the number provided by Cullity [45] for SiO_2. This confirms that sand is mainly composed of SiO_2 (Silicon dioxide).

Table 6.1: Interplanar spacing and diffraction planes in sand (fine aggregate)

2-Theta	d=λ/(2sinθ) (A)	hkl
20.677	4.2904	(100)
26.612	3.3455	(100)
39.423	2.2829	(102)
40.225	2.2392	(111)
42.364	2.1310	(200)
45.689	1.9833	(201)
50.032	1.8209	(112)
54.811	1.6729	(202)
55.223	1.6614	(103)
59.844	1.5436	(211)
64.034	1.4524	(113)
65.749	1.4186	(300)
68.031	1.3764	(213)
73.415	1.2882	(104)
77.561	1.2294	(220)
79.801	1.2004	(221)
81.375	1.1811	(310)
83.708	1.1541	(311)

Table 6.2: Lattice parameter for Silicon dioxide in sand

2θ	$\sin^2\theta$	H^2+hk+k^2	a_0
20.7	0.0322	1	4.956
42.4	0.1306	4	4.923
65.7	0.2946	9	4.916
81.4	0.4250	12	4.726

6.6 Conclusion

The unique features of concrete microstructure can be summarized as follows: first, there is the interfacial transition zone (ITZ), which represents a small region next to the particles of coarse aggregate, typically 10-50μm thick around large aggregate [43]. The ITZ is generally weaker than either of the two main components of concrete (bulk hydrated cement paste and aggregate) therefore exercises a far greater influence on the mechanical behavior of concrete than is reflected by its size.

Second, each of the three phases is itself a multiphase in character. For example, each aggregate particle may contain several minerals in addition to microcracks and voids. Similarly, both the bulk hydrated cement paste and the ITZ generally contain a heterogeneous distribution of different types and amounts of solid phases, pores, and microcracks.

Third, concrete microstructure is not an intrinsic characteristic of the material because the two components of the microstructure (bulk hydrated cement paste and ITZ) are subject to change with time, environmental humidity, and temperature.

CHAPTER 7

EFFECT OF ELEVATED TEMPERATURE ON RUBBERIZED CONCRETE

Human safety in the event of fire is one of the considerations in the design of residential, public and industrial buildings. Concrete has a good service record in this respect compared to wood and plastics since it is incombustible and does not emit toxic fumes on exposure to high temperature. Concrete is able to retain sufficient strength for reasonable long time when subjected to temperatures of the order of 700 to 800 °C (1290 to 1470°F) [43] thus permitting rescue operations by reducing the risk of structural collapse.

Durability refers to the ability of concrete to resist deterioration from the environment or service in which it is placed. The design of an engineering structure must ensure that under the worst loadings, the structure is safe, and during normal working conditions the deformation of the members does not detract from the appearance, durability or performance of the structure.

7.1 Procedure

Thermal expansion is an important factor in structures where differential heating may occur, either from environmental effects, such as solar heating or from service conditions such as furnace installations.

The effect of elevated temperature on rubberized (TDA) concrete was investigated. Three cylinders each from the Control Batch (no TDA) and the TDA Concrete (7.5% coarse aggregates replaced by TDA) were taken and placed in an oven set at 200°C (392°F) for 3 hrs as shown in Figure 7.1. Then the cylinders were left to cool to room temperature before they were examined and tested for compressive strength according to ASTM C39. The experiment was repeated again with another set of cylinders with the oven temperature set at 100°C (212°F) for 3 hrs.

A sample of TDA (Tire Derived Aggregate) was also placed in the same conditions above and its weight monitored to verify if TDA would decompose leading to deteriorating properties of the final structure.

Figure 7.1: Concrete Specimens placed in Oven

7.2 Results

The loss of ignition of TDA placed in the oven both at 100°C and 200°C for 3 hours did not show any significant loss of weight although some smoke was noticed coming from the TDA at 200°C. A smell of burning rubber was also felt.

The concrete that did not have TDA (Control) did not show cracks on the surface nor did spalling take place when exposed to 200°C in the oven for three hours as seen from Figure 7.2. With no visible damage to the Control Concrete at 200°C it was deemed unnecessary to run the experiment at 100°C for the Control Concrete.

However, after testing for compressive strength based on ASTM C39, it was found that compressive strength dropped by approximately 12% after exposure of the concrete to the elevated temperature. The Elastic Modulus also dropped by about 20% as shown in Table 7.1. Figure 7.3 shows the stress- strain curves for control concrete for different specimens with and without exposure to elevated temperature (200°C). The specimens which were not exposed to high temperature are labeled Control 1/2/3 and those that were exposed to 200°C for three hours

are labeled Control-Fire 1/2/3. From the curves, it is shown that both compressive strength and elastic modulus drop when concrete is exposed to high temperature.

Table 7.1: Compressive Strength of Control Concrete with and without exposure to elevated temperature

	Control Concrete after Exposure to 200 °C for 3 hrs		Control Concrete	
	Compressive Strength, psi (MPa)	Elastic Modulus, psi (MPa)	Compressive Strength, psi (MPa)	Elastic Modulus, psi (MPa)
Specimen 1	3646 (25.1)	2,231,677 (15,387)	4735 (32.6)	3,014,465 (20,784)
Specimen 2	4028 (27.8)	2,700,081 (18,616)	4038 (27.8)	2,937,778 (20,255)
Specimen 3	3909 (27.0)	2,522,990 (17,133)	4458 (30.7)	3,406,384 (23,486)
Average	3861 (26.6)	2,484,916 (17,133)	4410 (30.4)	3,119,542 (21,508)

When concrete containing TDA was exposed to 200°C for three hours, excessive cracking, spalling and pop-outs were observed on the surface of the concrete cylinders as shown in Figure 7.4. The pop-outs occurred where there was a TDA particle underneath and as seen from Figure 7.4 most cracks seem to originate from these pop-outs. The TDA concrete after exposure to 200°C could not sustain much load as the cracks already formed due to thermal stresses increased in size leading to premature concrete failure.

When TDA concrete was exposed to 100°C for three hours, cracks and pop-outs (spalls) also occurred on the surface of the concrete as shown in Figure 7.5 and Figure 7.6. Silica Fume addition to the concrete did not seem to have improved the thermal properties when comparing Figure 7.5 and Figure 7.6.

The TDA concrete after exposure to 100°C was able to sustain load although there was approximately 23% drop in compressive strength. The Elastic modulus also dropped by about 31% after exposure of concrete to 100°C. TDA concrete that contained Silica Fume had

compressive strength drop of about 24% and Elastic modulus drop of about 35%. Figure 7.7 and Figure 7.8 shows the stress-strain curves for TDA concrete with and without exposure to elevated temperature (100°C for three hours). The concrete becomes more non-linear with exposure to high temperature. The concrete that was not exposed to elevated temperature is labeled TDA 1/2/3 while that exposed to high temperature is labeled TDA 1/2/3–Fire.

Figure 7.2: Control Concrete (No TDA) after exposure to 200°C for 3 hrs, no noticeable cracks or spalling was observed.

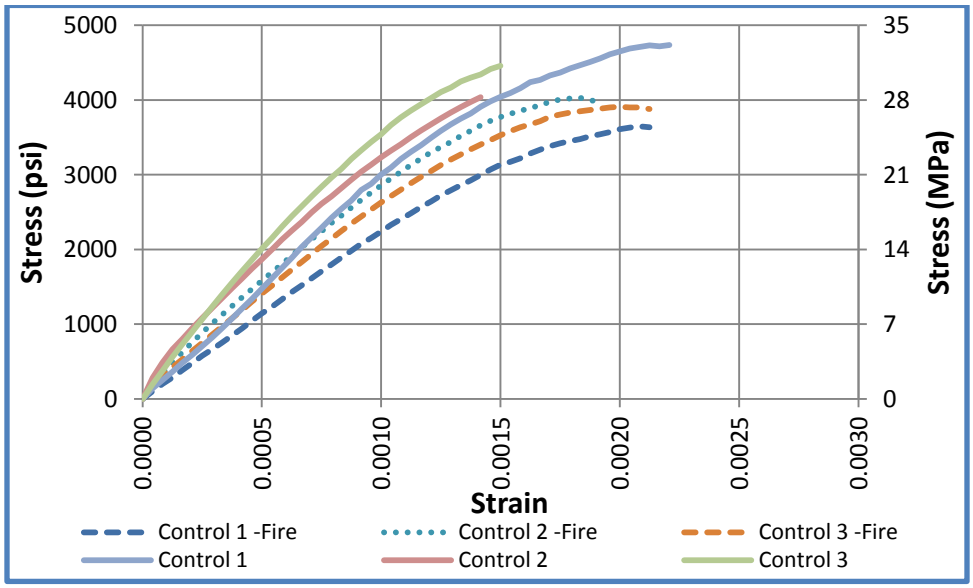

Figure 7.3: Stress vs. Strain curves for control concrete with and without exposure to elevated temperature

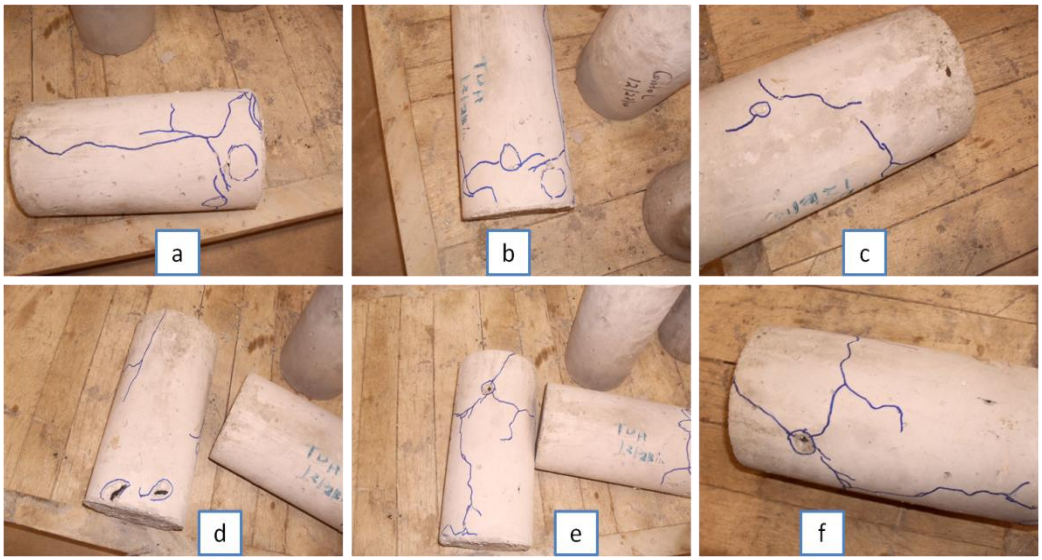

Figure 7.4: Cracks and spalling on TDA Concrete after exposure to 200°C for 3 hrs in the oven.

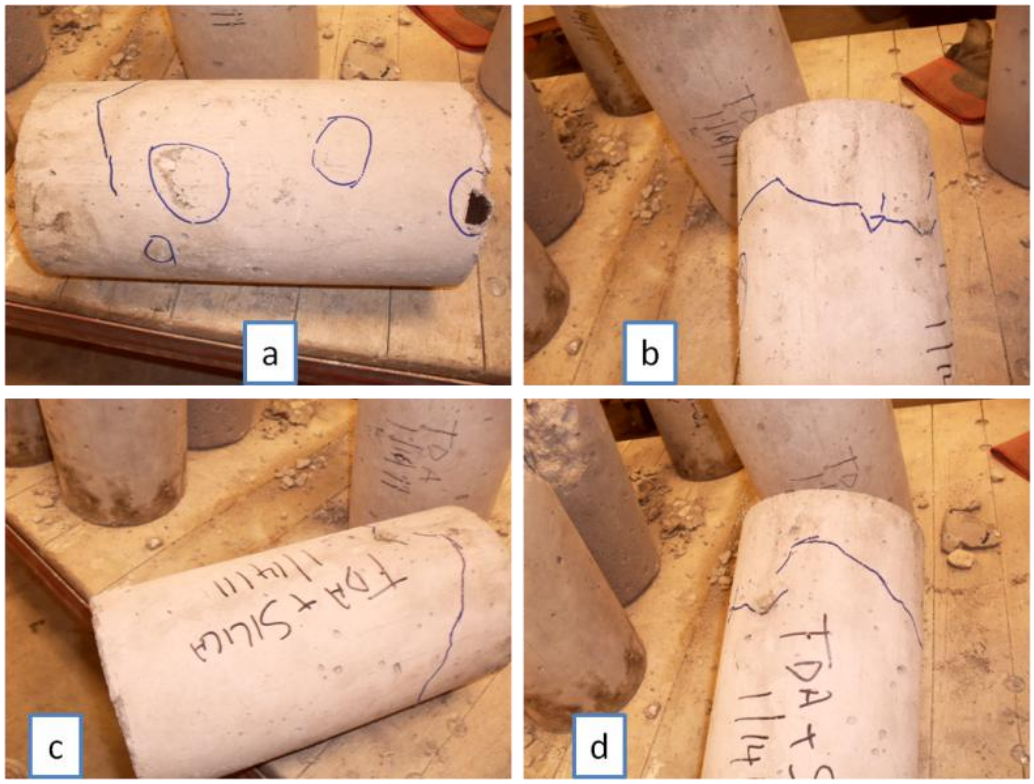

Figure 7.5: Cracks and spalling on TDA Concrete with Silica Fume after exposure to 100°C for 3 hrs in the oven.

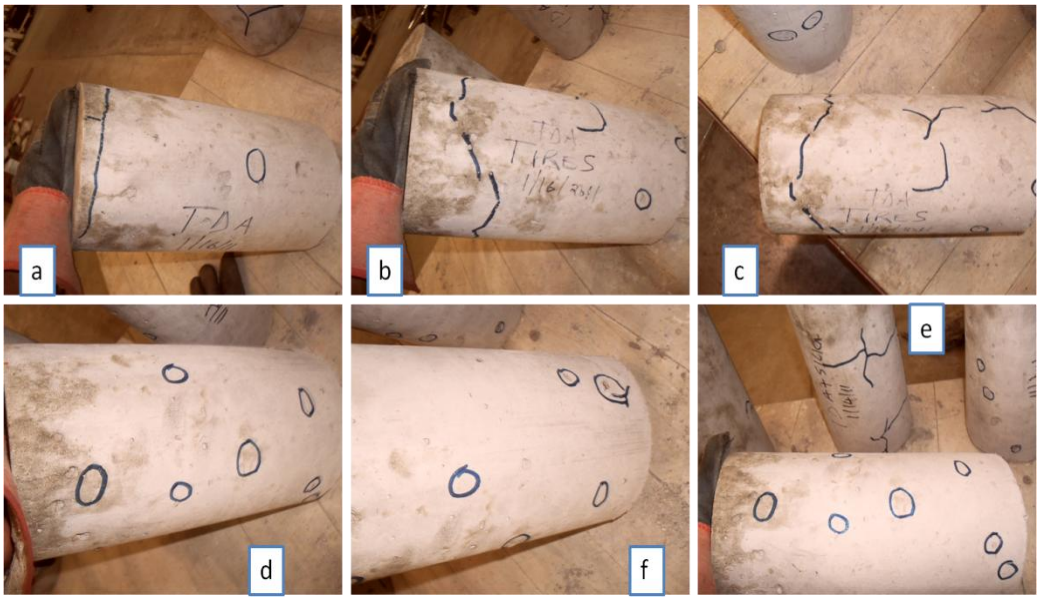

Figure 7.6: Cracks and spalling on TDA Concrete after exposure to 100°C for 3 hrs in the oven.

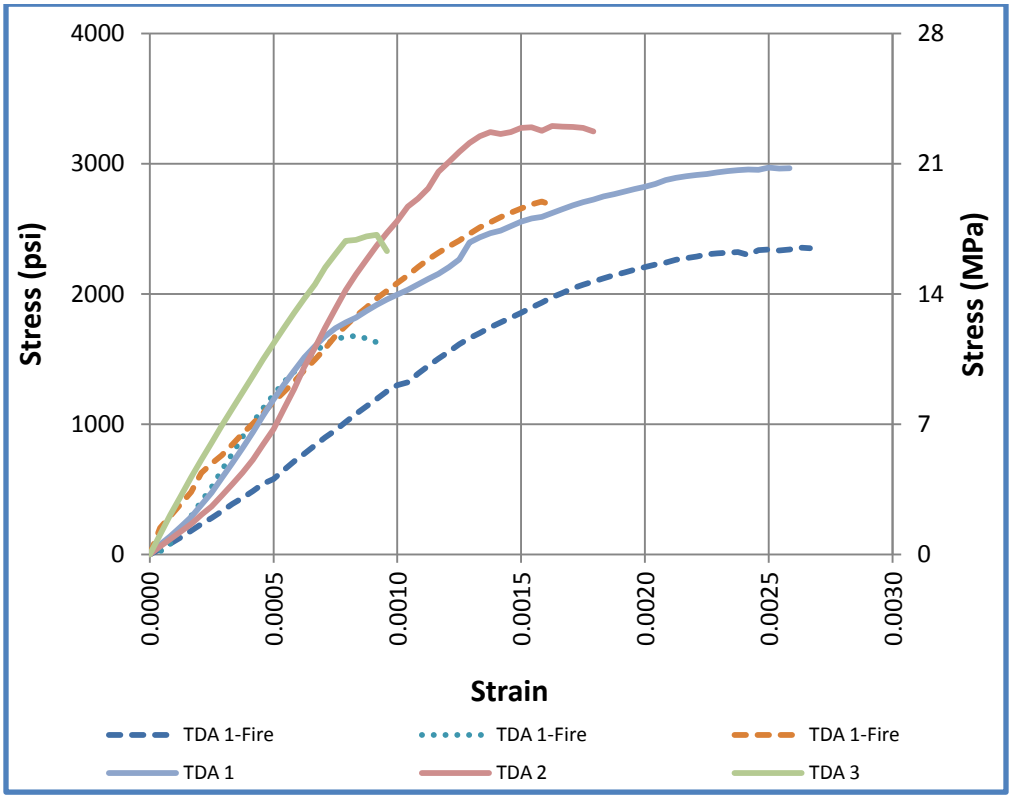

Figure 7.7: Stress vs. Strain curves for TDA concrete with and without exposure to elevated temperature (100°C for 3 hrs in the oven).

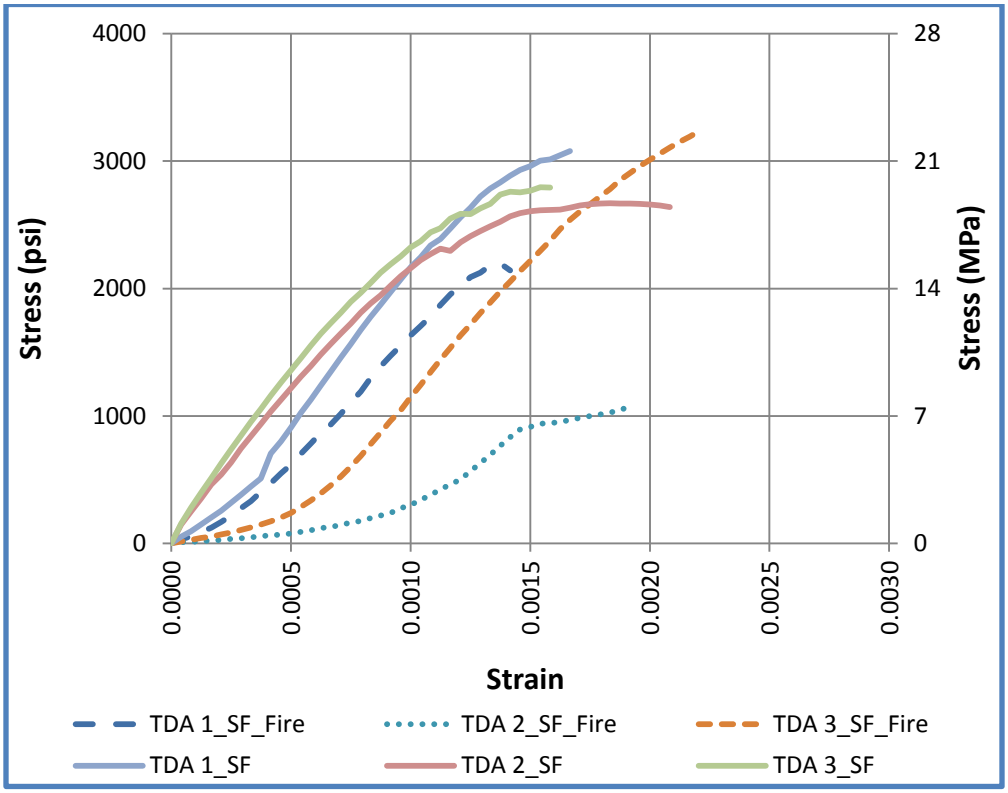

Figure 7.8: Stress vs. Strain curves for TDA concrete with Silica Fume (SF) with and without exposure to elevated temperature (100°C for 3 hrs in the oven).

7.3 Discussion of the Results

Within the normal environmental temperature range, concrete thermal properties (i.e. thermal expansion, thermal conductivity, and specific heat) can be considered to be constant provided that there is no change in moisture content [1]. However at elevated temperatures these properties change because of changes in the moisture content of concrete components and because of progressive deterioration of the paste and in some cases the aggregate.

Many factors control the response of concrete to fire. Composition of concrete is important because both the cement paste and the aggregate consist of components that decompose on heating. The permeability of concrete, the size of the element, and the rate of temperature rise are important because they govern the development of internal pressures from the gaseous decomposition products. Other factors to consider are the maximum temperature

and the time at elevated temperature. The response of concrete will generally depend on its initial properties and those of its constituents.

It was found that exposing concrete to 200°C for three hours led to a 12% compressive strength drop and a 20% drop in Elastic Modulus. The changes in both strength and modulus can be attributed to a combination of decomposition of the hydrated pastes, deterioration of the aggregates and thermal incompatibilities between the paste and the aggregate leading to stress concentrations and microcracking. The change in modulus of elasticity is more marked than in case of compressive strength probably due to internal microcracking at the paste-aggregate interface in addition to change in bonding energies.

When concrete is heated to elevated temperatures, drying shrinkage occurs due to additional loss of moisture from the paste. Drying shrinkage continues to increase at higher temperatures as structural decomposition of the hydration products continues, and much of this process is irreversible. Effect on increasing temperature on hydrated cement paste depends on the degree of hydration and moisture state. The rate of shrinkage being a factor of moisture loss from the concrete would thus depend on factors like water content, water/cement ratio, aggregate content, specimen geometry, and drying conditions at the surface.

The magnitude of the decrease in strength and modulus depend on the nature of the aggregate as seen from the catastrophic effect of high temperature to concrete containing TDA as an aggregate. Concrete containing TDA showed striking drop in compressive strength and elastic modulus, cracking on the surface and spalling and pop-outs beneath the TDA particle. Most cracks originated from areas where there was a TDA particle.

It was noted that smoke was coming off from TDA particles placed in the oven at the same conditions of elevated temperatures as those of TDA concrete. There was also a smell like that of burning rubber. From these two observations, it can be concluded that exposing the TDA to elevated temperature led to its decomposition hence producing gaseous compounds which were escaping in the form of smoke.

For the case of TDA concrete, since the TDA particles were trapped within the paste, the gaseous decomposition compounds could not escape leading to buildup of internal stress. Once the expansion joints were closed up, structure deformation and displacements occurred in different parts of the structure leading to cracking, spalling and pop-outs. Spalling and pop-outs must have occurred after the rate of increase of internal pressure in the concrete was faster than pressure relief of the decomposition gases into the atmosphere. Cracking of concrete in the field is very detrimental as it increases water permeability into the interior, thus accelerating the process of deterioration. Thermal cracks form when thermally induced strains produce localized stresses which exceed the fracture resistance of the concrete [46]. Thermal stresses are the greatest at the surface of the concrete because the temperature was highest at the surface hence the observed cracking on the surface.

The porosity and mineralogy of the aggregate therefore exercise an important influence on the behavior of concrete exposed to fire. Depending on the rate of heating and the size, permeability and the moisture state of the aggregate, the porous aggregate may themselves be susceptible to disruptive expansion leading to pop-outs. Low porosity aggregates should, however be free of problems related to internal moisture movement.

Aggregate mineralogy determines the differential thermal expansions between the aggregate and the cement paste and the ultimate strength of the interfacial transition zone. The inferior performance of TDA concrete at elevated temperature could also be a factor of differential expansion of the TDA particle and the concrete since the coefficient of thermal expansion of the two components is very different. Concrete has a coefficient of thermal expansion of 7.4 to 13 $\times 10^{-6}$/°C (4.1 to 7.3 $\times$ 10^{-6}/°F) [1] while elastomers used in tires have coefficient of thermal expansion of the order 10^{-4}/°C [47] and typical fillers such as carbon black and silica used in rubber compositions have coefficient of thermal expansion in the order of 10^{-5}/°C to 10^{-6}//°C [47]. In comparison most aggregates' coefficient of thermal expansion range from 4 to 13 $\times 10^{-6}$/°C (2.2 to 7.2 $\times$ 10^{-6}/°F) [1].

On relative basis then, the thermal expansion of concrete is not big enough to compensate for the much greater thermal expansion of TDA leading to internal pressures resulting in the observed cracking in TDA concrete. This may also explain why the observed cracks on the concrete surface seem to originate from the point where there is a TDA particle.

7.4 Conclusion

The concrete containing TDA was found to perform poorly at elevated temperatures when compared with concrete with similar composition except for the TDA. Cracking, spalling and pop-outs were observed in the concrete containing TDA and after exposure to heat; the concrete had a big drop in strength and elastic modulus. After exposure to 100°C (212°F), the TDA concrete strength dropped by as much as 23% in strength. In comparison, the concrete without TDA had only 12% drop in strength after exposure to 200°C (392°F) for the same duration.

The decline in strength and modulus is believed to be due to microcracking in the concrete due to internal pressures exerted by gaseous compounds escaping after decomposition of TDA particles and differential thermal expansion between the TDA and the concrete.

It is recommended that the concrete with TDA should be used in environments where temperatures would not exceed 100°C (212°F).

CHAPTER 8

MODELING OF CONCRETE IN ABAQUS

8.1 Purpose and Scope

The ultimate objective of design is the creation of a safe and economical structure. Advanced analytical tools can be an indispensable aid in the assessment of the safety and the serviceability of a proposed design. A major challenge facing the modern concrete technologist is the more accurate prediction of concrete durability under a variety of service loads [1].

Serviceability refers to suitability for everyday use and hard to wear. In order to ensure the serviceability requirement, it is necessary to predict the cracking and the deflections of concrete structures under service loads. To assess the margin of safety of concrete structures against failure, an accurate estimation of the ultimate load is essential and the prediction of the load-deformation behavior of the structure throughout the range of elastic and inelastic response is desirable. A capability for predicting stress and strain distribution and response for plain concrete and concrete containing Tire Derived Aggregate (TDA) and Crumb Rubber is proposed and analyzed in this study.

In many cases, analytical methods are more economical and expedient than laboratory or field testing and finite element models provides information that is not easily obtained through experimentation [48]. The development of reliable analytical models therefore reduce the number of required test specimens for the solution of a given problem, recognizing that tests are time-consuming and costly and often do not simulate exactly the loading and support conditions of the actual structure.

8.2 Methodology

Several experiments were designed to provide a basis for design equations and data which is invaluable in the preliminary model design stages. Three different concrete batches were

designed with compositions as shown in Table 8.1. From each batch, 6in x 12in (150mm x 300mm) cylinders, 20in x 6in x 6in (500mm x 150mm x 150mm) beams and 84in x 12in x 8in (2130mm x 300mm x 200mm) beams were cast.

Table 8.1: Batch Compositions for full scale beam testing

Component	Control (No TDA or Crumb used)	7.5% Fine Aggregate Replaced by Crumb	7.5% Coarse Aggregate Replaced by TDA
Designation	0%TDA	7.5%Crumb	7.5%TDA
Cement	350	350	350
Coarse Aggregate	1489	1489	1378
Fine Aggregate	981	907	981
Water	194	194	194
TDA 1/2"			36
Crumb Rubber		31	
Total	3014	2971	2938

The 6in x 12in (150mm x 300mm) cylinders were used to determine the ultimate compressive stress and stress-strain deflection curves for each concrete based on ASTM C39 [36] while 20in x 6in x 6in (500mm x 150mm x 150mm) beams were used to determine the concrete flexural strength (Modulus of Rupture) based on ASTM C78 [38]. The set-up for ASTM C39 and ASTM C78 is shown in Figure 8.1 and Figure 8.2 respectively. In both tests, the load applied to the concrete specimen was measured by a load cell while the displacement of the concrete was measured directly by two Linear Variable Differential Transducers (LVDTs). The information collected was load (LB) and displacement (inches) which was used to plot load-deformation curves for each specimen from each concrete type. From these two tests, the basic information for finite element models, such as material properties and stress-strain behavior under loading was extracted.

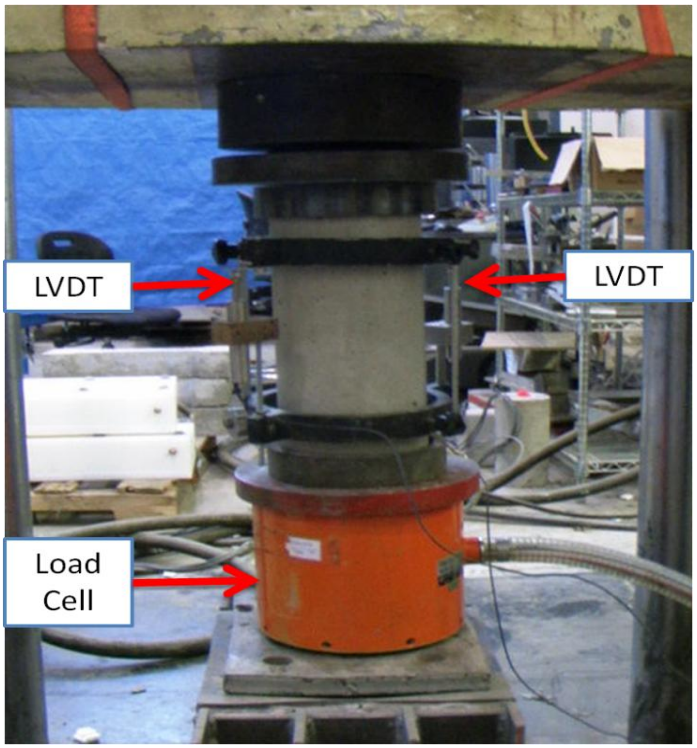

Figure 8.1: ASTM C39 (Compressive Strength) Set-Up

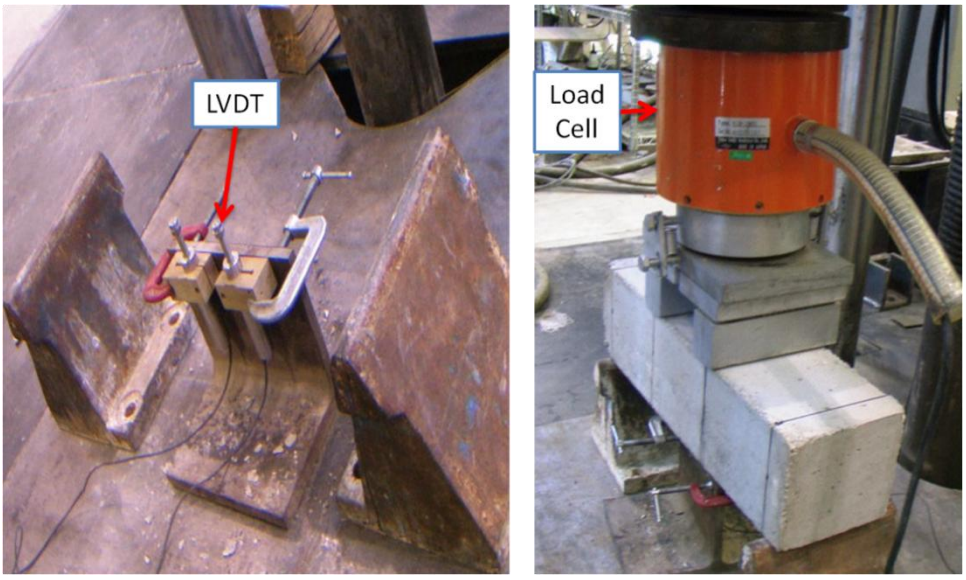

Figure 8.2: ASTM C78 (Flexural Strength) Set-Up

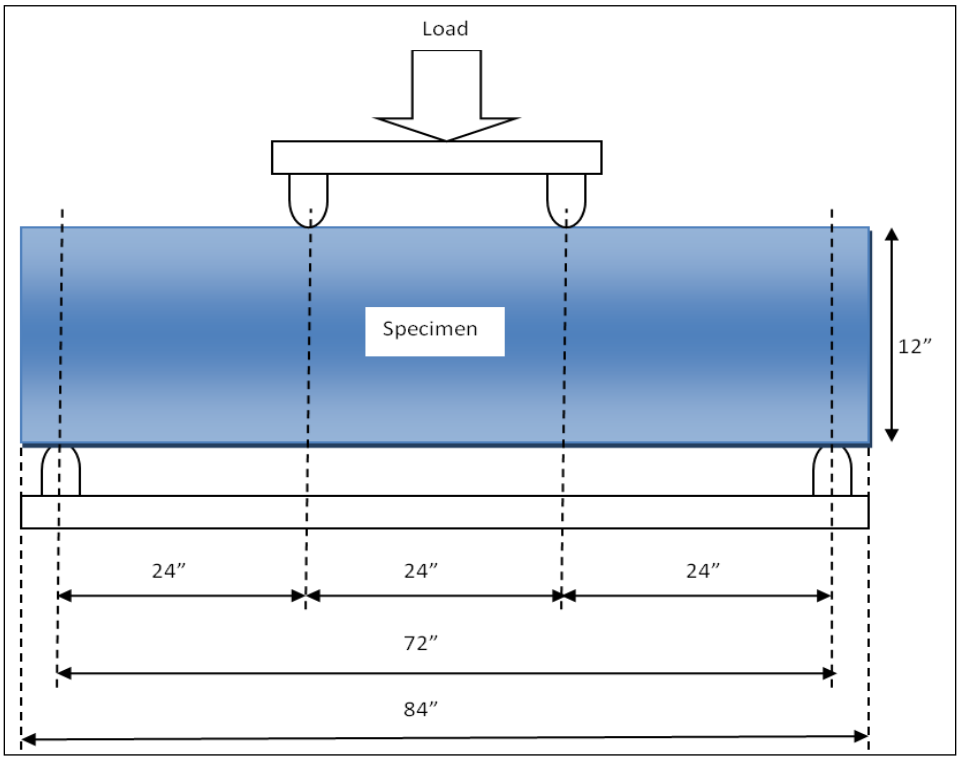

Figure 8.3: Experimental set-up for the full scale beam testing

The information was then used to design concrete models in ABAQUS software. The results of finite element models were then evaluated by comparing them with experimental results of the 84in x 12in x 8in (2130mm x 300mm x 200mm) full-scale beams. The schematic set-up for the full scale beam experiment is shown in Figure 8.3.

A complete analysis using ABAQUS requires a description of the material, the model configuration, boundary conditions and loading [49] {3220 Biggs, R.M. 2000}}. Concrete is subjected to essentially monotonic straining and a material point exhibits either tensile cracking or compressive crushing therefore a smeared crack model in ABAQUS would be used in the modeling.

Concrete smeared model was chosen due to its capability to models concrete behavior for relatively monotonic loadings under fairly low confining pressures (less than four to five times the magnitude of the largest stress that can be carried by the concrete in uniaxial compression)

[49]. For concrete smeared model, cracking is assumed to be the most important aspect of the behavior, and representation of cracking and of postcracking behavior dominates the modeling [49].

The concrete model is a smeared crack model in the sense that it does not track individual “macro” cracks. Constitutive calculations are performed independently at each integration point of the finite element model. The presence of cracks enters into these calculations by the way in which the cracks affect the stress and material stiffness associated with the integration point.

The main assumption of smeared crack model is that cracking is assumed to occur when the stress reaches a failure surface that is called the “crack detection surface. When a crack has been detected, its orientation is stored for subsequent calculations. Subsequent cracking at the same point is restricted to being orthogonal to this direction since stress components associated with an open crack are not included in the definition of the failure surface used for detecting the additional cracks. Cracks are irrecoverable: they remain for the rest of the calculation (but may open and close). No more than three cracks can occur at any point (two in a plane stress case, one in a uniaxial stress case). Following crack detection, the crack affects the calculations because a damaged elasticity model is used. Cracking dominates the material behavior when the state of stress is predominantly tensile. The model uses a “crack detection” plasticity surface in stress space to determine when cracking takes place and the orientation of the cracking. Damaged elasticity is then used to describe the postfailure behavior of the concrete with open cracks [49].

The shape of failure surface is defined by failure ratios as specified below:

a) Ratio 1: The ratio of the ultimate biaxial compressive stress to the ultimate uniaxial compressive stress. ABAQUS uses a default value of 1.16.
b) Ratio 2: The absolute value of the ratio of the uniaxial tensile stress at failure to the ultimate uniaxial compressive stress. Ratio 2 is calculated from the available data

from uniaxial compressive and tensile experiments for each of the three types of concrete as shown in Table 8.2.

Table 8.2: Failure Ratio 2 for failure surface description

Ratio 2	Control (0%TDA)	0.15
	Concrete with TDA (7.5%TDA)	0.16
	Concrete with Crumb Rubber (7.5%Crumb)	0.17

c) Ratio 3: The ratio of the magnitude of a principal component of plastic strain at ultimate stress in biaxial compression to the plastic strain at ultimate stress in uniaxial compression. ABAQUS uses a default value of 1.28.

d) Ratio 4: The ratio of the tensile principal stress at cracking, in plane stress, when the other principal stress is at the ultimate compressive value, to the tensile cracking stress under uniaxial tension. ABAQUS uses a default value of 1/3.

The four ratios are then used to define the failure surface in the property model under sub-options in the concrete smeared cracking as shown in Figure 8.4.

Two material constants are required to characterize the linear elastic behavior of the material: Young's modulus (E) and Poisson's ratio (γ). For nonlinear analysis, concrete uniaxial behaviors beyond the elastic range must be defined to simulate its behavior at higher stresses. The minimum input parameters required to define the concrete material are the uniaxial compression curve, the ratio of biaxial and uniaxial compressive strength, and the uniaxial tensile strength [49].

Boundary conditions represent structural supports that specify values of displacement and rotation variables at appropriate nodes. For concrete modeling, a model that simulates cracking, tension stiffening, shear capacity of cracked concrete, and crushing in compression is required.

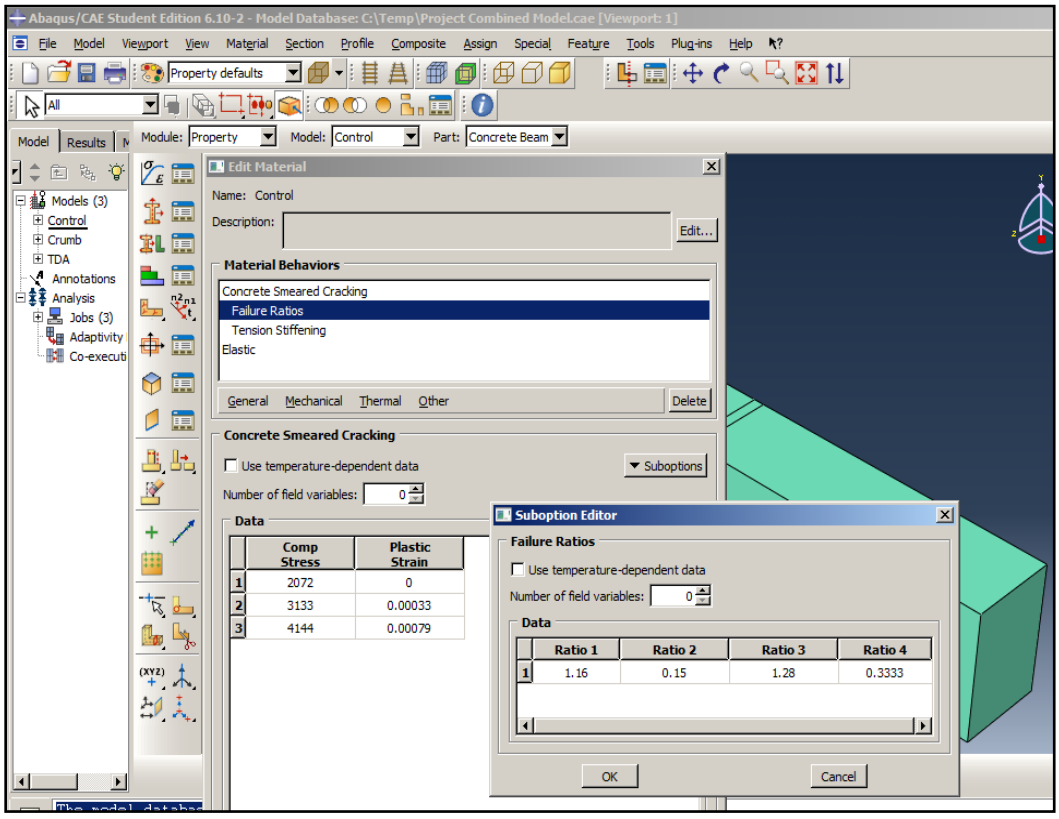

Figure 8.4: Failure Ratios definition in the Abaqus Model

Figure 8.5 shows the actual behavior exhibited by Control concrete without TDA (0%TDA), TDA concrete (7.5%TDA) and Crumb Concrete (7.5%Crumb) in tension. These curves would be used to simulate the tension stiffening behavior of the concrete elements in ABAQUS.

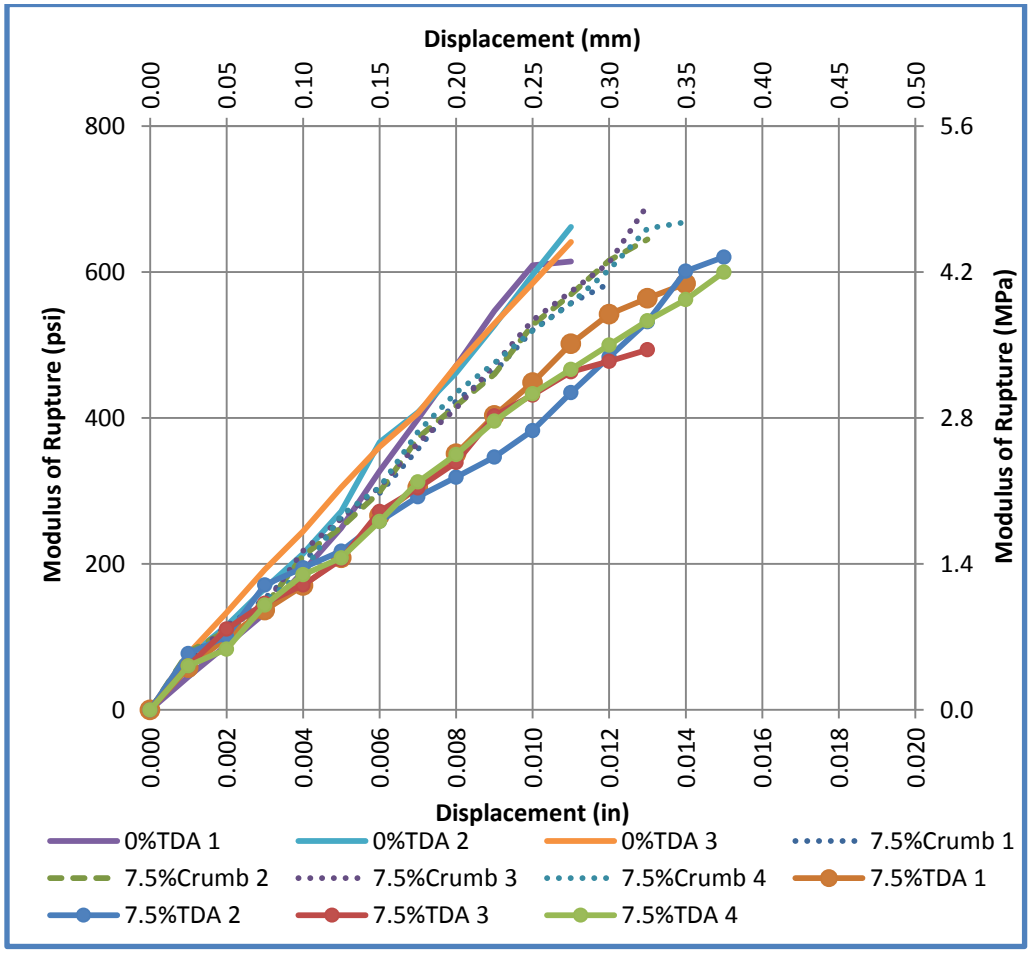

Figure 8.5: Behavior exhibited by different types of concretes in tension.

The response of a structure under load depends to a large extent on the stress-strain relation of the constituent materials and the magnitude of stress. The concrete stress-strain relation exhibits nearly linear elastic response up to about 30% of the compressive strength. This is followed by gradual softening up to the concrete compressive strength, when the material stiffness drops to zero. Beyond the compressive strength the concrete stress-strain relation exhibits strain softening until failure takes place by crushing. Figure 8.6 , Figure 8.7 and Figure 8.8 shows the behavior exhibited by Control Concrete (0%TDA), Crumb Concrete (7.5%Crumb) and TDA concrete (7.5%TDA) in Compression.

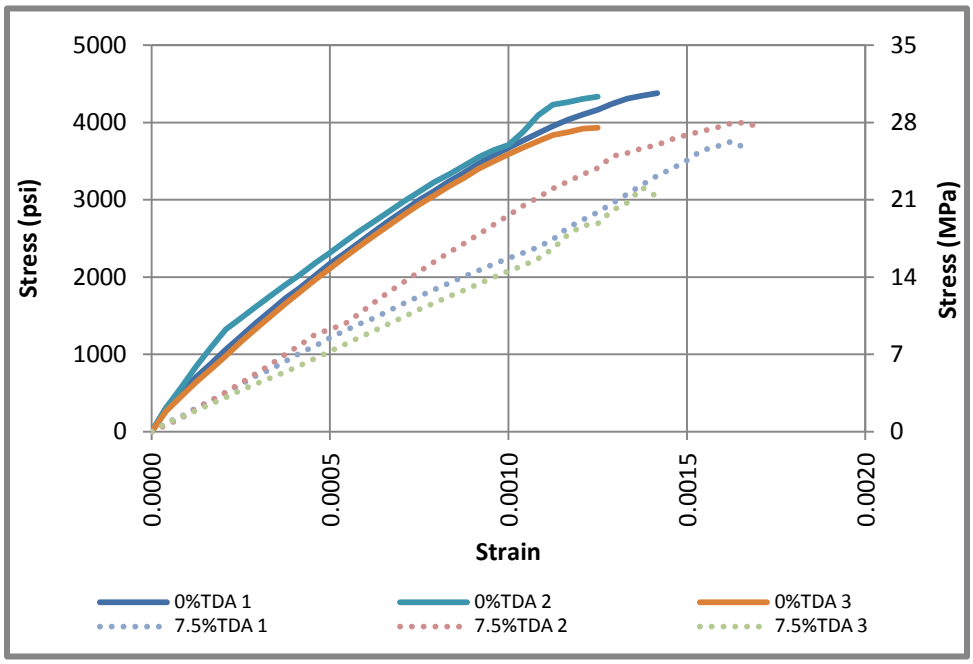

Figure 8.6: Stress vs. Strain Comparison between the Control Concrete (0%TDA) and Concrete containing TDA (7.5%TDA).

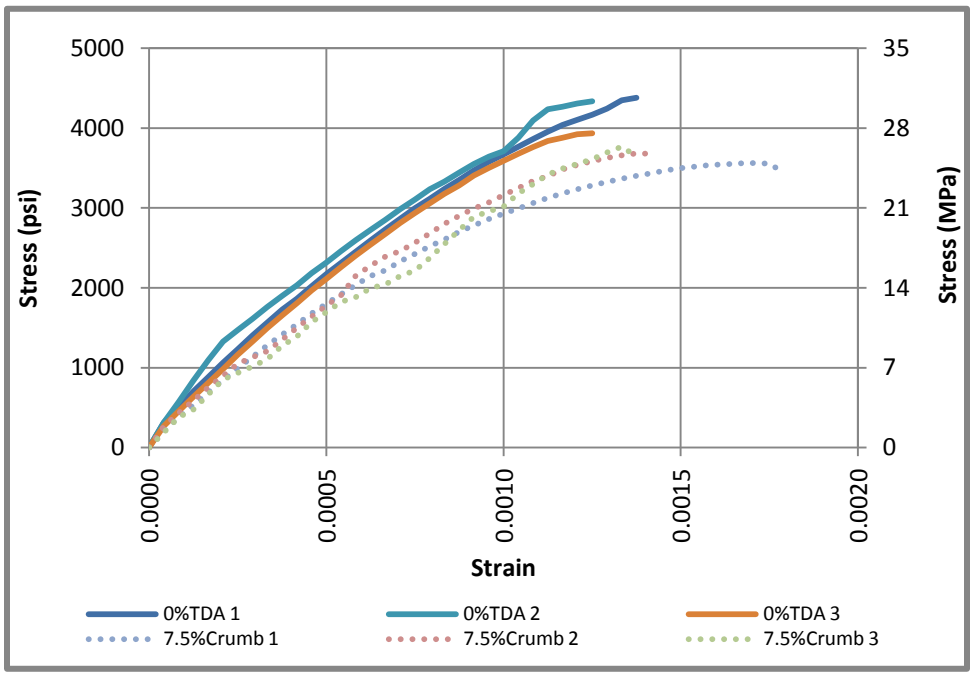

Figure 8.7: Stress vs. Strain Comparison between the Control Concrete (0%TDA) and Concrete containing Crumb Rubber (7.5%Crumb).

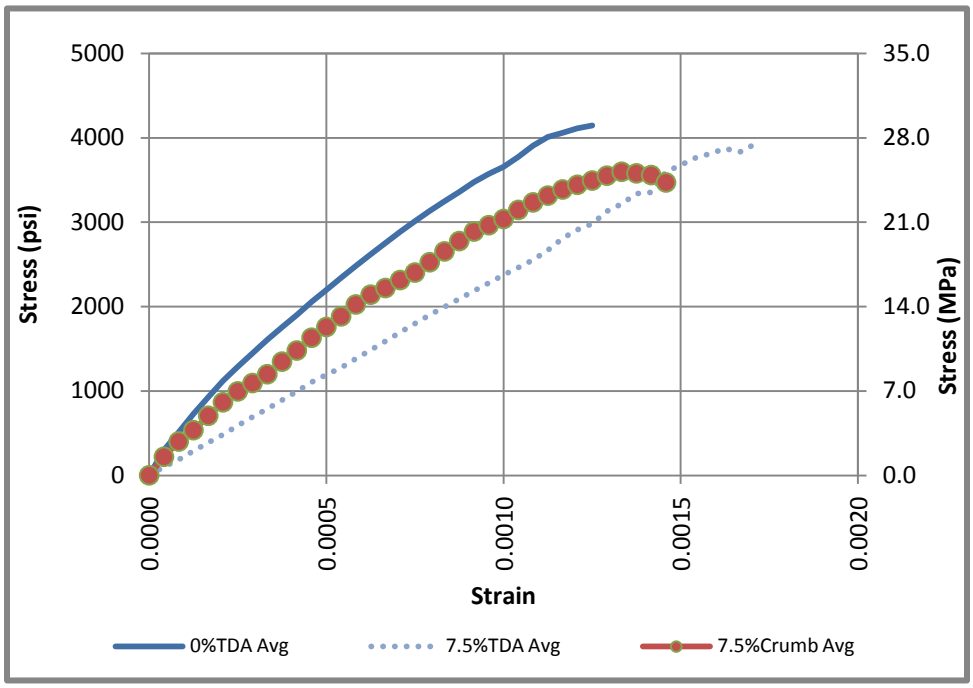

Figure 8.8: Average Stress vs. Strain Comparison for the three types of concrete

8.3 Specifying a Concrete Smeared Cracking Model

8.3.1 Element

The main problem examines a four –point bending test of a three-dimensional concrete beam. Therefore a three-dimensional, deformable extruded solid element in ABAQUS/CAE was chosen and defined in the part module as shown in Figure 8.9. Although concrete is a composite material, the solid was assumed to be homogenous and the different properties due to various concrete ingredients like TDA are accounted for in the material property definitions. The assumption of the material as a homogenous solid was done in the property module in the section manager as shown in Figure 8.10.

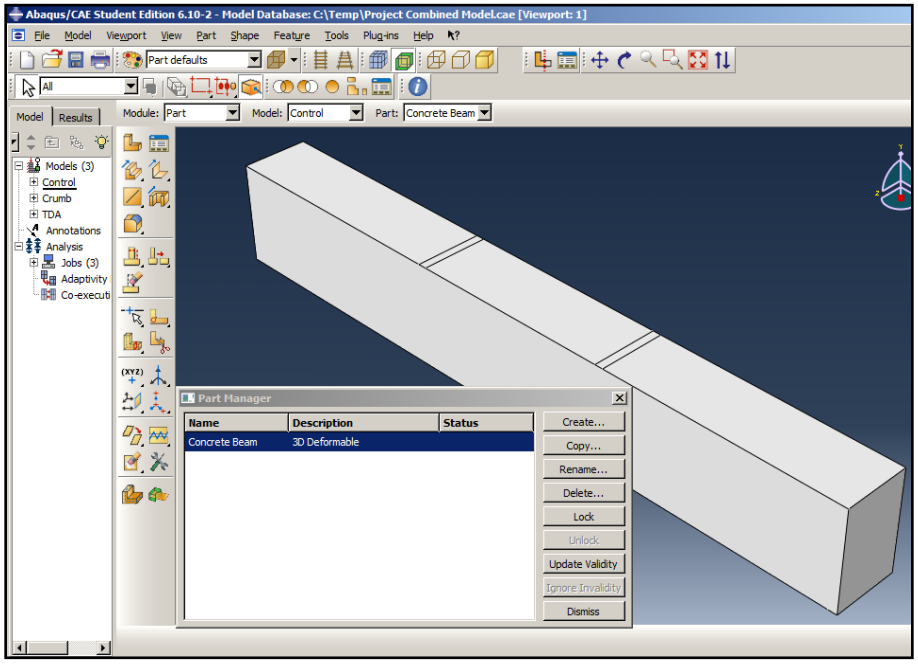

Figure 8.9: Definition of the concrete beam in the part module

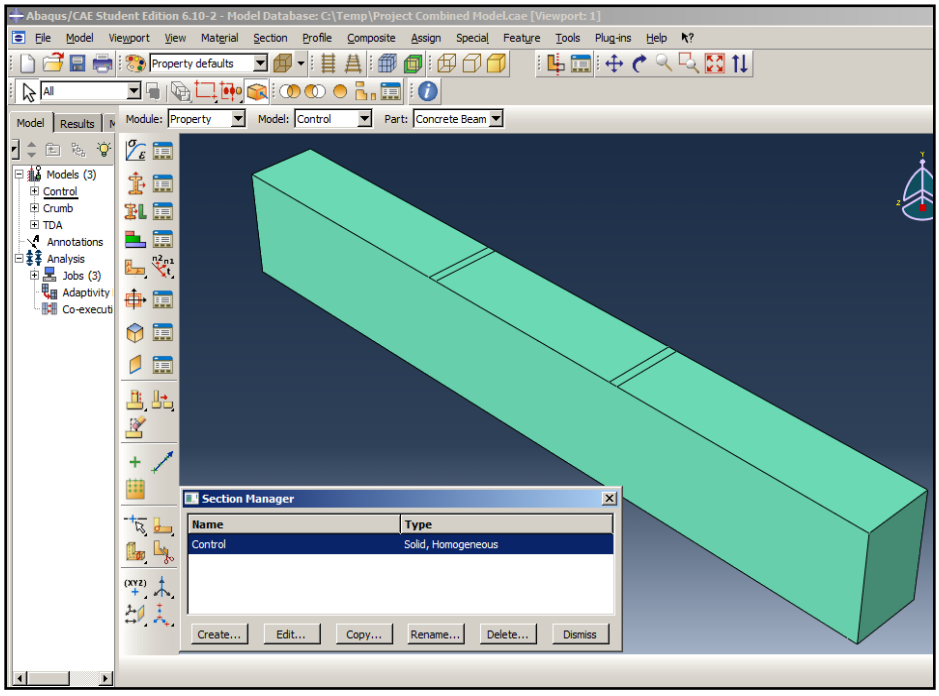

Figure 8.10: Definition of the material as a homogeneous solid

An 8-node linear brick, reduced integration (C3D8R) element is used for the ABAQUS/Explicit analysis. This was defined in the mesh module as an element type to be used in the analysis as shown in Figure 8.11. The mesh had a global size of 2.4" (36x5x3 elements). The reasonable agreement between the analysis results and the experimental data suggests that the mesh is adequate to predict overall response parameters with usable accuracy.

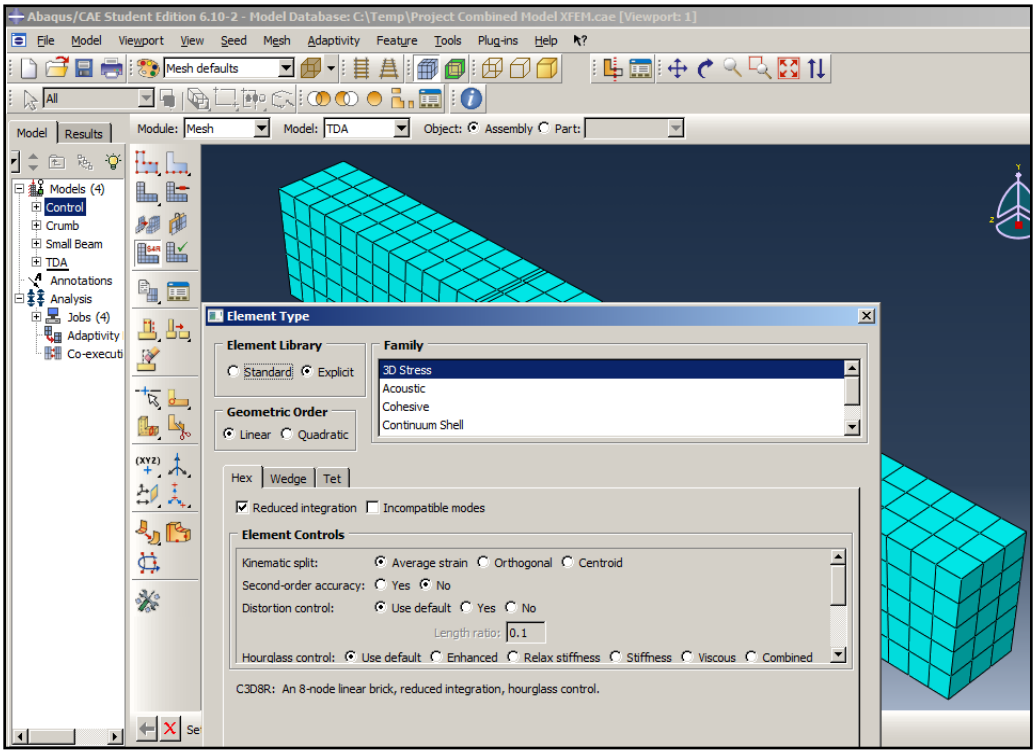

Figure 8.11: Definition of Element type in the mesh module

8.3.2 Material Properties

8.3.2.1 Elastic Range

Two material constants are required to characterize the linear elastic behavior of the material: Young's Modulus (E) and Poisson's ratio (γ). These are defined in the property module as shown in Figure 8.12. The Young Modulus (E) is calculated for the three types of concrete in this study from Figure 8.6 and Figure 8.7. These are summarized in Table 8.3.

Table 8.3: Young Modulus (E) of different types of concrete

	Young Modulus (E), psi
Control (0%TDA)	3,584,430
Concrete with TDA (7.5%TDA)	2,865,660
Concrete with Crumb Rubber (7.5%Crumb)	3,010,650

Poisson Ratio (γ) for concrete ranges from 0.15 - 0.20 [1] and an average value of 0.18 [1] would be used throughout. Poisson Ratio is usually lower in higher- strength concrete.

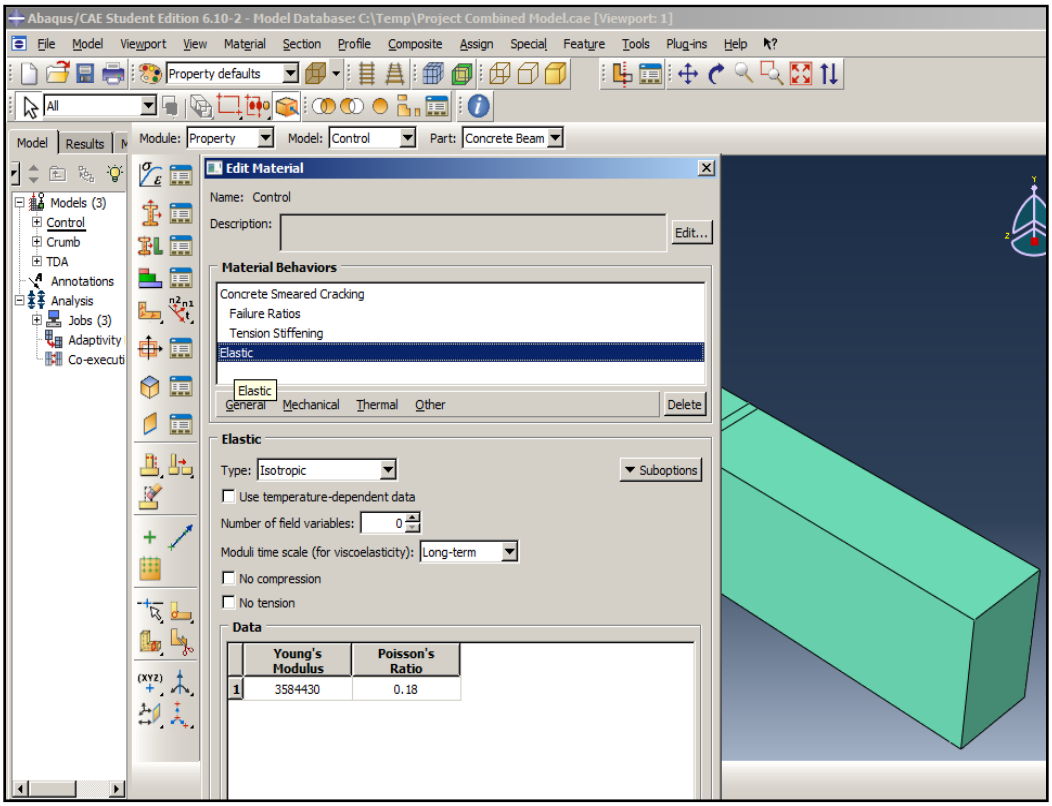

Figure 8.12: Definition of material property in the elastic range

8.3.2.2 Plastic Range

The concrete smeared cracking model was used to define the properties of plain concrete outside the elastic range in ABAQUS. The data required is the absolute value of compressive stress and the absolute value of plastic strain. The first stress-strain point given is at zero plastic strain and will define the initial yield point for that specific type of concrete. Values of

compressive and plastic strain are extracted from Figure 8.6, Figure 8.7 and Figure 8.8 and are summarized in Table 8.4. Figure 8.13 illustrates the definition of properties of plain concrete outside the elastic range using smeared cracking model in the property module.

Table 8.4: Values of absolute compressive stress and plastic strain in the plastic range

	% f'_c	**Stress (σ)**	**Plastic Strain (ε)**
Control (0%TDA)	50% f'_c	2072	0
	75% f'_c	3133	0.00033
	100% f'_c	4144	0.00079
Concrete with Crumb Rubber (7.5%Crumb)	50% f'_c	1797	0
	75% f'_c	2774	0.00038
	100% f'_c	3595	0.00083
Concrete with TDA (7.5%TDA)	50% f'_c	1961	0
	75% f'_c	2942	0.0004
	100% f'_c	3923	0.00088

When loading concrete under uniaxial compression up to 30-50% of ultimate strength, f'_c, microcracks in the ITZ would extend due to stress concentration at the crack tip even though no cracking occurs in the mortar matrix. Crack propagation is assumed stable (crack length reaches its final value if the applied stress is held constant). At 50-75% f'_c, ITZ cracks begin to grow again and crack system tends to be unstable. At >75% f'_c, the available internal energy is more than crack release energy and rate of crack propagation would increase and system become unstable. This stage is referred as *"Critical stress"* marking the onset of unstable propagation.

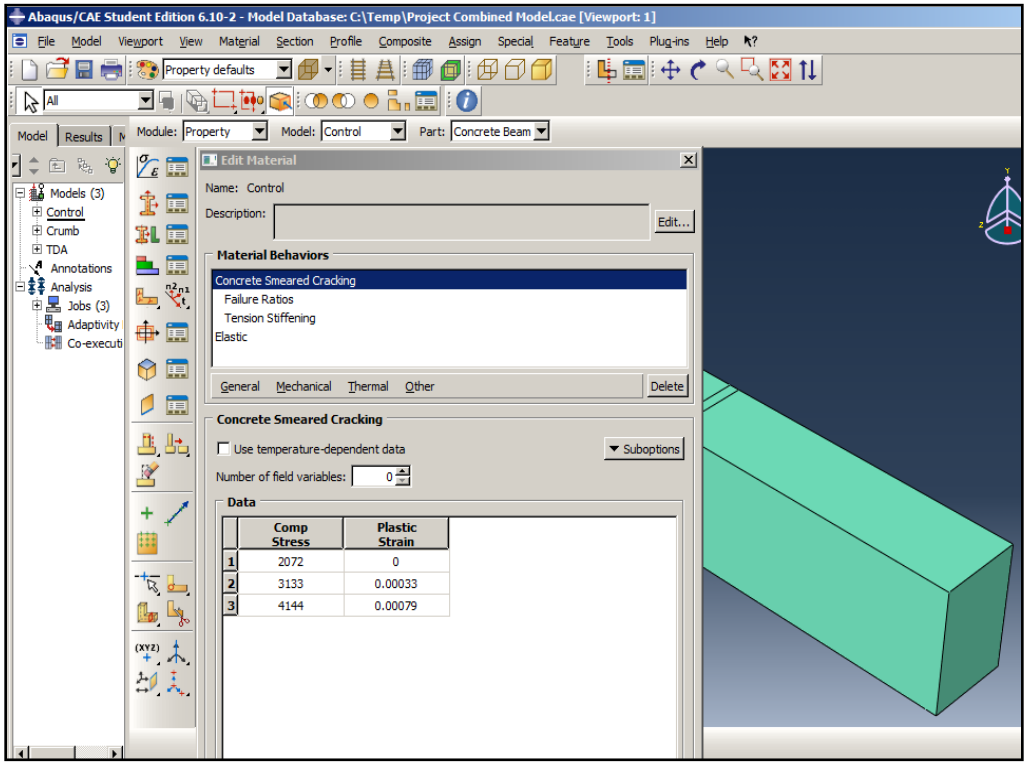

Figure 8.13: Description of material outside the elastic range using smeared cracking model

8.3.2.3 Tension Stiffening

Tension Stiffening is used to model the postfailure behavior for direct straining across cracks which allows for the strain-softening behavior for cracked concrete. Tension stiffening information is required for the concrete smeared cracking model. Tension stiffening would be specified by applying a fracture energy cracking criterion since no reinforcement was used in the concrete. Fracture energy cracking criterion is based on Figure 8.14.

For fracture energy cracking criterion, concrete's brittle behavior is characterized by a *stress-displacement* response rather than a *stress-strain* response. The energy required to open a unit area of crack is considered a material parameter.

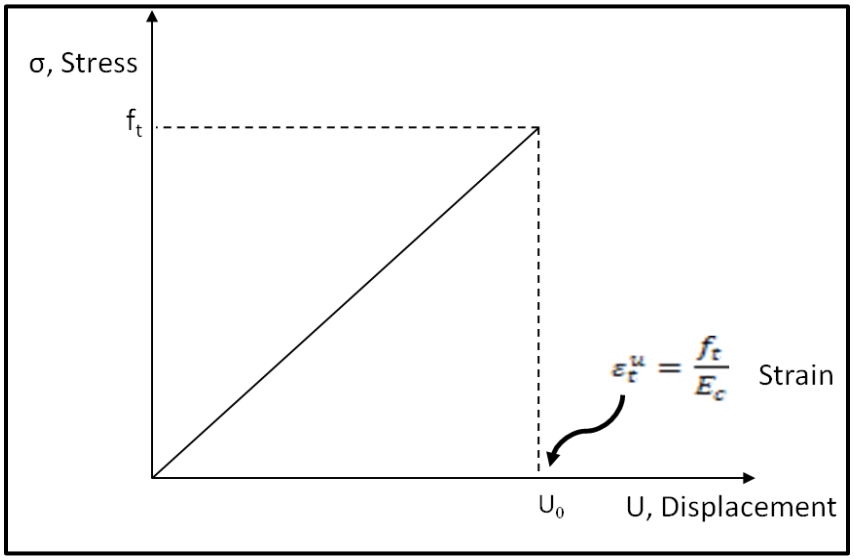

Figure 8.14: Fracture energy cracking criterion for Plain Concrete

The values of U_0 are extracted from Figure 8.5 and are summarized in Table 8.5. Tension stiffening is specified in the property module under the sub-options in the smeared cracking model as shown in Figure 8.15. These values of U_0 are cross checked with the condition given in Equation (8.1) where the length of specimen, L, is 20 inches and the values of ε_t^u are as calculated from Equation (8.2).

$\varepsilon_t^u < \frac{u_0}{L}$, L is the length of the specimen. (8.1)

Table 8.5: Values of U_0 for Tension Stiffening (Fracture Energy cracking criterion)

	U_0 (in)	ε_t^u
Control (0%TDA)	0.010	0.00018
Concrete with TDA (7.5%TDA)	0.014	0.00021
Concrete with Crumb Rubber (7.5%Crumb)	0.012	0.00022

In order to simulate the cracking of concrete, tension stiffening based on Figure 8.14 was required. Defining the maximum tensile strain as shown in Equation (8.2) and Figure 8.14, then ε_t^u can be calculated from the available experimental data for the three types of concrete and is shown in Table 8.5. For relatively heavily reinforced concrete modeled with a fairly detailed mesh,

an assumption that the strain softening after failure reduces the stress linearly to zero at a total strain of about 10 times the strain at failure can be made [49].

$$\varepsilon_t^u = \frac{f_t}{E_c} \tag{8.2}$$

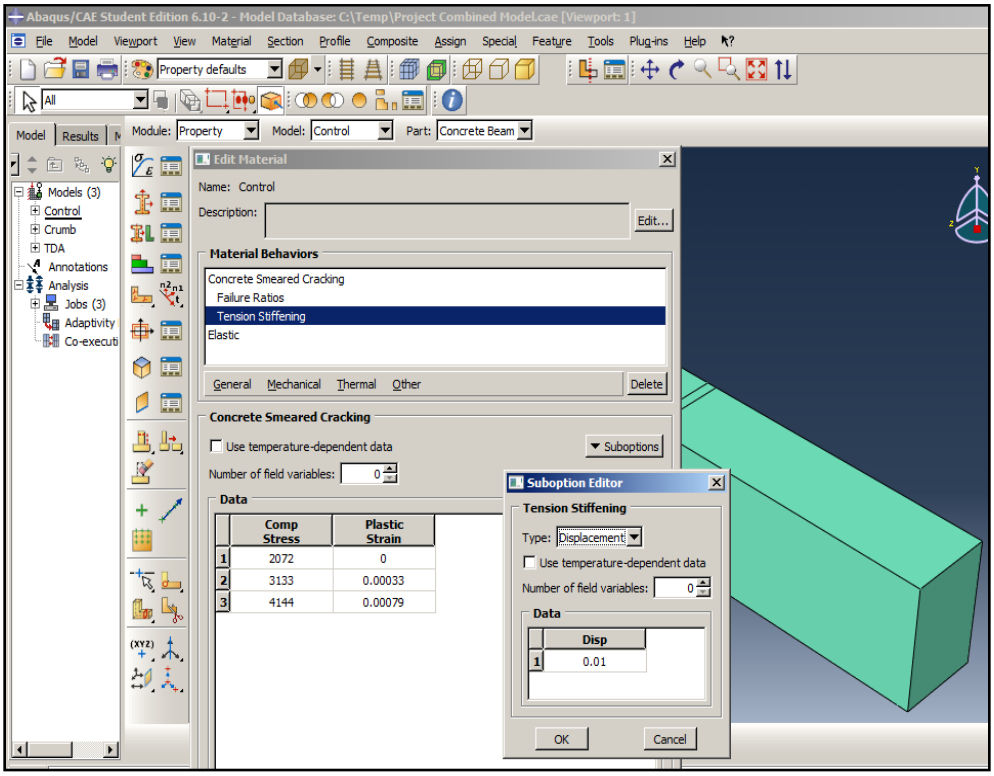

Figure 8.15: Definition of Tension stiffening in the property module

8.3.3 Crack Detection

The use Extended Finite Element Method (XFEM) to study the initiation and propagation of a crack along an arbitrary, solution-dependent path has been adopted in this study. XFEM is available for three-dimensional solid and two-dimensional planar models. Three-dimensional shell models are not supported. XFEM crack is defined in the Interaction Module of ABAQUS/Standard or ABAQUS/Explicit as shown in Figure 8.16.

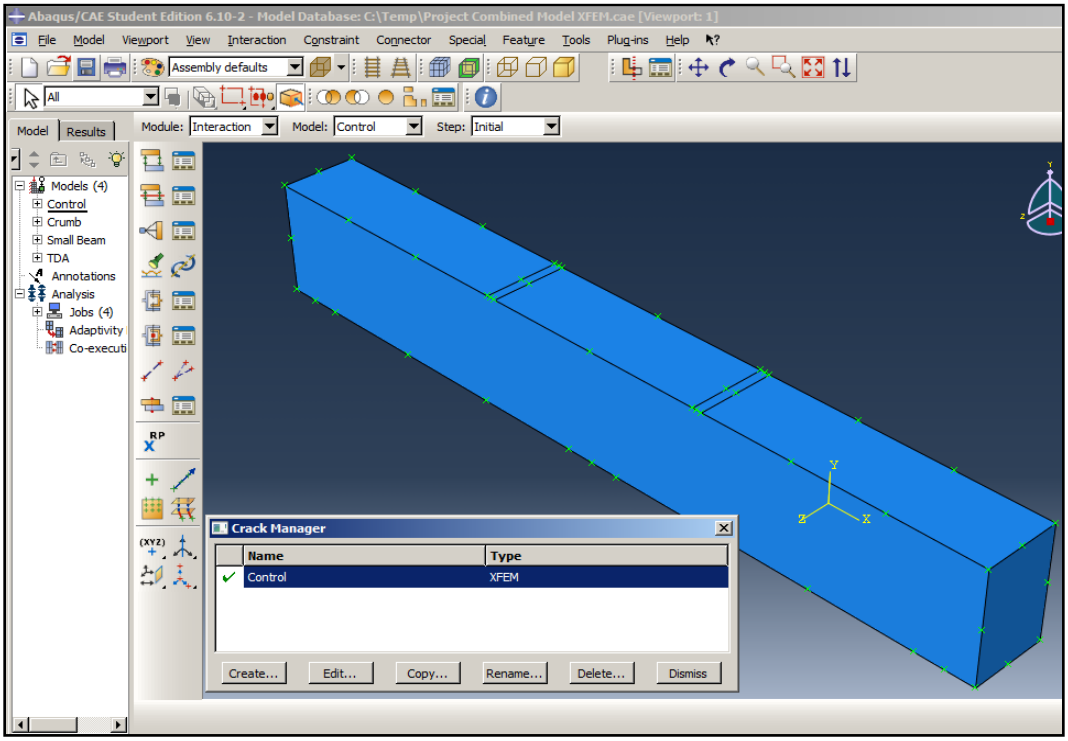

Figure 8.16: Definition of XFEM in interaction module

To define XFEM, one must also specify the conditions that will initiate a crack by specifying damage initiation criteria in the material definition. The criterion can be based on either maximum principal stress or maximum principal strain. Maximum principal stress was adopted in this study since the approximate peak value of flexural stress was already known from experimental data as shown in Table 8.6. This was defined in the property module as shown in Figure 8.17.

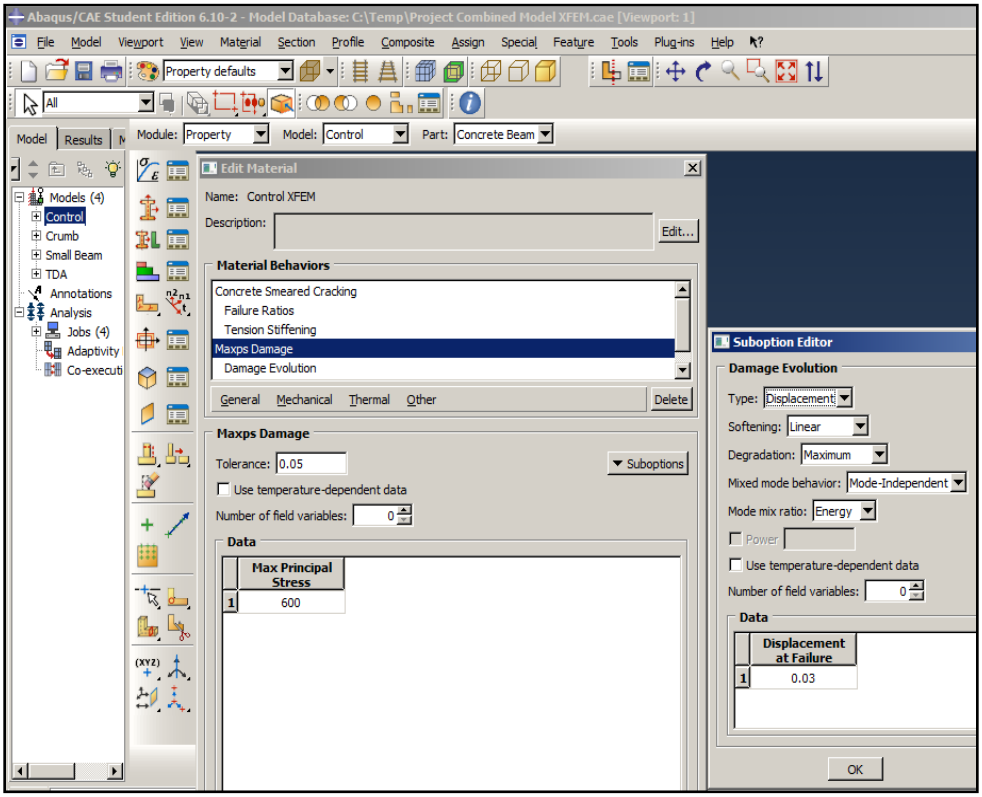

Figure 8.17: Definition of maximum principal criterion and damage evolution

The maximum principal stress criterion can be represented by Equation (8.3) and damage is assumed to initiate when the maximum principal stress ratio, f, (as defined in the expression (8.3)) reaches a value of one. Displacement was also defined in the material properties to define the evolution of damage leading to eventual failure. Displacement again was chosen Figure 8.17 in this regard since the maximum displacement for the beams was also known from experimental data.

$$f = \left\{\frac{\sigma_{max}}{\sigma^{o}_{max}}\right\}, \sigma^{0}_{max} = \text{the maximum principal stress} \qquad (8.3)$$

Table 8.6: Maximum Compressive and Flexural strength for different types of concrete

Component	0%TDA (psi)	7.5%TDA (psi)	7.5%Crumb (psi)
Average Max. Compressive Strength	4440	3907	3902
Average Max. Flexural Strength for 20"×6"×6" Beams	648	608	675
Average Max. Flexural Strength for Full-scale Beams (84"×12"×8")	662	530	544

A number of expressions have been developed to represent the relationship between flexural and compressive strengths of concrete. The relationship that is used by ACI [1] is shown in Equation (8.4). Based on the data in Table 8.6, the values of α in Equation (8.4) for the three types of concrete are 9.7 for 0%TDA and 7.5%TDA concrete and 10.8 for 7.5%Crumb concrete.

$$f_t = \alpha\sqrt{f_c'} \quad \text{Where } \alpha = 7.5. \tag{8.4}$$

The Modulus of Elasticity is also related to compressive strength and density. One of empirical relationships between the modulus of elasticity and compressive strength is given in the ACI Building Code (ACI 318) [1] as shown in Equation (8.5).

$$E_c = 57000\sqrt{f_c'} \tag{8.5}$$

Where E_c is the secant modulus of elasticity (at about 45% of the ultimate strength), f_c' is the compressive strength of the standard 150 x 300mm (6 x 12 in) cylinder and f_t is the flexural strength of concrete loaded in bending.

Based on data in Table 8.6 the elastic modulus for the three types of concrete is calculated as 3,798,100 psi, 3,562,840 psi, and 3,560,560 psi for 0%TDA concrete, 7.5%TDA concrete and 7.5%Crumb concrete respectively. The values of elastic modulus for Control concrete (0%TDA) closely match those values calculated from the stress vs. strain curves in Figure 8.6 and Figure 8.7 as shown in Table 8.3 but for the concrete containing TDA and Crumb Rubber, the equation overestimates the modulus by about 20%. This implies Equation (8.5)

cannot be used for concrete containing TDA or Crumb Rubber unless the right density for this concrete is incorporated into the equation.

8.3.4 Viewing of an XFEM Crack

In order to view an XFEM crack, a field output for the signed distance function, PHILSM must be requested. PHILSM is a signed distance function that describes the crack surface. To further investigate the crack in more detail a contour plot of the signed distance function (PHILSM) is created showing in which elements the signed distance values are negative or positive. The crack surface is situated in the elements where the value of PHILSM transitions from a negative number to a positive number.

Another ABAQUS function STATUSXFEM can also used to show the status of the enriched element. The status of an enriched element is 1.0 if the element is completely cracked and 0.0 if the element contains no crack. If the element is partially cracked, the value of STATUSXFEM lies between 1.0 and 0.0.

8.3.5 Solution control

Since considerable nonlinearity is expected in the response, including the possibility of unstable regimes as the concrete cracks the Nlgeom setting in ABAQUS was turned on in the step module as shown in Figure 8.18. Nonlinear effects result from large displacements and deformations. The Nlgeom setting for a step determines whether ABAQUS will account for geometric nonlinearity in that step [49]. Static, General step was used in the analysis.

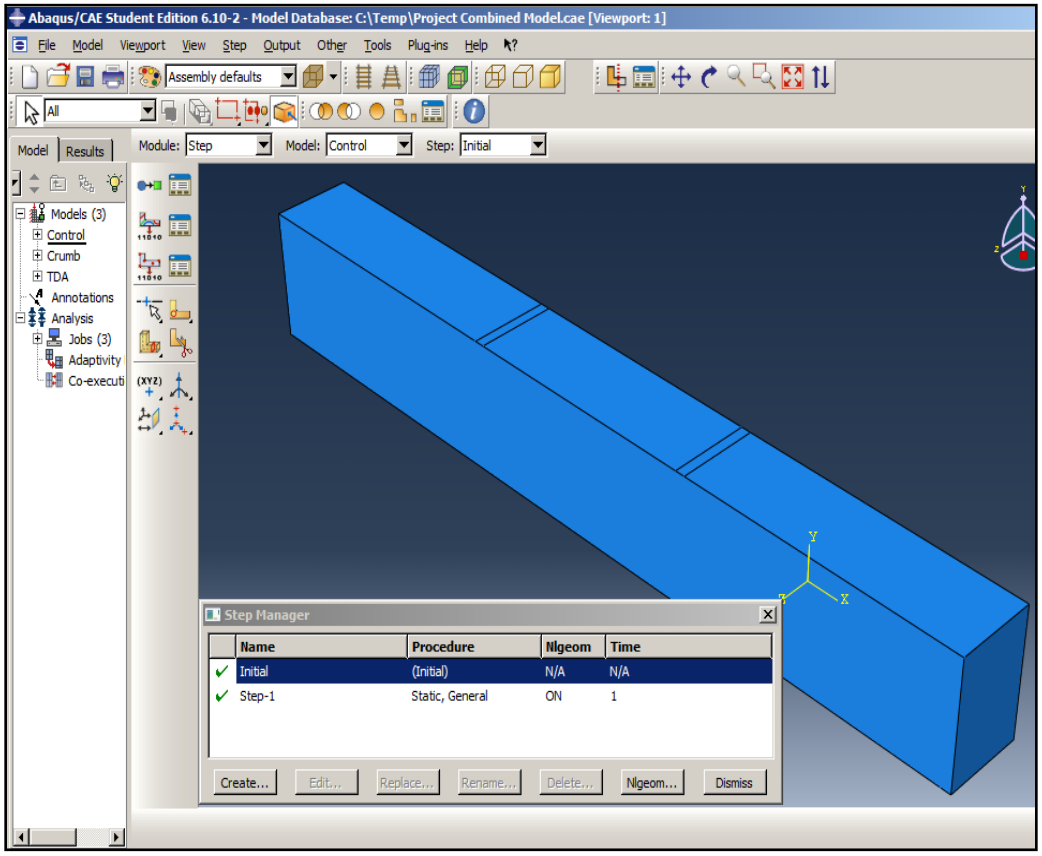

Figure 8.18: Nigeom Setting in the step module for solution

ABAQUS uses Newton's method to solve the nonlinear equilibrium equations therefore; the solution usually is obtained as a series of increments, with iterations to obtain equilibrium within each increment. Automatic incrementation scheme was preferred to let ABAQUS select increment sizes based on computational efficiency to ensure convergence of the solution. However the maximum increment size of 0.01 was specified.

In a nonlinear analysis the solution cannot be calculated by solving a single system of linear equations, as would be done in a linear problem. Instead, the solution was found by specifying the loading as a function of time and incrementing time to obtain the nonlinear response. Therefore the simulation was broken into a number of *time increments* to find the approximate equilibrium configuration at the end of each time increment.

Zero-valued boundary displacement conditions in the x, y and z directions were prescribed as model data in the initial step in ABAQUS/CAE. Rotation degrees of freedom were not constrained as only bending was expected from the response. A distributed load (pressure load) was applied at two points from the top of the beam to simulate four-beam bending as shown in Figure 8.3 and Figure 8.19.

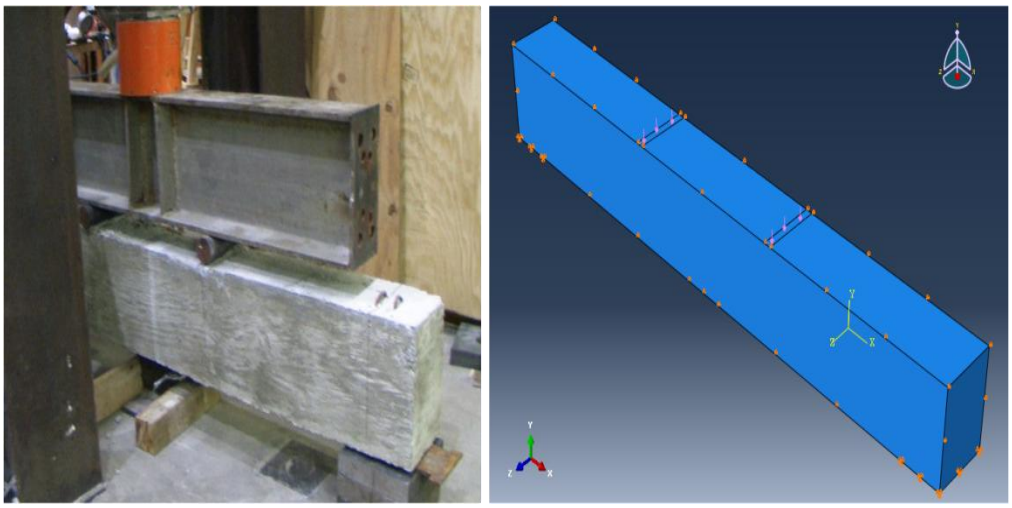

Figure 8.19: Boundary conditions and loading of full scale beams

8.4 Results and discussion

The numerical and experimental results are compared in Figure 8.20, Figure 8.22 and Figure 8.24 on the basis of Load versus Deflection at the center of the beam. The analysis shows a good agreement with the experimental data within the elastic limit. This analysis provides useful information from a design viewpoint. This means the assumption that the concrete beam was homogeneous therefore not accounting the Interfacial Transition Zone between the TDA and Crumb Rubber and the rest of the concrete was sufficient.

The plot contours for stress in the x-direction (tensile strength) is shown in Figure 8.21, Figure 8.23 and Figure 8.25. Superimposed on the contours are the experimental results of peak flexural stress (Modulus of Rupture) from field testing of beams.

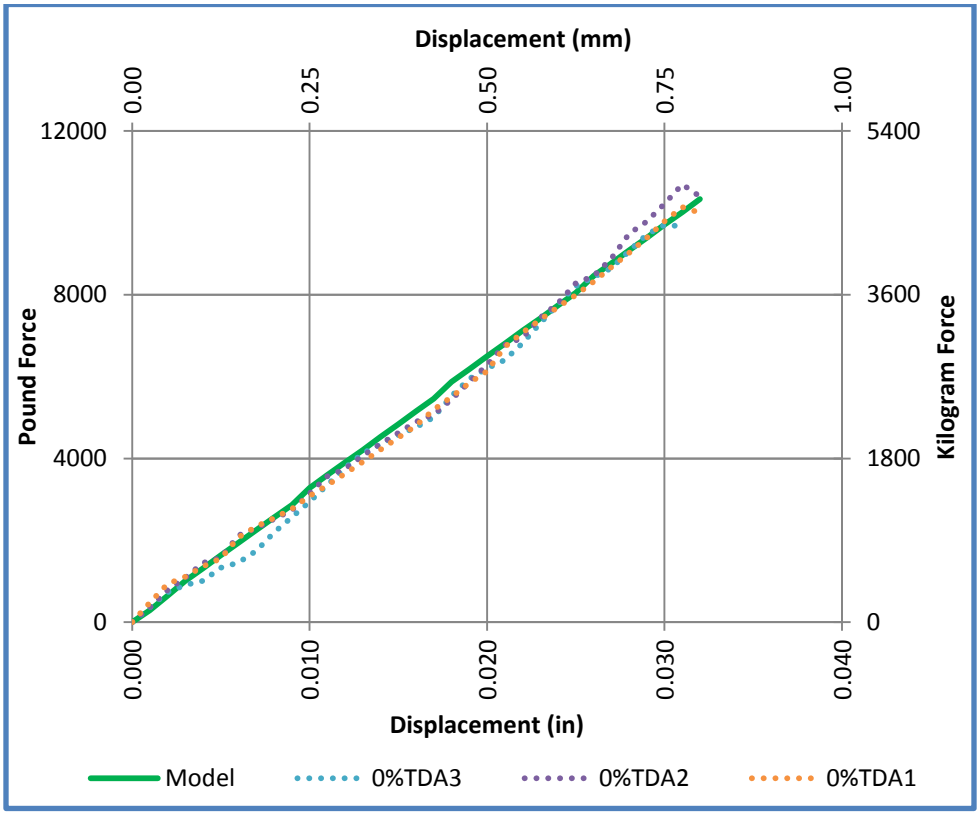

Figure 8.20: Numerical (Model) and Experimental results for Control Concrete (0%TDA)

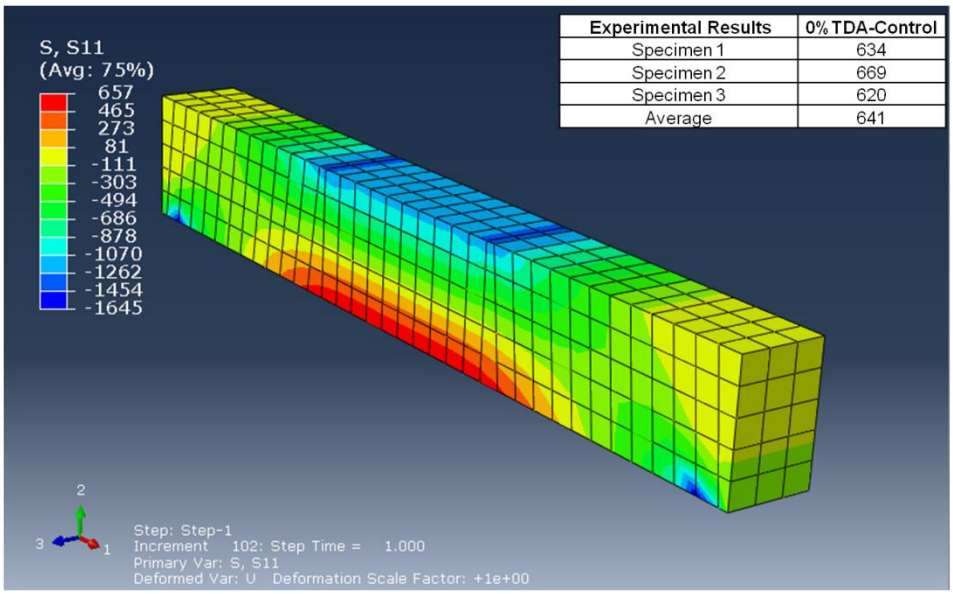

Figure 8.21: Numerical (Model) results for Control Concrete (0%TDA) (psi).

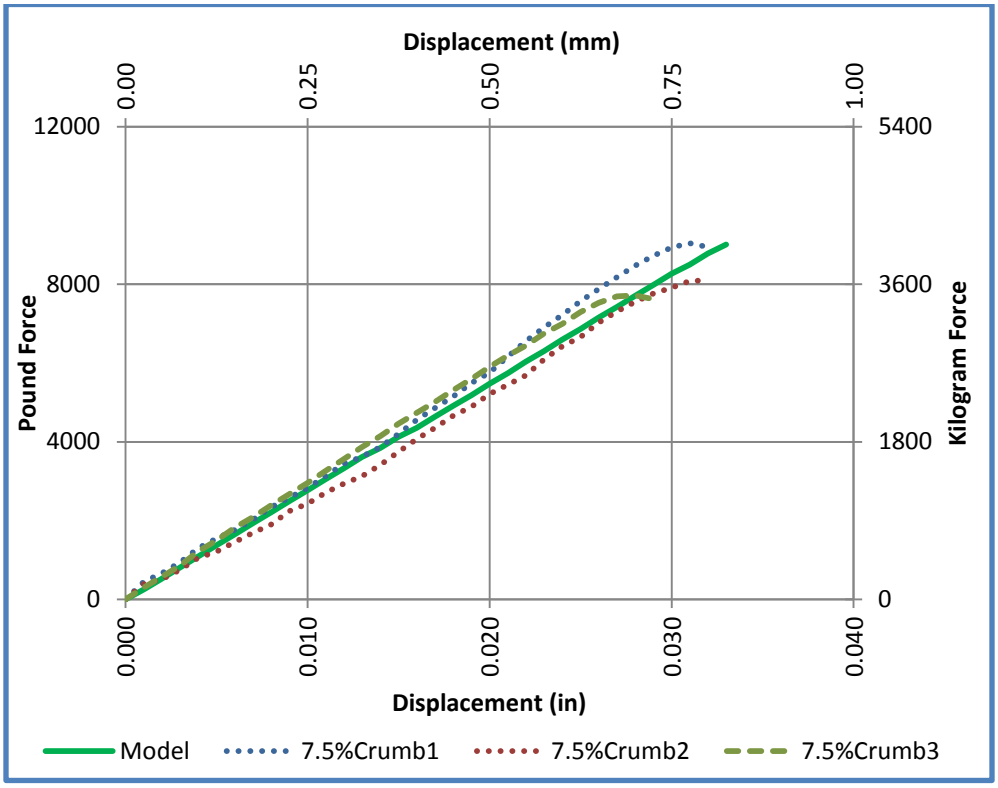

Figure 8.22: Numerical (Model) and Experimental results for Crumb Concrete (7.5%Crumb)

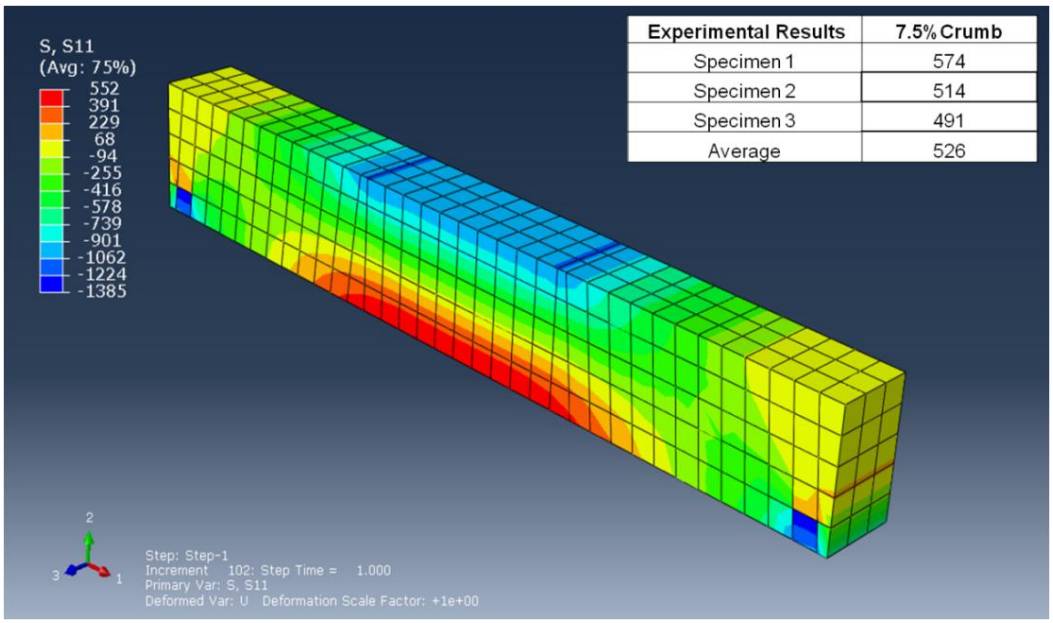

Experimental Results	7.5% Crumb
Specimen 1	574
Specimen 2	514
Specimen 3	491
Average	526

Figure 8.23: Numerical (Model) results for Crumb Concrete (7.5%Crumb) (psi)

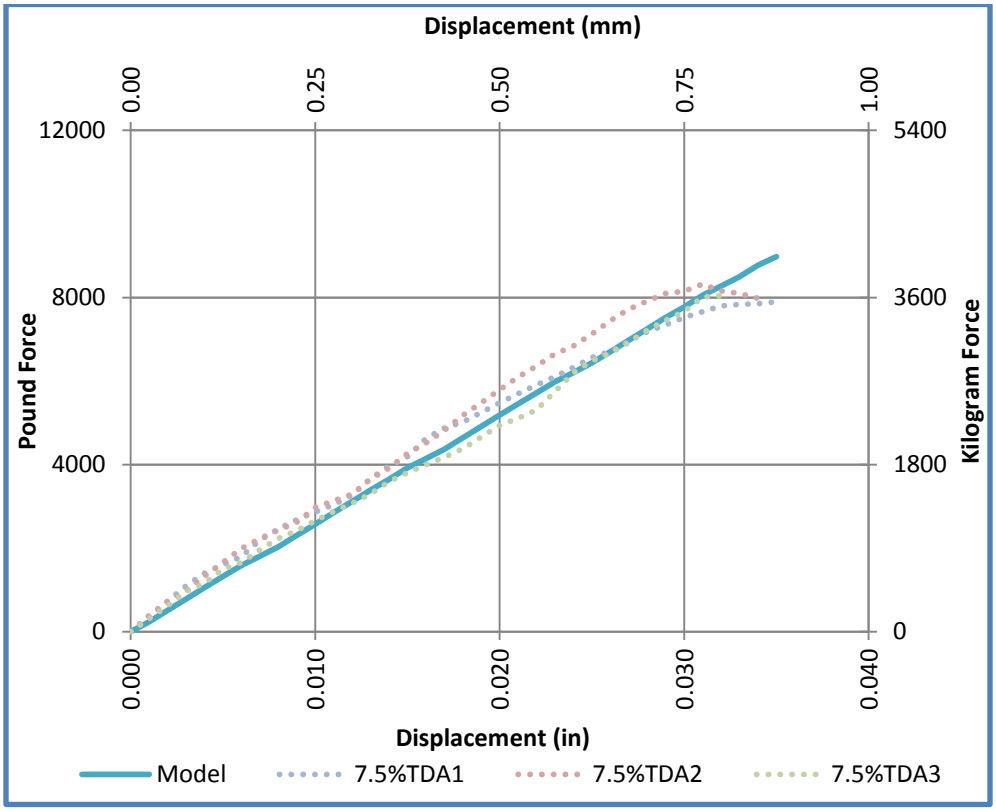

Figure 8.24: Numerical (Model) and Experimental results for TDA Concrete (7.5%TDA)

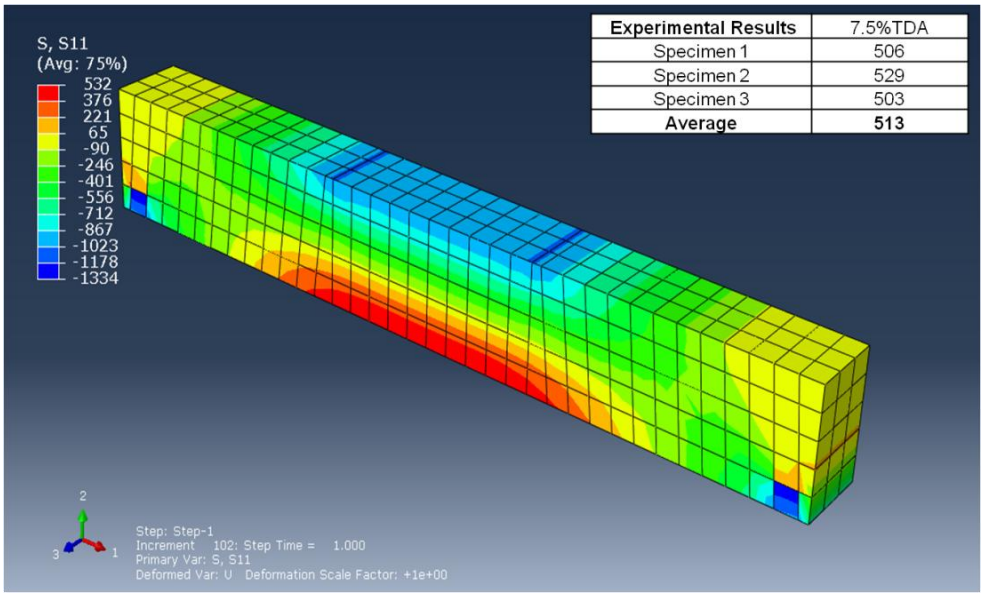

Figure 8.25: Numerical (Model) results for TDA Concrete (7.5%TDA) (psi)

The failure pattern in the control concrete (0%TDA) as predicted by the model is shown in Figure 8.26, which shows the predicted crack on the lower surface of the beam, generally at the center of the beam. This is consistent with the observed results from the experiment as shown in Figure 8.29.

For Concrete containing TDA and Crumb rubber, two possible locations for crack initiation are predicted by the model as shown in Figure 8.27 and Figure 8.28. The crack initiation locations predicted by the model are within the middle third hence the equation for modulus of rupture as given by ASTM C78 would still be valid. These predictions are also consistent with experimental results where it was observed that most of the specimens with TDA and Crumb Rubber did not fail at the center of the beam as shown in Figure 8.29, Figure 8.30, Figure 8.31 and Figure 8.32.

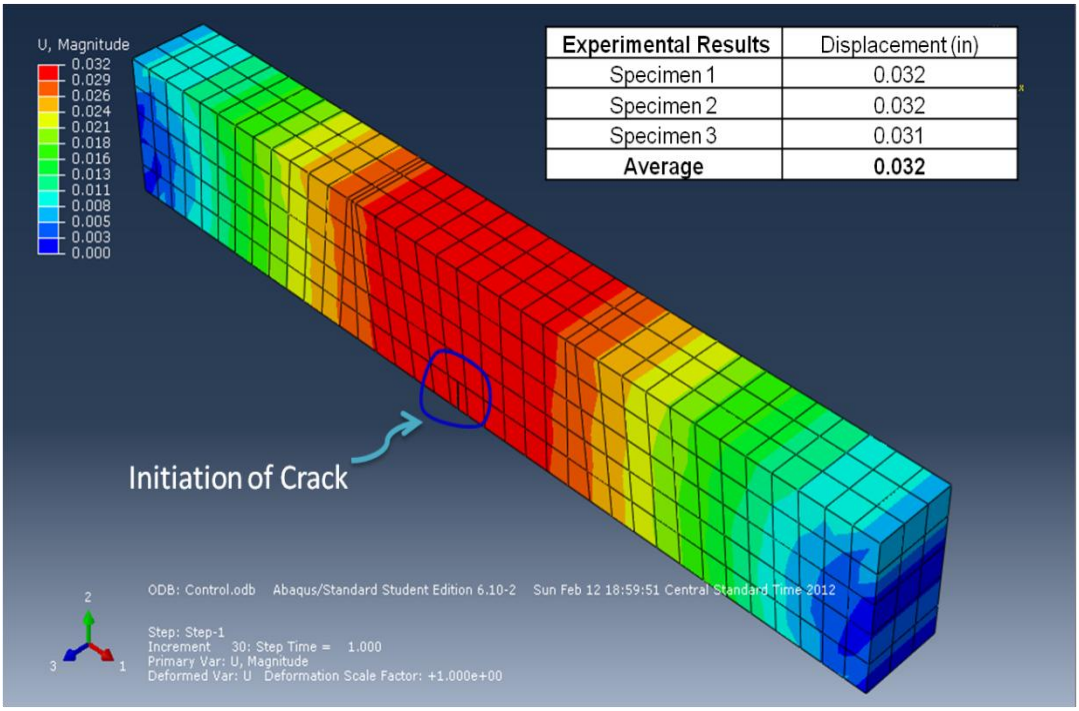

Figure 8.26: Initiation of Cracking in the control concrete (0%TDA)

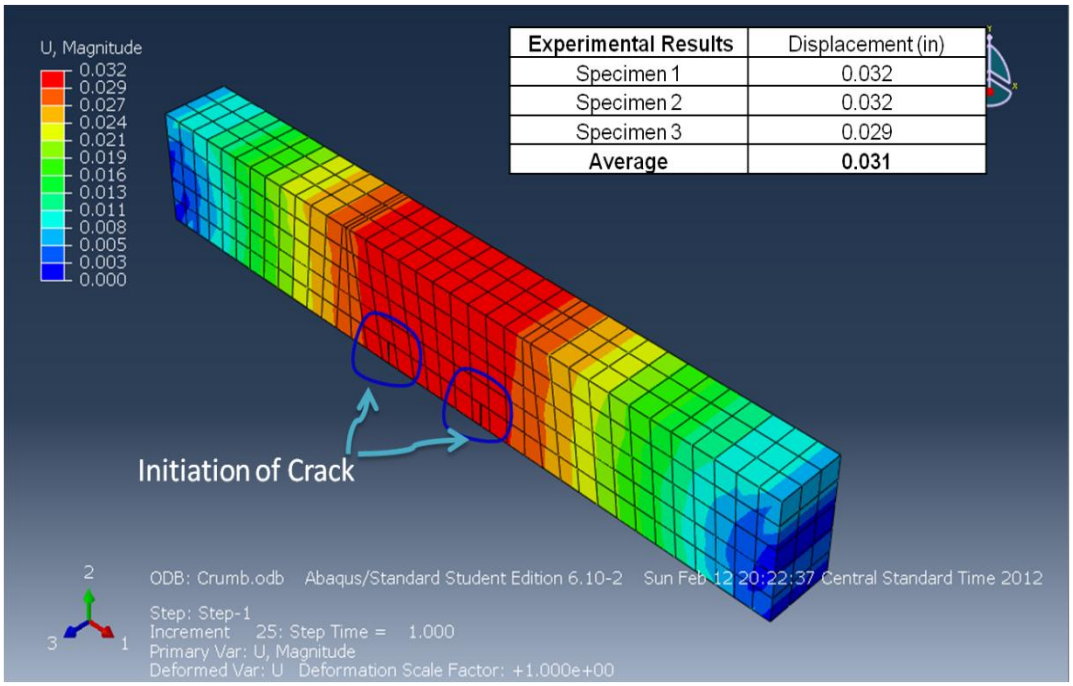

Figure 8.27: Initiation of Cracking in the crumb concrete (7.5%Crumb)

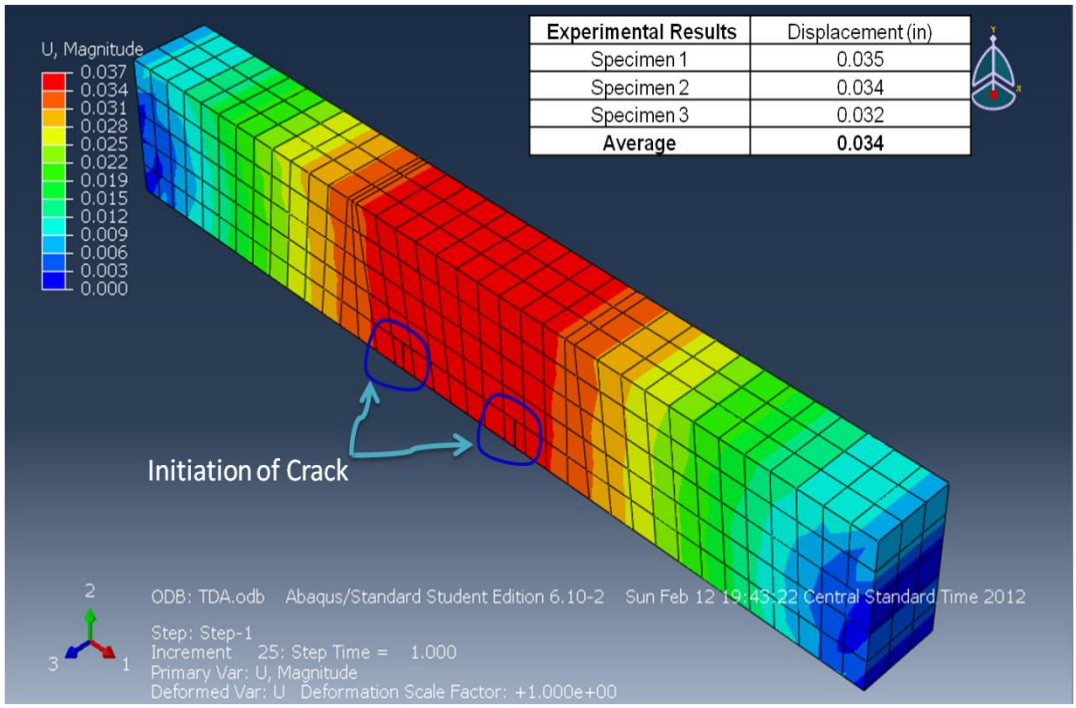

Figure 8.28: Initiation of Cracking in the TDA concrete (7.5%TDA)

Figure 8.29: Experimental Results for the Control concrete (0%TDA) Beam

Figure 8.30: Experimental Results for the Crumb concrete (7.5%Crumb) Beam

Figure 8.31: Experimental Results for the TDA concrete (7.5%TDA) Beam showing crack running at an angle to the direction of loading

Figure 8.32: Experimental Results for the TDA concrete (7.5%TDA) Beam. The Beam with TDA did not fall into two halves.

Notable failure differences between the concrete with TDA and the other two types of concrete is that concrete with TDA did not generally break into two halves and in some cases the crack was noted to be at an angle to the direction of loading as shown in Figure 8.31.

8.5 Mesh Convergence

A finite element (FE) analysis requires the idealization of an actual physical problem into a mathematical model and then the finite element solution of that model. A proper finite element solution should converge as the number of elements is increased to the analytical (exact) solution of the differential equations that govern the response of the mathematical model [50]. For a situation where the differential equations of motion are not known, convergence of an FE solution can only be measured on the fact that all basic kinematic, static and constitutive conditions contained in the mathematical model must be ultimately (at convergence) be satisfied [50]. By definition therefore, Finite element scheme exhibits convergence if the discretization error $\rightarrow 0$ as the mesh is made infinitely fine (i.e., element size $\rightarrow 0$).

Numerous control parameters are associated with the convergence and integration accuracy algorithms in ABAQUS. These parameters are assigned values that are chosen to optimize the accuracy and efficiency of the solution for a wide spectrum of nonlinear problems. The criteria used to establish convergence of nonlinear increments is the automatic adjustment of increment size based on the convergence rate. However, the most important consideration in the choice of the control parameters is that any solution accepted as “converged” is a close approximation to the exact solution of the nonlinear equations [49].

How ABAQUS Determines Convergence

Consider the external forces, *P*, and the internal (nodal) forces, *I*, acting on a body (see Figure 8.33(a) and Figure 8.33(b), respectively). The internal loads acting on a node are caused by the stresses in the elements that are attached to that node.

For the body to be in equilibrium, the net force acting at every node must be zero. Therefore, the basic statement of equilibrium is that the internal forces, *I*, and the external forces, *P*, must balance each other as shown in Equation (8.6).

$$P - I = 0 \tag{8.6}$$

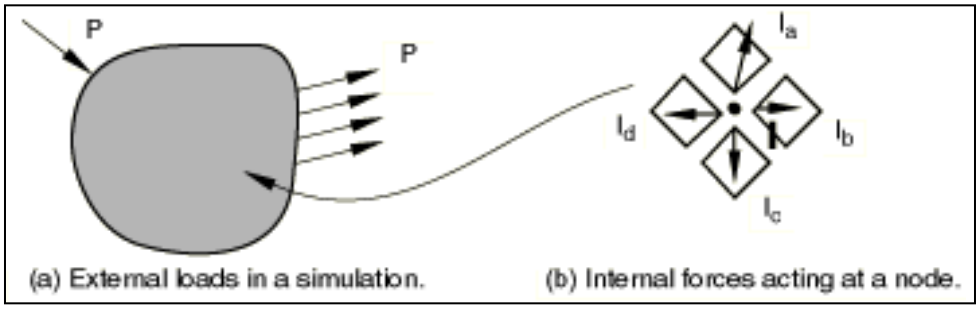

Figure 8.33: Internal and external loads on a body [49]

The nonlinear response of a structure to a small load increment, ΔP, is shown in Figure 8.34. ABAQUS uses the structure's tangent stiffness,K_0, which is based on its configuration at, u_0 to calculate a *displacement correction*,c_a for the structure. Using c_a the structure's configuration is updated to u_a.

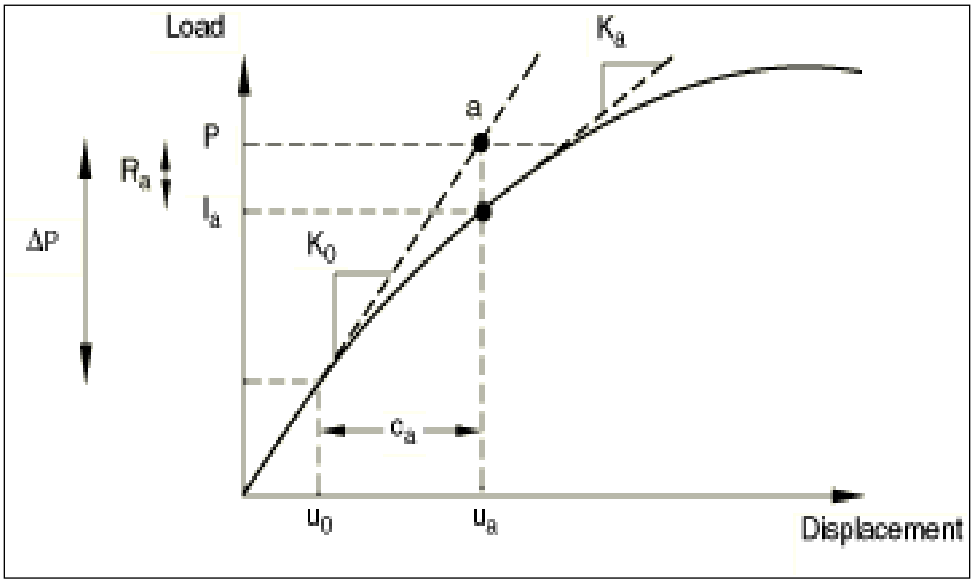

Figure 8.34: First iteration in an increment

ABAQUS then calculates the structure's internal forces, I_a, in this updated configuration. The difference between the total applied load, P, and I_a can now be calculated as shown in Equation (8.7), where R_a is the force residual for the iteration.

$$R_a = P - I_a \tag{8.7}$$

If R_a is zero at every degree of freedom in the model, point a in Figure 8.34 would lie on the load-deflection curve and the structure would be in equilibrium. In a nonlinear problem R_a will never be exactly zero, so ABAQUS compares it to a tolerance value. If R_a is less than this force residual tolerance at all nodes, ABAQUS accepts the solution as being in equilibrium. By default, this tolerance value is set to 0.5% of an average force in the structure, averaged over time.

If R_a is less than the current tolerance value, P and I_a are considered to be in equilibrium and u_a is a valid equilibrium configuration for the structure under the applied load. However, before ABAQUS accepts the solution, it also checks that the last displacement correction c_a is small relative to the total incremental displacement $\Delta u_a = u_a - u_o$. If c_a is greater than a fraction (1% by default) of the incremental displacement, ABAQUS/Standard performs another iteration. Both convergence checks must be satisfied before a solution is said to have converged for that time increment. If the solution from an iteration is not converged, ABAQUS performs another iteration to try to bring the internal and external forces into balance.

Three different meshes are used in ABAQUS/Explicit to assess the sensitivity of the results to mesh refinement: a coarse 4.0” × 4.0” mesh (22x3x2 elements), a medium 3.2” × 3.2” mesh (28x4x3 elements), and a fine 2.4” × 2.4” mesh (36x5x3 elements) of C3D8 elements. At least one hundred integration points are used through the thickness of the concrete beam to ensure that the development of plasticity and failure is modeled adequately. Mesh convergence studies were then performed by comparison of tensile stress-deflection response of the beam for the three different mesh densities as shown in Figure 8.35. Since the same model was used for the three different types of concrete, only the control concrete (0%TDA) was used in mesh convergence studies.

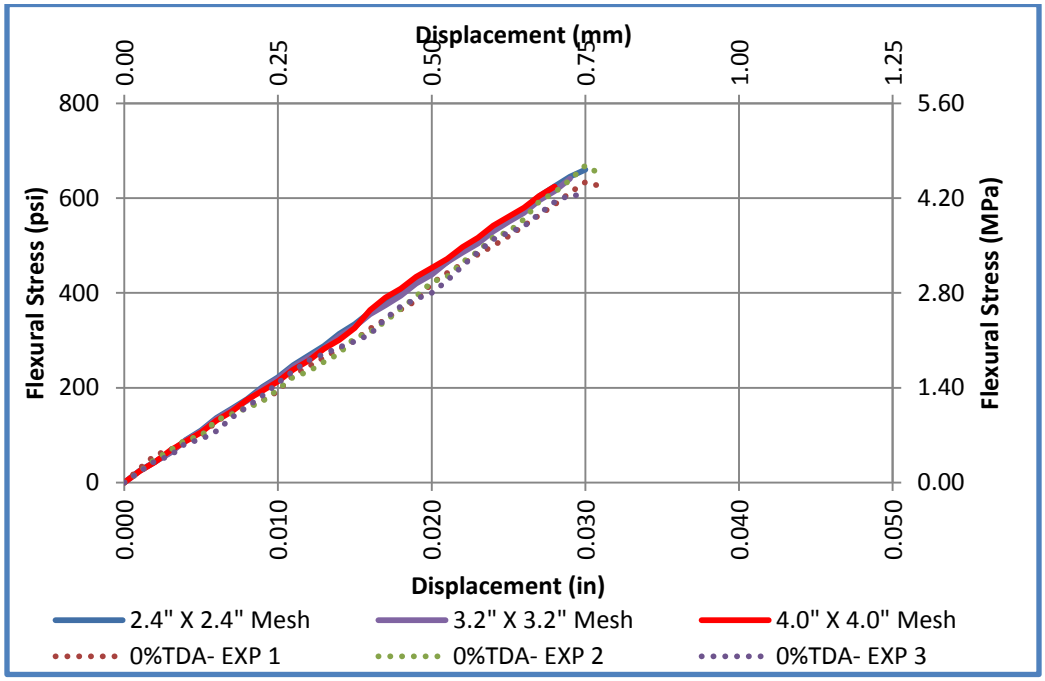

Figure 8.35: Mesh Sensitivity and convergence

8.6 Conclusion

In this study a three dimensional nonlinear Finite Element Model (FEM) of a concrete beam was proposed and developed for three types of concrete. The three types of concrete differed in composition by incorporating Tire Derived Aggregates of different sizes during batching. The material properties were defined with the smeared crack model in ABAQUS. The developed FEM is capable of predicting the ultimate load, deflections, Stress-deflection/strain curve and crack initiation which were all verified against the experimental tests. The experimental results showed close correlations when compared with those obtained from the FEM analysis.

CHAPTER 9

SUMMARY, CONCLUSIONS AND FUTURE WORK

9.1 Summary and Conclusions

The main question of this research was to find out if and how much Tire Derived Aggregate (TDA) or Crumb Rubber can be used in concrete without adversely effecting concrete strength and how properties of concrete change due to the introduction of these materials into the concrete mix. The difference between TDA and Crumb Rubber is size; otherwise they are all derived from used car tires. TDA for civil engineering applications generally ranges from 2" (50.8 mm) to ½" (12.7 mm) while Crumb Rubber size would be less than 3/8" (<10 mm).

It was found that small amounts TDA in the range of 7.5% to 10% with top size of 2" (50.8 mm) can be used to substitute for coarse aggregates in concrete with a target compressive strength of up to 4000 psi (27.5 MPa) but strength enhancing materials like silica fume need to be used. As the amount of TDA increases, the concrete compressive strength drops. At 7.5% of TDA replacing coarse aggregates, this drop is found to be averagely 10% compared to the control concrete if silica fume is added into the mixture. However, this amount of strength can also be achieved without using strength enhancing materials (Silica Fume) if the top TDA size is lowered from 2 in to 1 in.

Incorporating TDA into concrete was found to lower the modulus of elasticity of concrete by about 20% but the concrete toughness and ductility was increased. Silica Fume when used in concrete was found to increase compressive strength and consistency, but it has a negative effect to ductility. Workability of fresh concrete with TDA is slightly better as it has a slump of averagely 1 in. higher compared to the control concrete. At lower stresses of up to 3000 psi (20.6 MPa) concrete with TDA would deform elastically 20% more compared with concrete without TDA.

TDA lowers the Modulus of Rupture (Flexural Stress) of concrete but it increases displacement up to 50% (improved concrete deformation) during loading. The Splitting Tensile Strength improves by 12.7% with introduction of TDA into concrete. The Bond Strength of the TDA concrete is not significantly different from that of the control concrete but TDA improves post cracking behavior of the concrete as noted from the Pull-Out Tests.

It was found out that up to 15% of fine aggregates can be replaced with an equal volume of Crumb Rubber in a concrete mix without affecting the compressive strength of the concrete. Keeping the Silica Fume constant, the Crumb Rubber improves compressive strength by 5% at 7 days and 9% at 28 days.

Crumb Rubber was found to improve concrete workability slightly since the slump was higher by between ¼" to ½" (6.35 to 12.7 mm). Adding Crumb Rubber to the concrete mixture increased the strain at failure by about 33% with negligible loss of compressive strength. Strain being a measure of material deformation, it then shows the concrete with Crumb Rubber would experience more deformation before the concrete fails during compressive loading. However the deformation decreases with increase in quantity of Crumb Rubber used. At 15% replacement, the control concrete and Crumb Rubber concrete strains are averagely equal.

Crumb Rubber concrete exhibited good energy absorption and ductility as the concrete did not experience the typical brittle failure, but rather a ductile, plastic failure mode. At 7.5% replacement, Crumb Rubber improved the Modulus of Toughness by 54% while at 15% the Modulus of Toughness for Crumb Rubber concrete is 15% higher than the control concrete. Therefore addition of Crumb Rubber into the concrete would improve concrete toughness and impact resistance. However Crumb Rubber modified concrete has a lower elastic modulus, splitting tensile strength and modulus of rupture when compared with the control concrete.

At the micro level concrete was seen to have an interfacial transition zone (ITZ), which represented a small region next to the particles of coarse aggregate. The ITZ was seen to have micro pores and microcracks and was considered the weakest phase in concrete. The other

phases are bulk hydrated cement paste and aggregate. ITZ being the weakest link would then therefore exercises a far greater influence on the mechanical behavior of concrete than is reflected by its size.

The concrete containing TDA was found to perform poorly at elevated temperatures when compared with concrete with similar composition except for the TDA. Cracking, spalling and pop-outs were observed in the concrete containing TDA and after exposure to heat; the concrete had a big drop in strength and elastic modulus. After exposure to 100°C (212°F), the TDA concrete strength dropped by as much as 23% in strength. In comparison, the concrete without TDA had only 12% drop in strength after exposure to 200°C (392°F) for the same duration.

The decline in strength and modulus is believed to be due to microcracking in the concrete due to internal pressures exerted by gaseous compounds escaping after decomposition of TDA particles and differential thermal expansion between the TDA and the concrete. It is recommended that the concrete with TDA should be used in environments where temperatures would not exceed 100°C (212°F).

A three dimensional nonlinear Finite Element Model (FEM) for a concrete beam was proposed and developed for three types of concrete. The three types of concrete differed in composition by incorporating Tire Derived Aggregates of different sizes during batching. The material properties were defined with the smeared crack model in ABAQUS. The developed FEM was capable of predicting the ultimate load, deflections, Stress-deflection/strain curves and crack initiation which were all verified against the experimental tests. The experimental results showed close correlations when compared with those obtained from the FEM analysis. ABAQUS was found to be a useful tool for modeling of concrete.

9.2 Recommendations for Future Work

This research focused mainly on the effect of waste tires (TDA and Crumb Rubber) in concrete. It has been found that post cracking behavior of concrete is improved when you have rubber in concrete. However, only plain concrete (without reinforcement) was examined. In actual

civil engineering structures, reinforcement in concrete is normally used and it would be good to extend this research of Rubberized Concrete to concrete with reinforcement. Further modeling of post cracking behavior with reinforcement would then be required.

Rubberized Concrete was found to deteriorate at high temperatures (> 100°C). The temperature in some states in winter falls below 0°C. The study on the effect of temperature on Rubberized Concrete needs to be extended to find out how it would behave at very low temperatures and cycles of freezing and thawing.

REFERENCES

[1] S. Mindess, J.F. Young, D. Darwin, Concrete, Prentice Hall, Upper Saddle River, NJ, 2003.

[2] United States Environmental Protection Agency: Office of Solid Waste, Markets for Scrap Tires, Policy Planning and Evaluation PM-221, (1991).

[3] C.E. Pierce, Blackwell C M, Potential of Scrap Tire Rubber as Lightweight Aggregate in Flowable Fill.

[4] C. Hammer, T.A. Gray, Designing Building Products Made With Recycled Tires, Report 433-04-008 (2004).

[5] N. Segre, A.D. Galves, J.A. Rodrigues, P.J. Monteiro, I. Joekes, Use of Tyre Rubber Particles in Slag Modified Cement Mortars, (2003) 1546-1554.

[6] A.O. Atahan, U.K. Sevim, Testing and comparison of concrete barriers containing shredded waste tire chips, Materials Letters. 62 (2008).

[7] V. Petr, T.G. Rozgonyi, (2005).

[8] Texas Commission on Environmental Quality, Tracking the Fate of Scrap Tires in Texas: An Audit Report, Report SFR-078/08 (2010).

[9] Rubber Manufacturers Association, Scrap Tire Markets in the United States 9th Biennial Report (2009).

[10] Texas Department of Transportation, Using Scrap Tire and Crumb Rubber in Texas Highway Construction Projects, 2007 Annual Progress Report, (2007).

[11] Maryland Department of the Environment's Scrap Tire Program, Guidance Manual for Engineering Uses of Scrap Tires, Geosyntec Project No ME0012-11 (2008).

[12] ASTM International, ASTM Standard D6270: Standard Practice for Use of Scrap Tires in Civil Engineering Applications, ASTM International, West Conshohocken, PA, 2009.

[13] İ.B. Topçu, T. Bılır, Analysis of Rubberized Concrete as a Three-phase Composite Material, J. Composite Mater. 43 (2009) 1251-1263.

[14] D.N. Humphrey, Tire Derived Aggregate – A New Road Building Material.

[15] G.M. Engstrom, R. Lamb, Using Shredded Waste Tires as a Lightweight Fill Material for Road Sub grades, MN/RD No. 94/10 (1994).

[16] M.A. Aiello, F. Leuzzi, Waste tyre rubberized concrete: Properties at fresh and hardened state, Waste Management. 30 (2010) 1696-1704.

[17] N.N. Eldin, A.B. Senouci, Measurement and prediction of the strength of rubberized concrete, Cem. Concr. Compos. 16 (1994) 287-298.

[18] M. Emiroğlu, S. Yildiz, E. Özgan, Lastik Agregali Betonlarda Elastisite Modülünün Deneysel Ve Teorik Olarak İncelenmesi. (Turkish), Journal of the Faculty of Engineering & Architecture of Gazi University. 24 (2009) 469-476.

[19] A.M. Ghaly, J.D. Cahill IV, Correlation of strength, rubber content, and water to cement ratio in rubberized concrete, Canadian Journal of Civil Engineering. 32 (2005) 1075-1081.

[20] E. Güneyisi, M. Gesoğlu, T. Özturan, Properties of rubberized concretes containing silica fume, Cement & Concrete Research. 34 (2004) 2309-2317.

[21] B. Huang, G. Li, Su-Seng Pang, J. Eggers, Investigation into Waste Tire Rubber-Filled Concrete, J. Mater. Civ. Eng. 16 (2004) 187-194.

[22] A.R. Khaloo, M. Dehestani, P. Rahmatabadi, Mechanical properties of concrete containing a high volume of tire–rubber particles, Waste Management. 28 (2008) 2472-2482.

[23] Z.K. Khatib, F.M. Bayomy, Rubberized Portland Cement Concrete, J. Mater. Civ. Eng. 11 (1999) 206.

[24] Y. Li, Y. Wu, Y. Yang, Z. Han, M. Wang, Study on the structure properties of steel reinforced crumb rubber concrete, Beijing Gongye Daxue Xuebao / Journal of Beijing University of Technology. 34 (2008) 1280.

[25] F. Pelisser, N. Zavarise, T.A. Longo, A.M. Bernardin, Concrete made with recycled tire rubber: Effect of alkaline activation and silica fume addition, J. Clean. Prod. 19 (2011) 757-763.

[26] R.R. Schimizze, J.K. Nelson, S.N. Amirkhanian, J.A. Murden, Use of waste rubber in light-duty concrete pavements, Proceedings of the Materials Engineering Conference. (1994) 367.

[27] R. Siddique, T.R. Naik, Properties of concrete containing scrap-tire rubber – an overview, Waste Management. 24 (2004) 563-569.

[28] K.S. Son, I. Hajirasouliha, K. Pilakoutas, Strength and deformability of waste tyre rubber-filled reinforced concrete columns, Constr. Build. Mater. 25 (2011) 218.

[29] İ.B. Topçu, T. Bilir, Experimental investigation of some fresh and hardened properties of rubberized self-compacting concrete, Mater Des. 30 (2009) 3056-3065.

[30] İ.B. Topçu, A. Demir, Durability of Rubberized Mortar and Concrete, J. Mater. Civ. Eng. 19 (2007) 173-178.

[31] H.A. Toutanji, Use of rubber tire particles in concrete to replace mineral aggregates, Cem. Concr. Compos. 18 (1996) 135-139.

[32] C. Akisetty, F. Xiao, T. Gandhi, S. Amirkhanian, Estimating correlations between rheological and engineering properties of rubberized asphalt concrete mixtures containing warm mix asphalt additive, Construction & Building Materials. 25 (2011) 950-956.

[33] S.H. Kosmatka, W.C. Panarese, Design and Control of Concrete Mixtures, Portland Cement Association (PCA), Stokie, Illinois, 1994.

[34] ASTM International, ASTM Standard C192: Standard Practice for Making and Curing Concrete Test Specimens in the Laboratory, ASTM International;www.astm.org., West Conshohocken, PA, 2009.

[35] ASTM International, ASTM Standard C143: Standard Test Method for Slump of Hydraulic-Cement Concrete, ASTM International; www.astm.org., West Conshohocken, PA, 2009.

[36] ASTM International, ASTM Standard C39:Standard Test Method for Compressive Strength of Cylindrical Concrete Specimens, ASTM International; www.astm.org, West Conshohocken, PA, 2009.

[37] ASTM International, ASTM Standard C496: Standard Test Method for Splitting Tensile Strength of Cylindrical Concrete Specimens, ASTM International; www.astm.org, West Conshohocken, PA, 2009.

[38] ASTM International, ASTM Standard C78: Standard Test Method for Flexural Strength of Concrete (Using Simple Beam with Third-Point Loading), ASTM International; www.astm.org, West Conshohocken, PA, 2009.

[39] A. Dunster, Silica fume in concrete, Information Paper No. IP 5/09 (2009).

[40] T. Kuennen, Silica Fume Resurges, Concrete Products. (1996).

[41] S.P. Shah, K. Wang, Development of "Green" cement for sustainable concrete using cement kiln, (2004).

[42] L. Zheng, X.S. Huo, Y. Yuan, Strength, Modulus of Elasticity, and Brittleness Index of Rubberized Concrete, J. Mater. Civ. Eng. 20 (2008) 692-699.

[43] K.P. Mehta, P.J.M. Monteiro, Concrete: Microstructure, Properties, and Materials, McGraw-Hill, New York, 2006.

[44] D.R. Askeland, P.P. Phule, The Science and Engineering of Materials, 5th ed., Nelson (Division of Thomson), Toronto, Ontario, 2006.

[45] B.D. Cullity, Ements of X-RAY DIFFRACTION, Addison-Wesley Publishing Company, Inc., Reading, Massachusetts, 1956.

[46] R.Y. Kim, Modeling of Asphalt Concrete, 1st ed., McGraw-Hill Construction, 2009.

[47] G. Agostini, F.G. Corvasce, Tire with Low Thermal Expansion Component, 11/243,868 (2008).

[48] R.M. Biggs, P.J. Massarelli, Final Report Finite Element Modeling And Analysis Of Reinforced-Concrete Bridge Decks, (2000).

[49] Dassault Systèmes, Abaqus 6.10 Online Documentation, (2010).

[50] K. Bathe, Finite Element Procedures, PHI Learning Private Limited, New Delhi, 2009.

BIOGRAPHICAL INFORMATION

Gideon Siringi was born in Kisii District in Kenya where he started his primary education in the local schools from where he excelled in the Kenya Certificate of Primary Education in 1992 which earned him admission to the prestigious Alliance High School from where he sat his Kenya Certificate of Secondary Education in 1996 earning an overall grade of A Minus.

Gideon was then admitted to Moi University in Eldoret Kenya where he pursued a Bachelor of Technology degree in Chemical & Process Engineering graduating with a First Class Honors in 2003. While at Moi University, Mr. Siringi did his internship at Sony Sugar Company in Migori, Kenya and Kapa Oil refineries in Nairobi Kenya.

After graduation, Gideon started his professional career at Unilever Kenya Limited in October 2003, based Nairobi Kenya where he worked as an Industrial Engineer. In June 2004, Mr. Siringi moved to Bamburi Cement Limited, in Mombasa Kenya where he worked as a Process Engineer till December 2005 when he decided to pursue post graduate studies.

In January 2006, Mr. Siringi joined Lamar University in Beaumont Texas where he did his Master of Engineering degree in Chemical Engineering graduating in May 2007. Gideon then joined TXI's Midlothian Cement Plant in August 2007 where he worked as a Process Engineer till December 2011. While at TXI, Gideon started his PhD in Materials Science and Engineering at the University of Texas at Arlington in January 2008 which he has continued to pursue focusing on use of recycled rubber in concrete.

Currently Mr Siringi is working for Lhoist North America as a Senior Process Engineer and his future plan is to join the academic field. His research interests are in recyclable materials.